HEMATOPOIETIC STEM CELLS DERIVED FROM UMBILICAL CORD BLOOD: EFFECTS OF EX VIVO EXPANSION AND DESIGN OF A NOVEL CULTURE ENVIRONMENT

By

KORASHON LYNN WATTS

A DISSERTATION PRESENTED TO THE GRADUATE SCHOOL
OF THE UNIVERSITY OF FLORIDA IN PARTIAL FULFILLMENT
OF THE REQUIREMENTS FOR THE DEGREE OF
DOCTOR OF PHILOSOPHY

UNIVERSITY OF FLORIDA

2007

To Richard and Patricia Watts, founding members of the Fan Club.

ACKNOWLEDGMENTS

I would like to acknowledge my Ph.D. supervisory committee for providing me with outstanding guidance in their areas of expertise. I would like to extend special acknowledgement to Dr. Roger Tran-Son-Tay (for his assistance with cellular rheology concepts) and Dr. Vijay Reddy (for his aid in understanding stem cell biology). I would also like to thank the Stem Cell Lab of Shands Hospital for providing biological samples and for training me in proper cell culture technique.

In addition, this work would not have been possible without the help of the graduate students in the Cellular Mechanics and Biorheology Lab: Jessica Cobb (for teaching me to culture Caco-2 cells), Cecile Perrault (for assistance conducting rheology experiments), Adam Poniatowski (for training me in proper simulated microgravity culture technique), and Ethan Sherman (for support during fabrication of the mold for the cell culture chamber tested in this project). Finally, I would like to thank my family for fostering an environment of intellectual pursuit and scientific inquiry that will continue to propel me during pursuit of my goals.

TABLE OF CONTENTS

LIST OF TABLES

LIST OF FIGURES

LIST OF ABBREVIATIONS

AFM	Atomic force microscopy
BFU-E	Burst-forming unit: erythrocyte
BM	Bone marrow
BSA	Bovine serum albumin
CD	Cluster of differentiation
CFU	Colony-forming unit
CFU-E	Colony-forming unit: erythrocyte
CFU-GEMM	Colony-forming unit: granulocyte/erythrocyte/monocyte/megakaryocyte
CFU-GM	Colony-forming unit: granulocyte/macrophage
DMEM	Dulbecco's Modified Eagle's Medium
EDTA	Ethylene diamine tetra-acetic acid
EPO	Erythropoietin
FBS	Fetal bovine serum
FITC	Fluorescein isothiocyanate
FL	*flt*-3 ligand
G1	First gap (phase of cell cycle)
G2	Second gap (phase of cell cycle)
G-CSF	Granulocyte-colony stimulating factor
GVHD	Graft-versus-host disease
HARV	High aspect ratio vessel
HBSS	Hank's Balanced Salt Solution
HLA	Human leukocytic antigen

HSC	Hematopoietic stem cell
HSCT	Hematopoietic stem cell transplantation
IL-3	Interleukin-3
IL-6	Interleukin-6
IMDM	Iscove's Modified Dulbecco's Medium
M	Mitosis (phase of cell cycle)
MTC	Magnetic twisting cytometry
NASA	National Aeronautics and Space Administration
PBS	Phosphate buffered saline
PDMS	Polydimethylsiloxane
PE	Phycoerythrin
RCCS	Rotary cell culture system
S	Synthesis (phase of cell cycle)
SCF	Stem cell factor
STLV	Slow turning lateral vessel
TPO	Thrombopoietin
UCB	Umbilical cord blood

Abstract of Dissertation Presented to the Graduate School
of the University of Florida in Partial Fulfillment of the
Requirements for the Degree of Doctor of Philosophy

HEMATOPOIETIC STEM CELLS DERIVED FROM UMBILICAL CORD BLOOD: EFFECTS OF EX VIVO EXPANSION AND DESIGN OF A NOVEL CULTURE ENVIRONMENT

By

Korashon Lynn Watts

May 2007

Chair: Roger Tran-Son-Tay
Cochair: Vijay Reddy
Major: Biomedical Engineering

Umbilical cord blood (UCB) stem cell transplantation is a valuable treatment option for patients suffering from a range of hematopoietic and immune disorders. However, one of the major obstacles in this field is the limited number of transplantable cells available in a cord blood unit. Therefore, research and clinical trials are ongoing involving ex vivo expansion of the cells prior to transplant. However, this field is still in its infancy. This study was designed with the goal of determining the effects of ex vivo expansion on UCB CD34+ cells, and to investigate whether simulated microgravity offers promise for expanding these cells.

To this end, aspiration/recovery experiments and progenitor assays were conducted on fresh and ex vivo expanded UCB-derived CD34+ cells. Results were compared to determine whether a significant difference existed. In addition, a simulated microgravity culture chamber was designed, built, and validated using a control cell line. This device, which offers the benefit of requiring about one-tenth of the volume of traditional simulated microgravity devices, was subsequently used to study the effects of microgravity culture on UCB-derived CD34+ cells.

Results showed that ex vivo expanded cells had a significantly lower viscosity and cortical tension than fresh cells. Furthermore, expanded cells generated a significantly higher number of

myeloid progenitor colonies and a significantly lower number of erythroid progenitor colonies than their fresh counterparts. Additionally, this study proved that the culture chamber described above provides a cell-friendly environment in which the properties of microgravity are maintained. However, it was found that simulated microgravity is not a suitable environment for culture of UCB-derived CD34+ cells, as both short-term and long-term damage was observed in the cells.

In conclusion, ex vivo expanded UCB CD34+ cells are significantly different from fresh cells, and are expected to behave differently in the body. Consequently, patients transplanted with expanded cells should be monitored closely. Furthermore, although simulated microgravity did not prove to be an appropriate means of augmenting UCB-derived CD34+ cells, the device designed and fabricated here continues to offer merit as it broadens the field of simulated microgravity research and reduces supply costs.

CHAPTER 1
INTRODUCTION

Problem Statement

Hematopoietic stem cells (HSCs) are in high demand in both the research realm and in the clinical setting. Because of their potential to regenerate the entire hematopoietic cell line, these cells are especially valuable in the field of transplantation medicine, where patients are often in need of hematopoietic cells to replenish those lost during chemotherapy or radiation therapy.

Hematopoietic stem cell transplantation (HSCT) is a viable treatment option for patients diagnosed with a variety of different medical conditions, from cancers such as leukemia and lymphoma to autoimmune diseases such as rheumatoid arthritic and lupus. HSCT offers the advantage over chemo-radiotherapies of donor immune system reconstitution in the host, which results in graft-versus-tumor effects and thus leads to potential cure following the transplant. Treatment strategies range from autologous transplant (in which a patient's own cells are cryopreserved prior to radiation or chemotherapy for later re-transplant) to allogeneic or matched/unrelated transplant (in which cells from a different individual are transplanted with the goal of rebuilding a healthy immune system in the host). However, regardless of the treatment strategy implemented, the requirement is the same: a substantial source of healthy cells to encourage hematopoietic and immune system reconstitution and promote patient recovery.

Though the opportunities associated with stem cell transplant are exciting and offer enormous potential, there are limitations that stand in the way of complete success. One of these limitations is the difficulty of procuring sufficient numbers of cells from certain sources (such as umbilical cord blood) to engraft an adult of average size. In other cases, it is difficult to find a suitable match for many minority patients because of the under-representation of minority donors

and the resulting deficiency of appropriate cells in blood banks. Therefore, there is a clinical need for augmented numbers of cells that are in short supply. Two possible measures to overcome the shortage of HSCs include (1) ex vivo expansion of cells prior to transplantation and (2) implementation of simulated microgravity as a culture environment.

Transplantation of Ex Vivo Expanded Cells

In the past decade, researchers have made significant progress in the field of ex vivo expansion of hematopoietic stem cells. These advances have manifested themselves in the clinical world as well, and clinical trials are ongoing involving transplantation of cells cultured in vitro as a means of augmenting cell numbers prior to transplant (Shpall et al., 2002; Jaroscak et al., 2003). Transplantation of cultured cells offers the possibility for increased engraftment, reduced risk of infection, an increase in the pool of potential donors, and increased clinical applications (Devine et al., 2003). Many preliminary clinical trials show promise (Reiffers et al., 1999; McNeice et al., 2000; Paquette et al., 2000), and the overall conclusion that can be drawn from these studies is that ex vivo expanded cells may make a significant contribution to early hematopoietic recovery. It has been suggested, however, that culture may affect the functional properties of the cells (Devine et al., 2003). This is an issue that has not been explored in depth, and the current study attempts to make progress in this arena. It is important to understand the effects of ex vivo expansion on the properties of CD34+ cells in order to fully consider the health impacts that may result from transplanting these cells.

This study was designed to determine the effects of ex vivo expansion on the biological and rheological properties of umbilical cord blood-derived CD34+ cells. To investigate the *biological* impact of ex vivo expansion, the potential of fresh umbilical cord blood CD34+ cells and ex vivo expanded umbilical cord blood CD34+ cells to generate myeloid and erythroid precursors was studied. To investigate the *rheological* impact of ex vivo expansion, aspiration

and recovery experiments were performed on fresh CD34+ cells and cultured CD34+ cells to determine the viscosity and cortical tension of both populations of cells.

Simulated Microgravity

Conventional culture methods for expanding cell numbers have proven to be both expensive and time consuming, and it is often challenging to grow a sufficient number of cells to be of clinical significance. For these reasons, an efficient means of maximizing *ex vivo* stem cell growth would be both relevant and potentially useful to a wide range of medical practitioners and researchers.

Simulated microgravity offers promise as a technique to optimize ex vivo expansion. Preliminary studies have shown that simulated microgravity culture maintains bone marrow-derived hematopoietic stem cells in a quiescent state and promotes increased proliferation of the more primitive (and consequently, more valuable) phenotype upon initiation of secondary static culture (Plett et al., 2001). Unfortunately, current simulated microgravity facilities have proven to be costly and the volume requirement is too large to make this a realistic path to pursue. The cost of media and growth factors to fill the culture vessel is too high to make serious experimentation possible, and the high number of cells needed is difficult to obtain in a research setting. These restrictions comprise a frustrating limitation. There is vast potential to utilize microgravity for development of a new technique to induce growth and differentiation of HSCs, yet simulated microgravity culture cannot currently be carried out in a cost effective and realistic manner. Until an improved culture vessel can be engineered, the promise of simulated microgravity culture cannot be fully explored.

Consequently, a novel cell culture facility must be developed to imitate the conditions of microgravity while minimizing the volume requirement and promoting economical research into the effects of this environment on cell growth. Design of this facility will lead to a better

understanding of the impact of microgravity on the cellular mechanisms of HSC growth and function, and will allow for assessment of the effectiveness of this "micro-well" technique for culturing other types of cells in simulated microgravity as well. The outcome of this project will contribute not only to the advancement of the field of simulated microgravity study, but to the development of more economical cell culture as well.

Statement of Objectives

Very little is known about how the culture process affects the biological and rheological properties of the pivotal hematopoietic stem cells. For example, do these cultured cells have the same ability to reconstitute a patient's hematopoietic system as their non-cultured counterparts? Are these cultured cells more, less, or equally able to migrate through the tiny capillaries of the body? Therefore, the primary goal of this project was to elucidate some of the biological and rheological effects of ex vivo expansion and consider how these changes might affect a patient's health.

A secondary objective of this project was to design and test a convenient, economical device to facilitate experiments in simulated microgravity. Independent of the effects of simulated microgravity on the types of cells explored in this project, this micro-well chip will make an important contribution to simulated microgravity technology, as it will minimize volume requirements and decrease supply costs.

Specific Aims

- **Specific Aim 1**: Quantify the rheological properties of fresh and cultured cord blood stem cells and determine how these properties differ.
- **Specific Aim 2:** Study how the differentiation (colony generation) capability of cord blood-derived hematopoietic stem cells is affected by culture.
- **Specific Aim 3:** Design a novel, economical cell culture facility to reduce the volumetric requirements of current simulated microgravity research and validate the effectiveness of this device using a "control" cell line (human colon carcinoma cells).

- **Specific Aim 4:** Observe the short-term effects of simulated microgravity on cord blood stem cells (via primary simulated microgravity culture).

- **Specific Aim 5:** Observe the long-term effects of simulated microgravity by investigating the behavior of cord blood stem cells in secondary (a.) static culture, and (b.) progenitor culture.

Relevance

Autologous transplantation is used to treat cancers such as multiple myeloma, non-Hodgkin's lymphoma, Hodgkin's disease, and acute myeloid leukemia. It is also used for other diseases such as autoimmune disorders and amyloidosis. Annually, over 30,000 autologous transplants are performed worldwide; two thirds of these are used for patients suffering from multiple myeloma or non-Hodgkin's lymphoma (Copelan, 2006). Allogeneic transplantation is used to treat many of the same cancers as autologous transplantation; however, it is also used to treat acute lymphoblastic leukemia, chronic myeloid leukemia, myelodysplastic syndromes, myeloproliferative disorders, chronic lymphocytic leukemia, and juvenile chronic myeloid leukemia. Furthermore, it is used as a treatment option for various types of anemia, severe combined immunodeficiency, and inborn errors of metabolism. Annually, over 15,000 allogeneic transplants are performed worldwide; half of these are used for patients suffering from acute leukemias (Copelan, 2006). In addition, it is estimated that around 8,000 unrelated cord blood transplants have been performed worldwide since 1993 (Rubinstein, 2006). As clinical trials progress and more and more patients are transplanted with hematopoietic cells that have been expanded through ex vivo techniques, it becomes increasingly important to determine whether and how ex vivo expanded cells differ from fresh cells. Important properties of progenitor cells, such as the ability to reconstitute a patient's hematopoietic system and the ability to perform routine immune function, may be altered by ex vivo expansion; it is pivotal to

bring these dissimilarities to light in order to provide patients with the proper post-transplant care.

In addition, the effectiveness of simulated microgravity as a means of inducing growth of cord blood stem cells has not been able to be fully explored because of the high volume demanded by the current simulated microgravity culture vessel. By assessing this problem from an engineering standpoint and designing and constructing a novel microgravity culture vessel, simulated microgravity can be fully explored and it can be determined whether it offers merit as a culture environment for umbilical cord blood-derived stem cells. Furthermore, the large volume requirement associated with current simulated microgravity culture limits the types of cells and fields of research that can be explored. By reducing this volume requirement, the field of simulated microgravity research can be broadened.

CHAPTER 2
BACKGROUND

Hematopoietic Stem Cells

Hematopoietic stem cells (HSCs) are the precursor cells of the entire hematopoietic ("blood-forming") cell line; a single hematopoietic stem cell has the potential to generate all of the components of whole blood: white blood cells, red blood cells, and platelets. HSCs are unique in that they possess both the property of *proliferation* (self-renewal) and *differentiation* (ability to give rise to the various cell types that comprise whole blood). Figure 2-1 depicts the differentiation capabilities of an HSC.

Hematopoietic stem cells are primarily identified on account of the presence of the cell surface antigen Cluster of Differentiation (CD) 34. The CD34 antigen is a single-chained, trans-membrane glycoprotein, which decreases in density as cells differentiate into their terminal lineage (Lanza et al., 2001). Though other antigens are occasionally used for identification (such as CD117), CD34 is the antigen routinely used for clinical purposes. HSCs are obtained from three major sources: bone marrow, peripheral blood, and umbilical cord blood. Historically, the main source of HSCs for transplantation purposes has been the bone marrow; the limitation with bone marrow stem cell transplants is the difficulty of finding a suitable donor. Peripheral blood is an attractive source of HSCs because administration of growth factors can mobilize significant numbers of stem cells into circulation. However, there is a concern of splenic rupture upon administration of a certain growth factor, granulocyte colony-stimulating factor (G-CSF). Umbilical cord blood offers the advantages of ready availability, less stringent donor-host matching requirements, reduction of risk, and ease of procurement; however, the small volume of cells available limits the number of suitable patients (Heike and Nakahata, 2002). CD34+

cells are present at a frequency of about 1.08 to 2.5% in bone marrow, 0.048 to 0.24% in peripheral blood, and 0.42 to 1.325% in umbilical cord blood (Eridani et al., 1998).

Culture of Hematopoietic Stem Cells

Hematopoietic stem cells are routinely cultured for a variety of reasons, including optimization of culture conditions, observation of growth characteristics, and exploration of options related to transplantation of augmented quantities of cells. The two major types of culture are *conventional culture*, in which primitive cells are induced to proliferate, and *progenitor culture*, in which primitive cells are induced to differentiate into hematopoietic progenitors.

Conventional Culture

Historically, the two main aims of conventional culture of HSCs have been to compare the ex vivo expansion potential of cells from the three different sources (bone marrow, peripheral blood, and umbilical cord blood), and to optimize the growth factors used to promote expansion.

Eridani et al. (1998) studied the expansion potential of all three HSC sources in media containing stem cell factor (SCF), interleukin-3 (IL-3), and erythropoietin (EPO). They found that umbilical cord blood-derived stem cells demonstrated 100- to 220-fold expansion, while peripheral blood and bone marrow-derived stem cells demonstrated only 30- to 80-fold expansion. Peak expansion was observed at day 10, and these differences were significant. They concluded that umbilical cord blood-derived stem cells appear to be endowed with a higher amplification potential.

Gilmore et al. (2000) compared the growth of umbilical cord blood CD34+ cells and peripheral blood CD34+ cells; they showed that umbilical cord blood CD34+ cell cultures were significantly more successful and could be maintained for up to 16 weeks. They noted that one million cord blood CD34+ cells could be expanded to one hundred million CD34+ cells in eight

or nine weeks in media containing *flt*-3 ligand (FL) and thrombopoietin (TPO), while peripheral blood CD34+ cells showed limited, if any, expansion in media containing these two growth factors.

Tanavde et al. (2002) performed a similar study comparing umbilical cord blood stem cells and peripheral blood stem cells in culture and showed that, after 1-4 weeks in culture, umbilical cord blood stem cell cultures had greatly increased in total cell number, while peripheral blood stem cell cultures showed only minimal hematopoietic capacity. After 3 weeks of culture, the average cord blood CD34+ cell had divided around 5 times, while the average peripheral blood CD34+ cell had divided only about 2 times. They concluded that HSCs from neonatal umbilical cord blood have a significantly greater expansion capacity that those derived from mobilized adult peripheral blood.

Additional studies attempted to determine the most effective combination of growth factors to stimulate CD34+ cell growth. It was shown that bone marrow and peripheral blood CD34+ cells could be expanded in media containing FL, TPO, SCF, and interleukin-6 (IL-6) for up to 10 weeks, demonstrating up to 3000-fold expansion (Gammaitoni et al., 2003). Prior to these findings, umbilical cord blood was the only source of CD34+ cells that showed any encouraging results for ex vivo expansion.

Several teams of researchers have discovered that the optimal combination of growth factors to promote expansion of umbilical cord blood-derived CD34+ cells is FL and TPO (Piacibello et al., 1997; Gilmore et al., 2000; Heike and Nakahata, 2002). Piacibello et al. (1997) showed that the combination of FL and TPO was able to sustain the proliferation and renewal of umbilical cord blood CD34+ cells for more than 6 months without any sign of exhaustion. Gilmore et al. (2000) showed that these two growth factors were suitable for maintaining

cultures of CD34+ cells for up to 16 weeks, generating sufficient numbers of HSCs to be used for adult transplantation. Heike and Nakahata (2002) demonstrated greater than 200,000-fold expansion of cord blood CD34+ cells, using a combination of FL and TPO. The above findings have laid the foundation for the current study.

Progenitor Culture

When hematopoietic stem cells are cultured in a specialized semi-solid methylcellulose media, a small number of these cells form discrete colonies. These colonies are the progenitors of mature blood cells, and include cells from the erythrocyte, granulocyte, monocyte-macrophage, and megakaryocyte-myeloid lineages. Among others, the colonies formed include burst-forming units--erythroid (BFU-E), which are colonies containing at least 200 erythroblasts and colony-forming units--granulocyte/macrophage (CFU-GM), which are colonies containing at least 20 granulocytes, macrophages, or cells of both lineages[1]. These colonies can be easily enumerated based on morphology by viewing the cultures with an inverted light microscope. This technique is commonly used for characterization of hematopoietic progenitors, as a quality control for stem cell processing, and as a screening procedure for new growth factors.

Hematopoietic Stem Cell Transplantation

The concept of hematopoietic stem cell transplantation was originally explored over 50 years ago as a therapy for irradiation injury (Copelan, 2006). Today, it is used as a treatment option for patients suffering from various hematological and immune diseases. Strategies for treatment include autologous transplant, allogeneic transplant, and matched/unrelated transplant. During autologous transplant, a patient's own cells are cryopreserved prior to radiation therapy or chemotherapy; the cells are then re-infused post-therapy. During allogeneic transplant, a

[1] Definitions are derived from "Human Colony-Forming Cell Assays Using MethoCult", Technical Manual, October 2004.

matched relative acts as a donor for the patient. During matched/unrelated transplant, a matched, unrelated individual serves as the donor. Annually, over 30,000 autologous transplants and 15,000 allogeneic transplants are performed worldwide (Copelan, 2006).

The most novel source of transplantable stem cells is umbilical cord blood (UCB). The first umbilical cord blood transplant occurred in 1990, and since then there have been over 8,000 of these transplants performed worldwide. Over the past decade, significant advances have been made in the field of UCB stem cell transplantation, which have broadened the pool of potential recipients to include adult patients as well as the more traditional pediatric recipients (Tse and Laughlin, 2005). However, it has been shown that cell dose (number of transplanted cells per kilogram body weight) is the most significant obstacle in the field of umbilical cord blood-derived stem cell transplant (Wagner et al., 2002). In other words, the limited number of transplantable cells in a unit of cord blood restricts the number of suitable recipients. For this reason, clinical trials are ongoing involving transplantation of ex vivo expanded cord blood cells as a means of augmenting cell numbers prior to transplant (Shpall et al., 2002; Jaroscak et al., 2003).

The first report on the use of cultured cells to be used for transplantation came from Brugger et al. (1995) and was designed to show the safety and feasibility of using ex vivo expanded cells for transplantation. In this study, CD34+ cells derived from peripheral blood were cultured for 12 days prior to transplantation. The 10 patients receiving these cells achieved an absolute neutrophil count of >500/mm^3 by day 12 and platelet count CFU-recovered to >20,000/mm^3 by day 12. Since then, the transplantation of ex vivo expanded cells has grown in popularity and now includes cells from umbilical cord blood. Shpall et al. (2002) augmented conventional UCB transplants with ex vivo expanded cells. In this study, 37 patients received

high-dose chemotherapy followed by unrelated cord blood transplantation with either 40% or 60% of their graft expanded ex vivo. All evaluable patients achieved engraftment of neutrophils, and the study demonstrated that ex vivo expansion of UCB prior to transplantation is feasible. Similarly, Jaroscak et al. (2003) found that UCB grafts supplemented with expanded cells were well-tolerated; patients did not experience any adverse effects from these grafts.

Transplantation of cultured cells offers many opportunities, including the possibility for increased engraftment, reduced risk of infection, an increase in the pool of potential donors, and increased clinical applications (Devine et al., 2003). The goal of many preliminary clinical trials has been to expand the number of short-term repopulating cells in order to shorten the period of pancytopenia that follows high-dose chemotherapy or chemoradiotherapy. Results from clinical trials have been varied due to an inconsistency in culture conditions, but many show promise (Reiffers et al., 1999; McNeice et al., 2000; Paquette et al., 2000). The overall conclusion that can be drawn from these studies is that ex vivo expanded cells may make a significant contribution to early hematopoietic recovery and may be able to reduce post-chemotherapy nadirs. It has been suggested, however, that culture may affect pivotal properties of the cells (Devine et al., 2003). This is an issue that has not been explored fully, and consequently this topic provides part of the motivation for the current study.

Micropipette Experiments

One of the governing characteristics of blood cells is the ability to deform, flow through the tiny vessels of the body, and migrate to different regions of the anatomy (for example: sites of infection or tissue damage). Rheology is the study of the deformation and flow of matter, and the rheological properties of cells become even more pivotal in ill or immunocompromised patients. Therefore, one of the goals of this study was to determine the effects of ex vivo expansion on the rheological properties of umbilical cord blood-derived CD34+ cells. To this

end, aspiration and recovery experiments were performed on fresh CD34+ cells and cultured CD34+ cells to determine the viscosity and cortical tension of both populations of cells.

Aspiration and recovery experiments were performed according to the micropipette technique described by Evans and Yeung (1989). In short, a cell is aspirated under constant pressure into a capillary tube with a diameter less than that of the cell. As the cell flows into the tube, it behaves as a Newtonian liquid and deforms in a time-dependent manner. Following aspiration, the cell is expelled and recovers its spherical shape. By recording various dimensions of the cell during both aspiration and recovery, one can calculate the rheological properties or cytoplasmic viscosity and cortical tension. This technique has been used for several years to study the properties of various blood cells, include granulocytes (Evans and Yeung, 1989), neutrophils (Tran-Son-Tay et al., 1991), leukocytes (Kan et al., 1999), red blood cells (Maggakis-Kelemen et al., 2002), platelets (Thomas et al., 2003), and lymphocytes (Thomas et al., 2003; Perrault et al., 2004).

The manner in which a leukocyte responds to deformation is a function of either its cortical tension or its cytoplasmic viscosity. Cortical tension is related to a persistent tension provided by the cytoskeleton, and cytoplasmic viscosity is related to the flow resistance of the cytoplasm. The cytoskeleton consists of three main types of proteins: actin filaments, microtubules, and intermediate filaments. In addition, there are numerous associated proteins which perform such functions as controlling the length of the filaments, growth of filaments, cross-linking or bundling among filaments, and attachment of the filaments to the membrane. The shape of the cell, the motility of the cell, generation of force, and the way a cell responds to deformation are all a result of these proteins working together (Radmacher et al., 1996). It has been stated that the role of the membrane is primarily passive when responding to cytoskeletal

deformations (Sheetz, 1993). The cytoplasm of the cell consists of macromolecules, metabolites, ions and other solutes. The dominant component, however, is water. It is known that, even though water is the major component of the cytoplasm, the cytoplasm behaves quite differently from pure water (Clegg, 1984). For example, the viscosity of the cytoplasm varies with temperature (Needham and Hochmuth, 1990). Furthermore, Needham and Hochmuth (1990) showed that the cytoplasm of liquid-like cells (such as neutrophils) behaves as a Newtonian fluid with a constant viscosity over a large range of aspiration pressures.

Cell Models

There are two main types of cell models which have laid the foundation for subsequent rheological studies: continuum models and micro/nanostructural models. Continuum models are based on continuum mechanics; therefore, these models deal with continuous matter and ignore the heterogeneous microstructure within the matter. Continuum models can be broken down into the viscoelastic models and the biphasic model. The viscoelastic model can subsequently be further broken down into the liquid drop models, the solid models, and the fractional derivative model (Figure 2-2). The models that were developed based on micropipette experiments (and are therefore pertinent to this research) are the liquid drop models and the solid models. Therefore, these two families of models are the focus of the sections below.

The continuum approach is more straightforward than the micro-nanostructural approach, and is a more appropriate choice if the parameter of interest is the biomechanical response at the cell level (Lim et al., 2006). However, certain circumstances might require an understanding of the cell at the molecular level. In these cases, the micro/nanostructural approach would be more appropriate. This approach is largely based on the tensegrity model. Tensegrity models consider the cell as consisting of a tensed network of structural members, including discontinuous struts (microtubules) and continuous cables (actin filaments) (Volokh, 2003). Therefore, the tensegrity

model provides insight into the role of distinct elements of the cell and how they perform mechanically (Wang et al., 2001). However, it is important to mention that the tensegrity model is more appropriate for adherent cells than for suspension cells, and thus far no work has been published using the tensegrity model to study leukocytes.

Liquid-drop models

The liquid drop models are also called the cortical shell-liquid core models, and they are applied primarily to suspension cells. These models were developed to account for the rheology of neutrophils during micropipette aspiration, and include the Newtonian liquid drop model, the compound Newtonian liquid drop model, the shear thinning liquid drop model, and the Maxwell liquid drop model. A commonality of each of these four models is the presence of a cortex with a constant cortical tension; however, they differ in the manner in which the cell interior is modeled (Figure 2-3).

The *Newtonian liquid drop model* was developed by Evans and Yeung (1989) to simulate the flow of liquid-like cells into a micropipette. A Newtonian fluid is a fluid with a constant viscosity at a given temperature, regardless of the rate of shear. Newtonian fluids satisfy the Navier-Stokes equations. The local stress is linearly proportional to the local deformation rate or strain rate; Newtonian fluids can be characterized by a single value for bulk density (Roberson and Crowe, 1985). The development of this model was based on observations of Evans and Yeung that the cell adopts a spherical shape when suspended and will flow continuously into a micropipette as long as it is aspirated at a pressure above a certain "critical pressure." This "critical pressure" is the pressure at which the cell forms a hemispherical projection into the micropipette. In this model, the cytoplasm is represented as a Newtonian liquid (Figure 2-3a). Though this model holds for large deformations in the passive state, it is not able to explain the rapid entry of the cell into the micropipette.

The *compound Newtonian liquid drop model* (Dong et al., 1991; Hochmuth et al., 1993) is more complex than the previous model in that it is comprised of three heterogeneous parts: the outer layer, the middle layer, and the core layer. The outer layer consists of the plasma membrane and the ectoplasm (outer layer of cytoplasm), and it is under persistent tension. The middle layer consists of the endoplasm (inner layer of cytoplasm), and it is fluid-like in nature. The core layer consists of the condensed region of nucleus and the surrounding cytoskeleton. This surrounding cytoskeleton is also under constant cortical tension due to the presence of the nuclear envelope. In this model, there are two different viscosities, that of the cytoplasm and that of the nucleus (Figure 2-3b). It has been reported that, in order for the cell to exhibit Newtonian behavior, it must be held inside the micropipette for at least 5 seconds (Tran-Son-Tay et al., 1991). At hold times of >5 seconds, the nucleus has sufficient time to deform. As a result, the nucleus has a recovery time constant that is comparable to that of the cytoplasm-cortex complex, and the cell recovers as a Newtonian liquid drop. In addition, it has been found that the critical nucleus deformation index value in order for the cell to recover as a Newtonian drop is 1.4 (Kan et al., 1999). The nucleus deformation index is a ratio of the maximum deformed length over the initial diameter, and can be represented as L_i/D_0.

The *shear thinning liquid drop model* is based on the observation of Tsai et al. (1993) that the viscosity of the cytoplasm appears to decrease with increasing aspiration pressure. In order to account for the acceleration of the cell at the end of aspiration, the power-law constitutive relation was incorporated into the cortical shell-liquid core model. A power-law relation is any relation that is in the form $y=ax^k$, where a is a constant. This model is consistent with in vitro rheological studies because the cytoplasm is rich in polymers, and polymeric fluids are known to demonstrate shear thinning behavior. The polymers present in the cytoplasm

include actin filaments, microtubules, and intermediate filaments. In this model, the cytoplasm is modeled as a shear thinning liquid (Figure 2-3c).

The *Maxwell liquid drop model* (Dong et al., 1988) accounts for the small or initial deformation phase to explain the rapid, elastic-like entry of the cell during aspiration. This is the only of the liquid drop models to account for this observation. This model consists of a pre-stressed cortical shell containing a Maxwell fluid (Figure 2-3d). A Maxwell fluid is a viscoelastic material having the properties of both elasticity and viscosity (Roberson and Crowe, 1985). It has been observed that when the cell is held in the micropipette for less than 5 seconds, it undergoes an initial, rapid elastic rebound suggesting that it behaves as a Maxwell viscoelastic liquid rather than a Newtonian liquid with constant cortical tension (Tran-Son-Tay et al., 1991). During viscoelastic behavior, the front part of the cell (which enters the pipette first and exits last) deforms for a slightly longer time than the back part of the cell. The major drawback of this model is that, for large deformations, the model does not fit the data unless the values for viscosity and elasticity of the cytoplasm are allowed to increase continuously as the cell is aspirated. This validates the hypothesis that the cytoplasm seems to transition from a Maxwell material to a Newtonian material while being aspirated.

Solid models

The solid models are usually used for adherent cells. These models consider the cell to be homogeneous throughout and include the linear elastic solid model and the linear viscoelastic solid model (Figure 2-4).

The *linear elastic solid model* (Theret et al., 1988) is a simplification of the viscoelastic model in that the time factor has been neglected. However, this model is generally inadequate for describing the mechanics of cells, because the apparent viscosity of a viscoelastic material depends on both the loading rate and the loading history. This model serves as a basis for the

viscoelastic solution according to the correspondence principle (Fung, 1965). The correspondence principle states that as a system becomes large enough, quantum mechanics can be approximated by classical physics. During micropipette aspiration, when the pipette is very small compared to the cell (or conversely, the cell is very large compared to the micropipette), the cell can be approximated as an incompressible elastic half-space. Likewise for adherent cells, if the diameter of the tip used to stress the cell is small compared to the cell, the cell can be approximated as a half space. In this model, the cell consists of a homogeneous elastic solid (Figure 2-4a).

The *linear viscoelastic solid model* is similar to the linear elastic model, but a time factor is incorporated. This model was originally proposed to explain the small–strain deformation of leukocytes undergoing micropipette aspiration (Schmid-Schonbein et al., 1981); however, it was later found that the liquid drop models were more appropriate for modeling leukocytes. Though the formulas have been simplified in order to make this model more approachable, it has been found that the experimental values compare favorably with the numerical solutions. Anchorage-dependent cells and cell nuclei exhibit this behavior. In this model, the cell consists of a homogeneous viscoelastic solid (Figure 2-4b).

Other continuum models

The fractional derivative model mentioned in Figure 2-2 is represented by the *power-law structural damping model* (Alcaraz et al., 2003). This model is used for studying the dynamic behavior of adherent cells, while the previous models are used for transient loading conditions. This model is frequently used when performing tests via oscillatory magnetic twisting cytometry (MTC) or atomic force microscopy (AFM). During MTC, oscillating mechanical stresses are applied to cell surface receptors using magnetic beads. During AFM, a force probe is used to study topography by measuring attractive and repulsive forces between the tip and the sample.

For these tests, it has been found that a low amplitude sinusoidal force signal resulted in a sinusoidal displacement at the same frequency but with a phase lag. This model helps to explain cellular behavior that can't be explained by spring-dashpot models, because spring-dashpot models will always overestimate the power of the frequency dependence.

The final continuum model is the *biphasic model* (Shin and Athanasiou, 1999). This model is used to study musculoskeletal cell mechanics, and is especially useful for studying the interaction of chondrocytes with the extracellular cartilage matrix. This model is based on the knowledge that the cytoplasm exists in both solid and liquid form. The solid component is comprised of the polymer contents, and the liquid form is comprised of the interstitial fluid. The biphasic model treats these two phases separately. However, the complexity of the biphasic theory and the irregular geometry associated with it often make it too difficult to solve analytically.

Relevant Formulae

Needham and Hochmuth (1990) derived a formula for cytoplasmic viscosity based on the flow of a Newtonian liquid from either a hemisphere or a spherical segment into a cylinder. They used a linearized version of the previous theoretical results of Yeung and Evans (1989). According to this method, the slope of the linear portion of the tracking profile of a single cell undergoing aspiration was matched with the slope from the theoretical results of Yeung and Evans (1989), and a formula for calculating cytoplasmic viscosity was derived. This formula is presented and all variables are defined in Chapter 3: Materials and Methods.

After the cell is expelled from the micropipette, it recovers its original spherical shape. (This procedure is detailed in Chapter 3 and represented by Figure 3-1b.) The shape recovery process is analyzed according to a Newtonian liquid drop model. In this analysis, a variational method is used to simultaneously solve the hydrodynamic equations for low Reynold's number

flow and the equations for membrane equilibrium with constant surface tension (Tran-Son-Tay et al., 1991). The shape recovery equation gives the ratio of length to initial undeformed diameter (L/D_0) of the cell at a given time as a function of the dimensions before recovery (initial deformation ratio, L_i/D_0) and as a function of time; the shape of the cell can then be approximated by third order polynomials. This formula is presented and all variables are defined in Chapter 3: Materials and Methods.

Cortical tension can also be determined by a more direct method based on the Law of Laplace. The Law of Laplace states that the larger a vessel radius, the larger the wall tension required to withstand a given internal fluid pressure. For a given vessel radius and internal pressure, a spherical vessel will have half the wall tension of a cylindrical vessel (Roberson and Crowe, 1985). To use this method, a cell is aspirated until the point that it just begins to form a hemispherical projection into the micropipette. At this point, the cell is in equilibrium and the cortical tension can be solved by a relatively simple formula (Zhelev et al., 1994). This formula is presented and all variables are defined in Chapter 3: Materials and Methods.

Simulated Microgravity

Intent of NASA

The simulated microgravity system was developed by the National Aeronautics and Space Administration (NASA) at the Johnson Space Center with two goals in mind: to provide an in vitro technique for studying the effects of altered gravity on cell and tissue cultures[2], and as a means of protecting fragile cultures during space missions[3]. Most crucial of these goals, however, was to model the unique conditions encountered in space in order to study the effects of space travel on the human body with a focus on astronaut health. Specific considerations

[2] Information obtained from the Synthecon, Inc. website, www.synthecon.com. Accessed May 2005.

[3] Information obtained from the Rotary Cell Culture System User's Guide (from Synthecon, Inc.)

included anemia, loss of bone density, and abrogated immune function; all of these are common problems noted in astronauts returning from space (Plett et al., 2001).

Within a relatively short time, however, it became evident that the advantages offered by this system (low shear, high mass transfer, and lack of a net gravitational force) were not only helpful for modeling the phenomena occurring during spaceflight, but were also useful for growing cells in a traditional stationary incubator. Researchers discovered that cell lines which were notoriously difficult to culture in conventional culture could be grown with ease in this environment. Originally, NASA intended for this system to be used as a means of culturing suspension cells, but further research showed that this environment was also conducive to growth of anchorage-dependent cells.

The simulated microgravity bioreactor is currently manufactured by Synthecon, Inc. as a Rotary Cell Culture System (RCCS), and is marketed for a wide range of clinical and research applications. Current research includes tissue regeneration, pharmaceutical testing on a patient's own tissue, virus growth, and vaccine development. Many research teams have taken steps to improve the existing system; however, it is imperative that the established mechanism of operation is not changed; in other words, modified simulated microgravity systems must be identical to the original, un-modified parent system in terms of the mode of operation.

Mechanism of Operation

The mechanism of operation of simulated microgravity is relatively simple: cells and media are added to a disc-shaped or cylindrical culture vessel, which is rotated about its horizontal axis (Figure 2-5). The media becomes established in a cyclical orbit which effectively maintains cells in a constant state of suspension in a low shear, laminar flow environment. The standard gravitational field encountered in conventional culture is replaced with a randomized gravitational vector (Gao et al., 1997; Hammond and Hammond, 2001). By filling the inner

chamber completely and eliminating an air-liquid interface, the motion of the fluid within the vessel approximates the motion of the vessel itself, thereby causing shear forces on a particle to be minimal.

There are two different culture vessels available for simulated microgravity culture. The one which was used for this project is the High Aspect Ratio Vessel (HARV), a disc-shaped vessel with a gas permeable membrane covering one planar surface to allow for the exchange of oxygen and carbon dioxide (Figure 2-6 a, b, c). The second vessel, the Slow Turning Lateral Vessel (STLV) is a more elongated, cylindrical vessel with an oxygenator core (Figure 2-6d). For either vessel, rotation is necessary for proper gas exchange and nutrient mixing.

The rotational speed of the culture vessel can be varied to accommodate the spectrum of settling rates encountered. The appropriate rotational speed is one which balances the forces on a cell such that the cell attains an equilibrium state. When the HARV first begins to rotate, a cell exhibits spiraling motion as a result of Coriolis forces (Gao et al., 1997; Hammond and Hammond, 2001). Coriolis-induced spiraling of a cell is illustrated in Figure 2-7. The Coriolis effect (as observed in the spiraling of a hurricane) is caused by the Earth's rotation; this phenomenon results in the seemingly anomalous appearance of an object following a straight-line path with respect to the inertial reference frame but a curved path with respect to the rotating reference frame.

As long as the particle (cell or microcarrier bead) is less dense than the surrounding medium, it will reach an equilibrium state in which all forces balance. At this time, the particle remains in a fixed point relative to a rotating reference frame. If the particle is more dense than the surrounding medium, however, it will migrate toward the outer wall of the vessel (Gao et al., 1997). This behavior causes collisions with the vessel wall and results in cell damage. It has

been found that the time it takes for a dense particle to reach the vessel wall is affected by the following factors: rotational speed, fluid viscosity, density difference between the particle and the fluid, particle size, and particle position (Gao et al., 1997).

The forces acting on a cell in simulated microgravity once it achieves its equilibrium state are shown in Figure 2-8. These forces include a buoyancy force (F_B), a force due to the weight of the object (W), a centripetal force (F_{Cp}), and a drag force (F_D). The buoyancy force is an upward force on the cell caused by the fluid displaced by the cell. This force has a magnitude of $F_B=\rho gv$, where ρ is the density of the fluid, g is the acceleration due to gravity, and v is the volume of the cell. The force due to the cell's weight is in the direction of gravity and is equal to $W=mg$, where m is the mass of the cell. The centripetal force causes the cell to follow a circular path; this force is always directed toward the center of rotation (perpendicular to motion) and has a magnitude of $F_{Cp}=m\omega^2 r$ where ω is the angular velocity and r is the radius of rotation. The drag force is a result of the fluid's motion relative to the cell; the drag force pulls the cell along in the direction of flow.

Simulated microgravity can also be used to culture adherent cells on either planar discs or microcarrier beads. In these cases, the mechanism of operation is the same as with suspension cells. The above principles of physics can be applied to both adherent cells grown on a substrate and individual suspension cells.

What Constitutes "Simulated Microgravity"?

Upon first inspection, it may appear that rotation forms the crux of the scientific definition of "simulated microgravity". The rotation of the culture vessel causes both constant suspension and the randomization of the gravitational vector. However, constant suspension can be achieved with any rotary culture vessel (for example: stirred bioreactors); therefore, the actual

root of "simulated microgravity" lies in the fact that the culture vessel operates with zero air space. In other words, the fluid entirely fills the chamber and no air bubble is present. This causes the cell to constantly change its spatial orientation with respect to the *stationary reference frame* while remaining fixed with respect to the *rotating reference frame*; consequently, this phenomenon results in randomization of the gravitational vector as shown in Figure 2-9.

There is debate as to whether or not this system should actually be termed "simulated microgravity", as the gravitational force itself has not been minimized (only the *net* gravitational force has been minimized, due to the changing spatial orientation of the cell). Many argue that "rotating wall vessel" is a more accurate nomenclature. However, the Rotary Cell Culture System designed by NASA is currently the best *ground-based model* of "microgravity", and therefore this term is commonly used in practice and is understood by experts in the field. For this reason, this term "simulated microgravity" is used in this project.

Advantages of Simulated Microgravity

For several reasons, the Rotary Cell Culture System effectively mimics *in vivo* conditions[4]. First, the gas exchange system is comparable to the exchange system of the human lung. Specifically, the oxygenator membrane provides a very good analogue to the membrane surrounding the lungs and functions by delivering oxygen while removing carbon dioxide. Likewise, the constant supply of oxygen available in the circulating medium is analogous to the nearly unlimited supply available for diffusion from the blood. Second, without the threat of settling, cells are able to grow three-dimensionally, which increases size and density potential. Third, because the bioreactor lacks impellers, bubbles, or agitators, cell damage is minimized.

[4] Information derived from the Synthecon, Inc. website, www.synthecon.com. Accessed May 2005.

Collisions with the vessel wall are avoided and shear stress is negligible; therefore, a gentle, non-abrasive environment is maintained.

Disadvantage of Simulated Microgravity

The main disadvantage of simulated microgravity is that the existing culture vessels require a large volume of media (at least 10 mL), which makes simulated microgravity research more suitable for culturing anchorage-dependent cells or cells that are available in large quantities. For cells that are rare or difficult to procure (for example: hematopoietic stem cells), it is nearly impossible to obtain a high enough culture concentration to promote growth. In addition, this large volume requirement results in significant material and supply costs.

Effects of Simulated Microgravity on Cells

The effects of simulated microgravity on cells are wide-ranging and diverse, and it is difficult to draw a single conclusion as to how cells will behave in this environment. The performance of cells in simulated microgravity appears to depend on both the type of cell (for example: bone cells versus colon cancer cells versus CD34+ cells) and also on the interaction of the cells with the surrounding environment (for example: suspension cells floating freely in media versus adherent cells seeded onto scaffolds versus tissue-like conglomerations of cells).

Non-CD34+ Cells

Ovarian tumor cells generated in simulated microgravity were shown to be very similar to those generated in vivo in terms of their immunocytochemical, oncogenic and morphologic characteristics; these cultures also demonstrated a high degree of cellular diversification (Goodwin et al., 1997). Likewise, heart cells grown in simulated microgravity in a HARV culture vessel generated a 3-dimensional organization that was ideal for promoting a tissue-like assembly of cardiac cells (Atkins et al., 1997). Furthermore, simulated microgravity has been shown to cause reduced apoptosis and increased differentiation of human colon cancer cells

(Jessup et al., 2000), and to induce colon cancer cells to grow longer and wider than in traditional static culture (Anderson, 2004).

However, simulated microgravity has been shown to negatively affect cells as well. Prostate cancer cells grew more slowly in simulated microgravity as compared to traditional static culture, and differences in cell cycle kinetics and immunostaining became more pronounced (Clejan et al., 1996). In addition, the interleukin-2 signaling pathway was almost completely abrogated in simulated microgravity cultures of peripheral blood mononuclear cells (Licato and Grimm, 1999). Bone cells cultured in simulated microgravity have been shown to demonstrate loss of the mature osteoblast phenotype, disrupted mitochondrial function, and increased apoptosis (Bucaro et al., 2004). Chondrocytes in simulated microgravity at the early phase of chondrogenesis showed very little proliferation and did not differentiate or mineralize (Klement et al., 2004). In heart cells, simulated microgravity reversibly suppressed growth and inhibited the synthesis of interleukin-6, an event that may contribute to growth retardation (Cotrupi et al., 2005). Furthermore, simulated microgravity was shown to interfere with the shuttling of a specific growth factor receptor to the nucleus in leukemic cells, resulting in decreased signaling and enhanced cell death (Vincent et al., 2005). Twenty-four hours of simulated microgravity culture resulted in almost total loss of viability of T-cells and failure of T-cells to activate (Simons et al., 2006).

CD34+ Cells

Studies suggest that a period of *primary* simulated microgravity culture can induce bone marrow CD34+ cells to proliferate and differentiate when placed in *secondary* static culture (Plett et al., 2001). In this study, bone marrow CD34+ cells were first cultured in simulated microgravity and secondarily maintained in static cultures. Results showed that, during the period of primary simulated microgravity culture, cells showed reduced growth as compared to

static controls. Cell cycle analysis confirmed that cells cultured in simulated microgravity exited the G_0/G_1 phase slower than those in static culture. However, it was noted that the differentiation potential upon initiation of secondary static culture was *higher* for cells initially cultured in simulated microgravity. It appears that the simulated microgravity environment helped preserve the more primitive phenotype (by undergoing self-renewal in lieu of differentiation) which resulted in a higher potential for growth in secondary static culture. This discovery lays the foundation for Specific Aims IV and V of the current study. Lui et al. (2006) cultured umbilical cord blood-derived mononuclear cells in a rotating wall vessel fabricated in their laboratory, the Stem Cell and Tissue Engineering Laboratory at Dalian University of Technology. Their system differs from Synthecon's Rotary Cell Culture System in many ways; most significantly, it allows for rotational speeds much lower than those offered by Synthecon Inc.'s system. They showed that, after 200 hours of culture at a speed of 6 rpm, the total number of cells increased over 400-fold and the number of CD34+ cells increased over 32-fold. However, they were unable to grow CD34+ cells in traditional T-flasks and showed that CD34+ cell number decreased daily in static culture and died out completely by day 8. Since many other researchers have successfully cultured CD34+ cells in static culture, this makes the results of Lui et al. questionable. Furthermore, their results are incongruent from those of Plett et al., who stated that stem cells become quiescent in simulated microgravity culture.

As with other types of cells, simulated microgravity has also been shown to have negative effects on CD34+ cells. Savary et al. (2001) generated dendritic cells from peripheral blood CD34+ cells in both simulated microgravity and traditional static cultures. It was shown that dendritic cells from simulated microgravity resulted in poorer yield, decreased function, lower density of the phenotypic cell surface marker Human Leukocytic Antigen (HLA)-DR, and

reduced production of interleukin-12 as compared to those from static cultures. In summary, the simulated microgravity environment had a suppressive effect on both the growth and function of dendritic cells derived from CD34+ cells. In addition, Sytkowski and Davis (2001) showed that erythroid differentiation of CD34+ cells occurred at one-half the rate in the simulated microgravity environment as it did in the traditional static culture environment. Furthermore, Plett et al. (2004) showed that bone marrow CD34+ cells cultured in simulated microgravity demonstrated reduced migration and alterations in cell cycle kinetics resulting in prolonged S-phase. In agreement with the Sytkowski and Davis study, the Plett et al. study showed that CD34+ cells in simulated microgravity favored myeloid differentiation at the expense of erythroid differentiation.

Summary of the Effects of Simulated Microgravity on Cells

In conclusion, simulated microgravity tends to be advantageous for modeling of in vivo conditions (due to the similarity between the gas exchange system of the vessel and that of the human lung, the three-dimensional growth opportunity for cells, the vast supply of oxygen in the circulating medium, and the lack of bubbles or agitation), as well as for studying the interaction of cells and tissues with their environment. It also tends to be valuable for generating 3-dimensional spheroid cultures or for inducing organization of cells at the tissue level. Additionally, it appears to be beneficial for growing cancer cells, and thus for cancer research. On the contrary, simulated microgravity tends to be damaging to cells on an individual level, evidenced by increased apoptosis, disrupted cell signaling, delayed cell cycle kinetics, lower proliferation, and reduced migration. The results from Plett et al., though somewhat of an anomaly, offer immense promise if the results can be replicated with the most promising source of CD34+ cells: umbilical cord blood.

Currently, however, it is difficult to study the effects of simulated microgravity on cord blood-derived CD34+ cells because the cells are only available in small quantities. When placed in the large, volume-demanding HARV, the cells struggle because of the low concentration and lack of interaction with their neighbors. The design and fabrication of a smaller, more economical simulated microgravity culture vessel promises to allow more in-depth study of the effects of microgravity on cord blood stem cells, as well as other cells that are only available in small quantities.

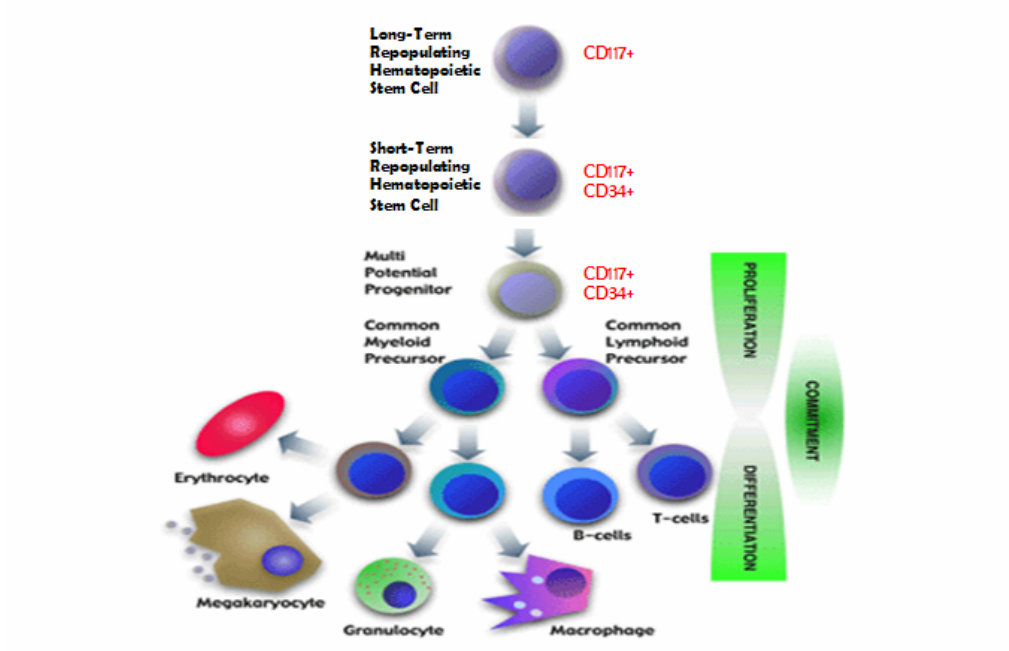

Figure 2-1. Differentiation of a hematopoietic stem cell into the components of whole blood. (Modified from: http://www.mdc-berlin.de/englisch/research/research_areas/e_index2.htm, with permission from Dr. Archim Leutz); Material also incorporated from Chan and Yoder, 2004.

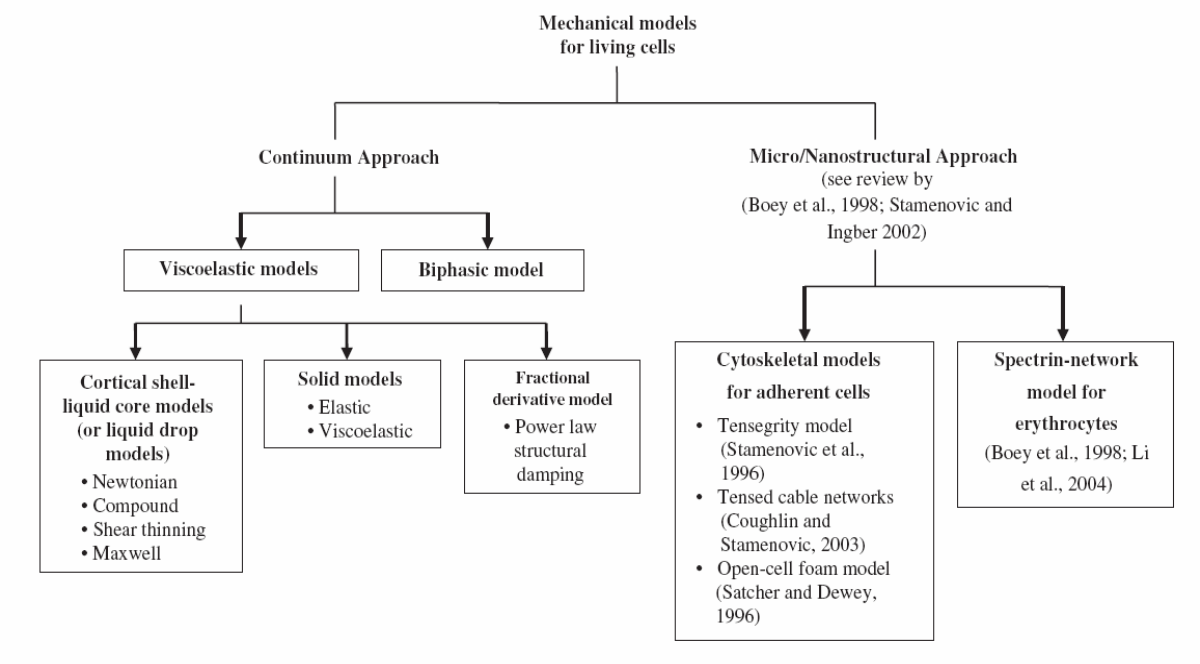

Figure 2-2. Mechanical models of the cell. (Reprinted from: Lim CT, Zhou EH, Quek ST. Mechanical models for living cells – a review. J Biomech 2006;39:198, with permission from Elsevier.)

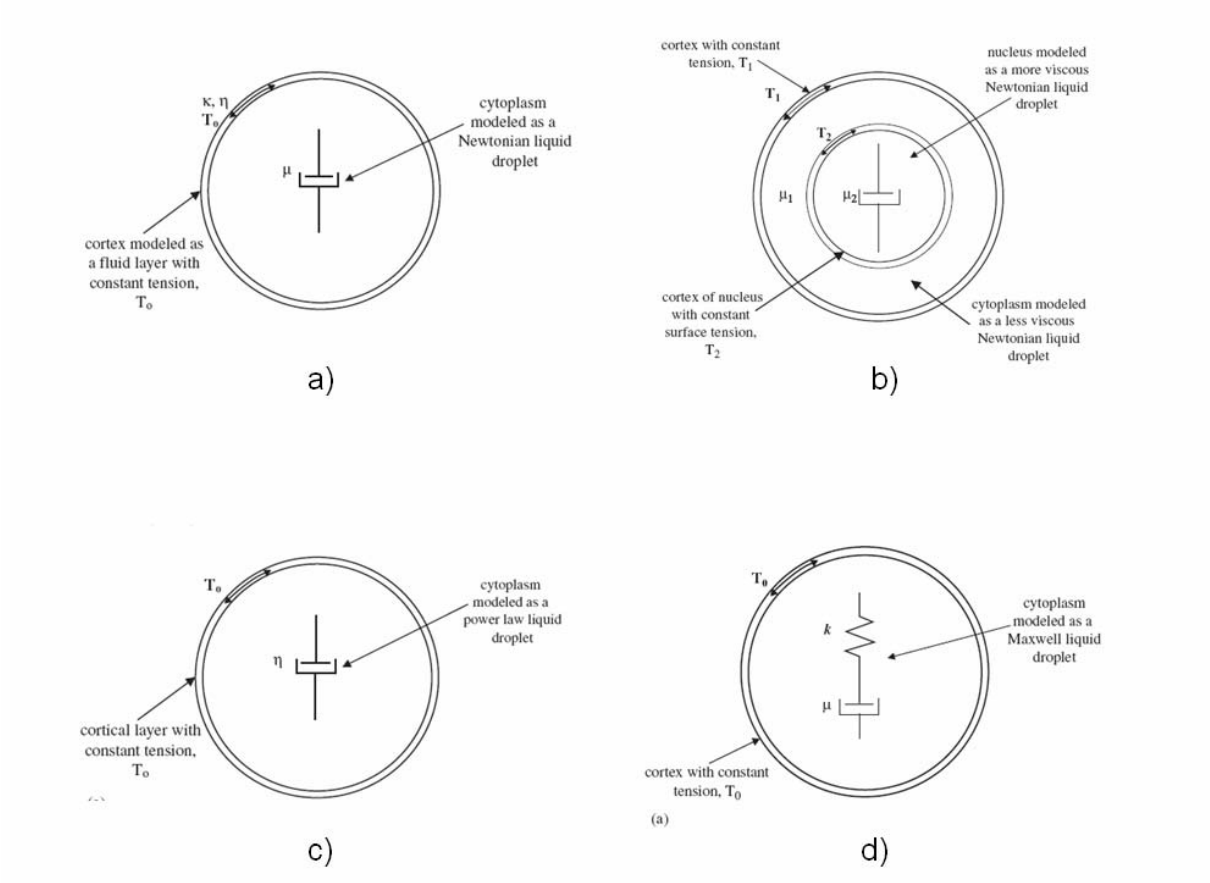

Figure 2-3. Liquid-drop models of the cell. (a) Newtonian liquid drop model. (b) Compound Newtonian liquid drop model. (c) Shear thinning liquid drop model. (d) Maxwell liquid drop model. T = cortical tension, κ = coefficient of viscosity for surface area dilation, η = coefficient of viscosity for shear, μ = viscosity, k = spring constant. (Reprinted from: Lim CT, Zhou EH, Quek ST. Mechanical models for living cells – a review. J Biomech 2006;39:195-216, with permission from Elsevier.)

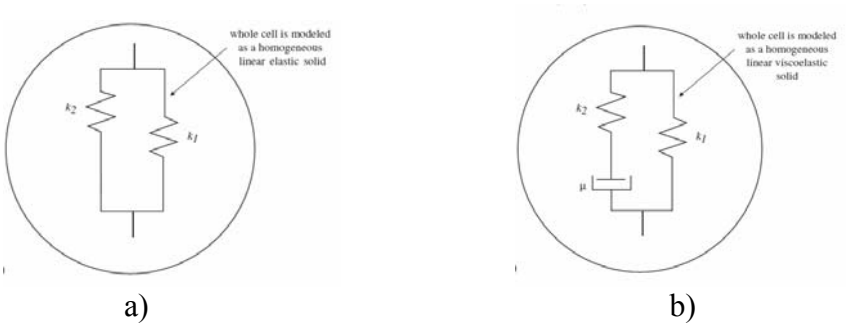

Figure 2-4. Solid models of the cell. (a) Linear elastic solid model. (b) Linear viscoelastic solid model. k = spring constant, μ = viscosity. (Reprinted from: Lim CT, Zhou EH, Quek ST. Mechanical models for living cells – a review. J Biomech 2006;39:195-216, with permission from Elsevier.)

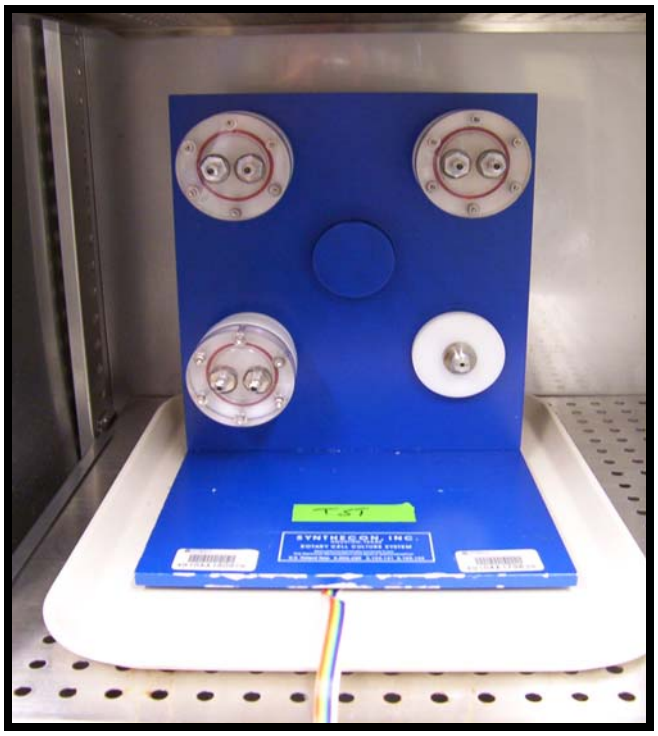

Figure 2-5. Rotary Cell Culture System

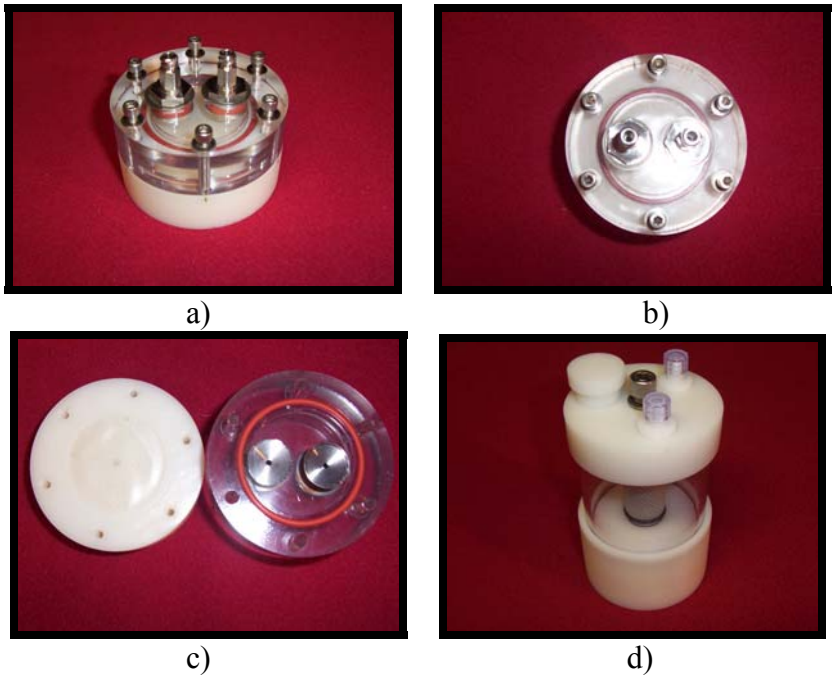

Figure 2-6. Rotary Cell Culture System culture vessels. a) High Aspect Ratio Vessel (HARV). (b) HARV, assembled. Visible surface is the *external* surface of the vessel. (c) HARV, unassembled. Visible surfaces are the *internal* surfaces of the vessel. (d) Slow Turning Lateral Vessel (STLV).

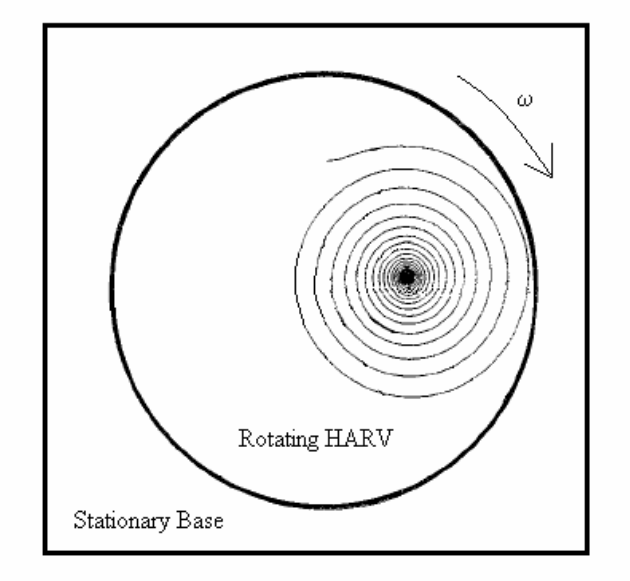

Figure 2-7. Coriolis-induced spiraling of a cell as the HARV first begins to rotate, as seen from the stationary reference frame. As centrifugal forces and Coriolis forces balance, the particle reaches equilibrium. (Modified from: Gao H, Ayyaswamy PS, Ducheyne P. Dynamics of a microcarrier particle in the simulated microgravity environment of a rotating wall vessel. Microgravity Sci Technol 1997;3:154-65, with permission from ZARM Technik Publishing Division.)

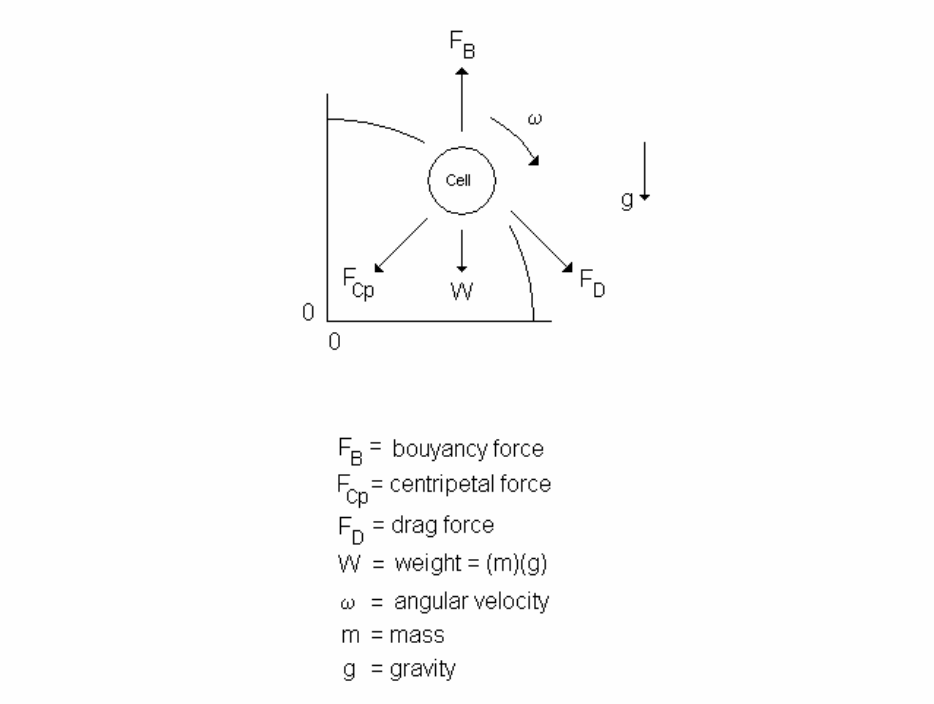

Figure 2-8. Forces acting on a cell at equilibrium in simulated microgravity (as seen from the stationary reference frame.)

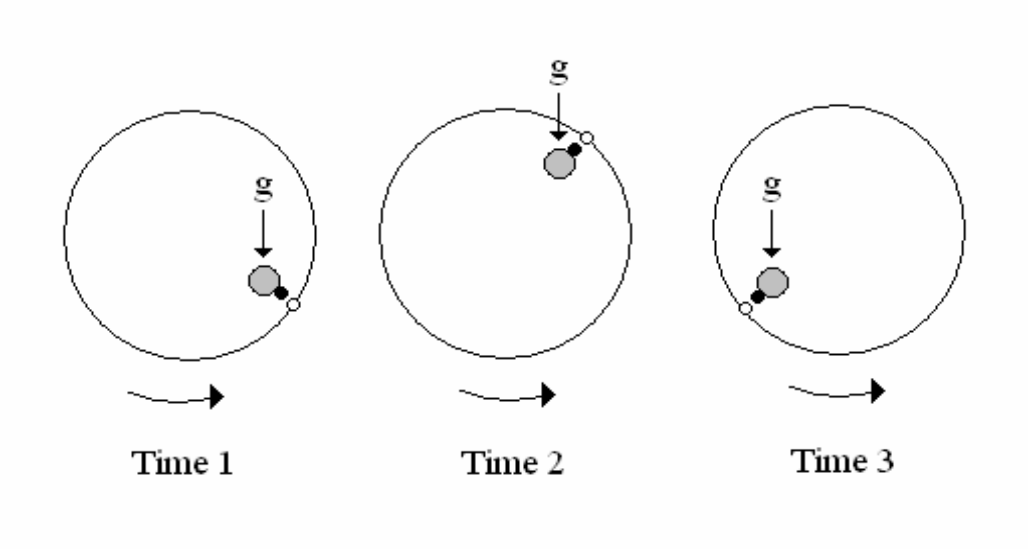

Figure 2-9. Randomization of the gravitational vector in simulated microgravity. The cell is represented by a shaded gray circle. The solid black dot represents a single location on the cell surface. The open dot represents a single location on the culture vessel. With time, the cell changes it's orientation with respect to the stationary reference frame (and hence, the gravitational vector, g), but remains fixed with respect to the rotating reference frame.

CHAPTER 3
MATERIALS AND METHODS

Cell Sources

Hematopoietic stem cells used in this study were derived from neonatal umbilical cord blood. Samples were obtained from the Stem Cell Lab of Shands Hospital at the University of Florida under an approved IRB protocol with written, informed consent. In order for umbilical cord blood samples to be used for research purposes, they were first checked for nucleated cell content by laboratory technologists. Units with fewer than $8x10^8$ nucleated cells were used for research, while units having greater than $8x10^8$ nucleated cells were considered to be bankable for future donation. Umbilical cord blood samples were stored at 4°C and were processed within 36 hours of collection.

Colon carcinoma cells used in this study were derived from the human cell line Caco-2. These cells were obtained as a gift from the University of Illinois at Chicago.

Mononuclear Cell Separation

Mononuclear cells from umbilical cord blood were separated by centrifugation over a buoyant density solution. First, the full volume of blood was diluted in a 1:1 ratio with 1X phosphate buffered saline (PBS) (Sigma-Aldrich, St. Louis, MO). Next, the diluted blood was allocated into 50-mL centrifuge tubes, each with 15 mL of blood carefully layered atop 10 mL of Lymphoprep solution (Axis-Shield, Oslo, Norway). Tubes were centrifuged at 1200 rpms and 25°C for 25 minutes.

The physical-chemical properties of Lymphoprep solution (density of 1.077±0.001 g/mL and osmolality of 290±15 mOsm) cause aggregation of the erythrocytes, resulting in increased sedimentation. Leukocytes, on the other hand, are only moderately affected. The differential sedimentation rates of the constituent parts of blood cause clearly visible layers to form after

centrifugation. When tubes are removed from the centrifuge, erythrocytes form the bottom layer, Lymphoprep solution is visible as the second layer, mononucleated cells form the third layer, and plasma makes up the topmost layer. The mononuclear cell layer was removed by aspiration and washed with PBS in preparation for CD34+ cell separation.

CD34+ Separation

After mononuclear cell separation, CD34+ cells were isolated using the MACS magnetic column separation system developed by Miltenyi Biotec (Auburn, CA). The MACS system utilizes a positive selection technique. CD34+ cells are magnetically labeled using a hapten-conjugated primary monoclonal antibody and an anti-hapten antibody that is incorporated with MACS magnetic MicroBeads. When the magnetically-labeled cells are placed in the field of the MACS magnet, the CD34+ fraction adheres to the separation column while the CD34- fraction passes through, allowing for CD34+ enrichment.

Umbilical cord blood mononuclear cells were suspended in a volume of 300 μL of MACS buffer per 10^8 total cells. MACS buffer is a solution of 1X PBS with 0.5% bovine serum albumin (BSA) and 0.4% 0.5 M ethylene diamine tetra-acetic acid (EDTA). One hundred microliters of FcR Blocking Reagent were added per 10^8 cells, followed by 100 μL of Hapten-Antibody per 10^8 cells; mixture was incubated at 4°C for 15 minutes. The Blocking Reagent binds to certain receptors on nucleated cells, inhibiting non-specific binding of the MicroBeads. Next, cells were washed by addition of buffer followed by centrifugation and removal of the supernatant. The cell pellet was then resuspended to a volume of 400 μL per 10^8 total cells. One hundred microliters of Anti-Hapten MicroBeads were added per 10^8 cells and the mixture was incubated at 4°C for 15 minutes. Finally, cells were washed and resuspended in 500 μL buffer per 10^8 total cells in preparation to be run through the magnetic columns.

One MACS LS column was placed on the MACS magnet and rinsed with buffer. The cell solution was applied to the column; the column was subsequently rinsed 3 times with 3 mL buffer, allowing the CD34- fraction to pass through. The column was then removed from the magnet and placed on a clean 15 mL centrifuge tube, filled with 5 mL buffer, and the CD34+ fraction was eluted using the accompanying plunger. Magnetic separation was repeated twice to obtain a final CD34+ purity of 85 to 98%.

Cell Counting

To assess cell number and cell viability, cell counts were performed using microscopy. Depending on the hypothesized cell number, a 1:2 or 1:10 dilution of cell solution to 0.4% Trypan Blue Stain (Fisher Scientific, USA) was prepared. After significant mixing, 10 μL of this mixture was carefully loaded into a Bright Line (Hausser Scientific, Horsham, PA) hemacytometer channel and viewed using an inverted light microscope with 20X objective and 10X ocular eyepiece. Total cell counts and cell viability were recorded. Because Trypan Blue Stain is only able to permeate the ruptured membranes of dead and dying cells, healthy cells appeared translucent blue under the microscope while dead or dying cells appeared opaque blue. This technique was used for both hematopoietic stem cells and colon carcinoma cells.

Flow Cytometry

CD34+ cell viability and CD34+ purity were assessed using flow cytometry. Flow cytometry measures the properties of laser light-scattering and fluorescence emission of cells. By plotting these results on a bivariate graph, cells within a certain region are able to be identified on the basis of morphology and level of emission with a relatively high degree of confidence.

All labeling reagents were obtained from Becton Dickinson (San Diego, CA). Two aliquots of $1x10^6$ cells each were pulled from the general population and placed in separate vials

for labeling. One of these samples of cells served as the test subject while the other served as the control. Cells in each vial were washed and resuspended with 90 µL of staining buffer (1X PBS supplemented with 0.5% BSA and 0.01% sodium azide), followed by addition of 10 µL of 10% human AB serum to block non-specific binding (performing the same role as the FcR Blocking Reagent used during CD34+ separation). Next, vials were incubated for 20 minutes at 4°C.

Following incubation, 20 µL of CD34 phycoerythrin (PE)-conjugated antibody were added to the test subject, while 20 µL of an isotype matched control, IgG_1 Control PE-conjugated antibody, were added to the control vial. (As per the instructions of the CD34+ separation system manufacturer (Miltenyi Biotech, Auburn, CA), these antibodies recognized an epitope different from that recognized by the CD34 monoclonal antibody used in the purification step.) The control antibody possesses the same non-specific binding properties as the CD34-specific antibody, yet exhibits no specificity for the CD34 antigen. Its main purpose is to set the level of background fluorescence emission inherent to cells from a certain sample; cells that emit a level of fluorescence above this threshold are therefore likely to be CD34+. The vials were once again incubated for 20 minutes at 4°C.

Cells were then washed two times and resuspended with 100 µL of staining buffer and 20 µL of Via-Probe fluorescein isothiocyanate (FITC)-conjugated antibody for viability testing, followed by incubation for 10 minutes at 4°C. Via-Probe stain contains a nucleic acid dye which binds to the DNA of dead cells by penetrating their membrane. Finally, 880 µL of staining buffer were added to achieve a final workable volume of 1 mL. Samples were then run on a FACScan flow cytometer and analyzed using CellQuest software to produce plots depicting cell viability and CD34+ cell purity.

Conventional Cell Culture

The term "conventional cell culture" refers to cells cultured in the traditional static manner, in either 24-well plates or T-25 flasks in an incubator.

Hematopoietic Stem Cells

Conventional culture of CD34+ cells was initiated in 24-well plates. Cells were plated at a concentration in the range of $8x10^4$ to $4x10^5$ CD34+ cells/mL, as determined by preliminary experiments to promote satisfactory growth. Cells were grown in Iscove's Modified Dulbecco's Medium (IMDM) (GIBCO, Long Island, NY), supplemented with 10% fetal bovine serum (FBS), 5 ng/mL thrombopoietin (TPO), and 50 ng/mL *flt*-3 ligand (FL). All growth factors were obtained from PeproTech, Inc. (Rocky Hill, NJ). Cultures were incubated at 37°C in 100% humidity and 5% CO_2. At intervals of 3-4 days, cultures were re-supplemented with fresh growth factors. Cultures were maintained for 7-14 days.

Colon Carcinoma Cells

Conventional culture of Caco-2 cells was initiated in non-coated T-25 flasks (Fisher Scientific, USA). Cells were grown in media consisting of 40% Dulbecco's Modified Eagle's Medium (DMEM), 40% Ham's Nutrient Mixture F-12, and 20% FBS. All media components were obtained from Fisher Scientific (USA). Cultures were incubated at 37°C in 100% humidity and 5% CO_2. At intervals of 3-4 days, depleted media was removed and replaced with fresh media. Cells were split every 6-7 days, or when they reached approximately 80% confluence. At this time, cells were washed once with Hank's Balanced Salt Solution (HBSS) (Fisher Scientific, USA) and induced to detach with 0.25% trypsin/EDTA (Fisher Scientific, USA). Once they detached, half of the solution was transferred to a clean T-25 flask and fresh media was added to both flasks.

Progenitor Cell Culture

Progenitor cell assays were performed in duplicate. CD34+ cells were added to 1.1 mL of MethoCult 4434 methylcellulose media (StemCell Technologies, British Columbia, Canada) at a concentration of 1,375 CD34+ cells/mL as specified by the manufacturer, and transferred to 35-mm Corning culture dishes (Corning, NY). The two 35-mm culture dishes were placed within a 100-mm Corning culture dish, along with an additional (uncapped) 35-mm culture dish filled with sterile water to provide humidity. Cultures were incubated for 14 days.

The media used in these assays is specialized for detection of colony-forming units--granulocyte/macrophage (CFU-GM), burst-forming units--erythroid (BFU-E), colony-forming units--erythroid (CFU-E), and colony-forming units--granulocyte/erythrocyte/monocyte/megakaryocyte (CFU-GEMM). CFU-E and CFU-GEMM colonies make only a minor contribution to the total number of colonies and consequently were not enumerated in this study. For example, less than 4% of progenitor colonies generated by cord blood are CFU-E, and less than 10% are CFU-GEMM[5]. Furthermore, these additional colonies are not as visually distinctive as CFU-GM and BFU-E, and their enumeration can be subject to classification error. Therefore, only CFU-GM and BFU-E were of interest in this study.

Progenitor Colony Enumeration

After 14 days of incubation, cultures were enumerated for CFU-GM and BFU-E using a Nikon TMS inverted light microscope (Nikon, USA) with 4X objective and 10X ocular eyepiece. Each culture dish was scanned twice and the colony counts from each scan were averaged to determine the total number of colonies of each type.

[5] Information is derived from "Human Colony-Forming Cell Assays Using MethoCult," Technical Manual, October 2004

BFU-E are characterized by growth in clusters. As it can sometimes be difficult to distinguish between multiple colonies and a single colony with multiple clusters, a counting scheme must be used to maintain consistency. Therefore, in circumstances where the distance between adjacent clusters was less than half the diameter of the individual clusters, the colony was recorded as one single colony with multiple clusters. If the distance between adjacent clusters was greater than half the diameter of the individual clusters, the clusters were recorded as separate colonies.

Micropipette Experiments

Glass capillary tubes (1.0 mm x 0.5 mm, 4") were pulled on a Narishige model PB-7 pipette puller (Narishige Company, Ltd., Tokyo, Japan) to create micropipettes of a desired diameter. Micropipettes used for fresh cell experiments had an average inner diameter of 6.6 μm, and micropipettes used for cultured cell experiments had an average diameter of 7.8 μm. (Cultured cells were found to be 10 to 20% larger than fresh cells; therefore, micropipette diameters were scaled according.)

CD34+ cells were suspended in PBS in a clear chamber which was affixed atop of the stage of an Axiovert 100 inverted light microscope (Carl Zeiss Microimaging, Germany). The proximal end of the micropipette was inserted into the cell chamber; the distal end of the micropipette was connected to two coupled water reservoirs in order to provide hydrostatic pressure control. Individual cells were aspirated under constant pressure until the cell was located fully inside the micropipette (Figure 3-1a).

The cell was held in place inside of the micropipette for 10 seconds, and then expelled. After expulsion, the cell was observed until it fully recovered its original, undeformed shape (Figure 3-1b). An attached video system was used to record each experiment, and the Adobe Premiere 6.0 program (Adobe Systems Incorporated, San Jose, CA) was used to create still

frames at regular time intervals from the recorded experiments. From the still frames, a variety of different dimensions were recorded (Figure 3-2).

Rheological Analysis

During aspiration experiments, the leading edge of the cell within the micropipette was tracked as a function of time (Figure 3-1a). From this data, a plot of L_p (the length of the cell inside the micropipette) versus time was generated (Figure 3-3). Viscosity (μ) values (in units of Pa•s) were determined by the following equation (Needham and Hochmuth, 1990).

$$\mu = \frac{(\Delta P) D_p}{2(dL_p / dt) m \left(1 - \frac{1}{\overline{D}}\right)} \qquad (3\text{-}1)$$

In the above equation, ΔP is the pressure (in Pascal) as indicated by the height difference between the water reservoirs, D_p is the diameter of the micropipette (in meters), dL_p/dt is the slope of the linear portion of the aspiration curve (in meters/second), $\overline{D} = D_{out}/D_p$, and D_{out} is the diameter of the portion of the cell outside of the pipette (in meters). The constant $m \approx 6$, and is proportional to the ratio of surface dissipation in the cortex to the dissipation in the cytoplasm, discovered empirically by Evans and Yeung (1989).

During recovery experiments, the length of the major axis of the recovering cell was monitored as a function of time (Figure 3-1b and Figure 3-4). The equation below governs this relationship for white blood cells (Tran-Son-Tay et al., 1991).

$$\frac{L}{D_0} = \frac{L_i}{D_0} + A\bar{t} + B(\bar{t})^2 + C(\bar{t})^3 \qquad (3\text{-}2)$$

In the above equation, L is the length of the major axis of the recovering cell (in meters), D_0 is the diameter of the resting cell (in meters), L_i is the length of the cell when completely inside the

micropipette (in meters), A, B, and C are known function of (L_i/D_0) as defined previously (Tran-Son-Tay et al., 1991), and $\bar{t}$ is a dimensionless time defined by:

$$\bar{t} = \frac{2t(T_0)}{\mu(D_0)} \tag{3-3}$$

In the above equation, t is time in units of seconds and T_0 is cortical tension in units of Newton/meter. By substituting Equation 3-3 into Equation 3-2 and rearranging the terms, the following cubic equation is obtained, which can be solved for cortical tension (T_0).

$$0 = \frac{L_i}{D_0} + A\left(\frac{2tT_0}{\mu D_0}\right) + B\left(\frac{4t^2T_0^2}{\mu^2 D_0^2}\right) + C\left(\frac{8t^3T_0^3}{\mu^3 D_0^3}\right) - \frac{L}{D_0} \tag{3-4}$$

As described in Chapter 2: Background, cortical tension can also be calculated based on a derivation of the Law of Laplace. This method was used in addition to Equation 3-4 in order to compare values obtained by each method. This second method is more straightforward and uses the following equation (Zhelev et al., 1994):

$$\Delta P = 2T_0\left(\frac{1}{R_p} - \frac{1}{R_{out}}\right) \tag{3-5}$$

In the above equation, R_p is the radius of the micropipette (in meters) and R_{out} is the radius of the portion of the cell outside of the micropipette (in meters).

Design of Simulated Microgravity Cell Culture Chamber

The HARV was chosen as the culture vessel of interest (as opposed to the STLV) because it is more conducive to modification; the HARV lacks an oxygenator core and therefore it is possible to design a cell culture insert with a centrally-located culture chamber.

The simulated microgravity cell culture chamber was designed to fit snugly into the HARV's inner chamber, which dictated that it have a thickness of 0.6 cm and a diameter of 4.3 cm. It was designed to have a central well with a depth of 0.5 cm and a diameter of 1.7 cm

(Figure 3-5). The dimensions of the central well were chosen to model the size of one well of a 24-well plate; consequently, this allows for an appropriate static control. Furthermore, when culturing cells in simulated microgravity it is imperative that static controls and experimental microgravity cells are cultured at the same ratio of "surface area available for oxygenation" to "volume of cell suspension" so that both populations of cells have equal opportunity for oxygen exposure. The cell culture chamber designed in the present study allows for this uniformity. The chamber also has a built-in O-ring that is offset from the central well by 0.4 cm to promote a tight seal and prevent fluid from exiting the well.

The volume requirement of this novel cell culture chamber is approximately 1 mL, which is only 1/10 of the requirement of the unmodified HARV. This significantly reduces supply costs and allows cells to be cultured at a higher concentration. Since the center of rotation of the culture chamber coincides with the center of rotation of the HARV, the physics of simulated microgravity are not altered by implementation of this cell culture insert.

Fabrication of Simulated Microgravity Cell Culture Chamber

The simulated microgravity cell culture chamber was built based on a rapid prototyping technique that was developed in order to sort cells (Gill, 2003) and to study the effects of surface roughness of cell spreading (Branham et al., 2002).

The mold for fabrication of the cell culture chamber (Figure 3-6 and Figure 3-7) was constructed of stainless steel and was manufactured in a machine shop utilizing a lathe and a milling machine. It consists of a "base" and a "ring". After construction, a mirror finish was achieved by polishing all critical surfaces of the base (Figure 3-6) with size-600 sandpaper, followed by further polishing using a series of 15-μm, 5-μm, 1-μm, and 0.3-μm graduated aluminum oxide particles in a water-based slurry. This process resulted in a high degree of optical clarity in the final molded prototype, which was necessary in order to ensure a uniform

topography. The ring (Figure 3-7) was machined from aluminum stock. This ring is removable and is attached to the base by 4 screws.

The cell culture chamber was constructed of polydimethylsiloxane (PDMS), which is a clear, biocompatible, biochemically inert, silicone elastomer. PDMS was made by blending Sylgard 184 elastomer and the corresponding curing agent (Dow Corning Corporation, Midland, MI) in a 9:1 ratio. Bubbles that formed during the mixing process were removed by allowing the mixture to sit under vacuum for 15-20 minutes. To create the cell culture chamber, the PDMS mixture was poured into the mold and left to cure for 48 hours. After curing, the PDMS portion was carefully detached from the mold by first removing the ring and then slowly peeling the cured polymer from the base (Figure 3-8).

Simulated Microgravity Cell Culture

The term "simulated microgravity cell culture" refers to cells cultured in an incubator in the Rotary Cell Culture System using the "as-is" (unmodified with the aforementioned cell culture chamber) HARV.

Hematopoietic Stem Cells

Simulated microgravity cultures were initiated at identical cell number/volume/unit of oxygenation surface area as those grown in conventional static culture. Likewise, simulated microgravity cultures were grown using media and growth factors that were identical to their static counterparts.

To load the HARV, the top and bottom portions were screwed together. A sterile stopcock (Mallinckrodt Critical Care, Glens Falls, NY) was added to each port, and both were turned to the "open" position. The cell solution (containing cells, media, and growth factors) was prepared in a 15-mL centrifuge tube, and then 10 mL of solution was carefully injected into the HARV using a 12-cc syringe via one of the external ports. A second 12-cc syringe was

placed on the second port, and air was simultaneously removed as the cell solution was injected, until the HARV was completely filled with media and no air space was present. The stopcocks were turned to the "closed" position, capped, and the HARV was then attached to the RCCS base and rotated at 8 rpms, as suggested by the manufacturer for lymphoid suspension cells.

Cultures were maintained at 37°C in 100% humidity and 5% CO_2. At intervals of 24 hours, simulated microgravity cultures were de-bubbled to remove waste. In order to de-bubble the HARV, a 12-cc syringe partially filled with fresh media was applied to one of the ports, while an empty syringe was applied to the other. Once again, the air bubble was slowly pulled into the empty syringe while media was simultaneously added from the other syringe, until the bubble was completely removed. Cultures were maintained for up to 4 days.

Colon Carcinoma Cells

Caco-2 cells in simulated microgravity were cultured on planar discs. Planar discs were fabricated from Thermanox plastic cover slips (Nalge Nunc International, Rochester, NY) using a standard ¼" hole punch. Discs were sterilized by soaking in ethanol and sitting under UV light overnight. After sterilization, three discs were placed in each well of a 24-well plate. Caco-2 cells (previously grown in T-25 flasks in conventional static culture, see above) were trypsinized, and cells were added to the well at a concentration of 60,000 cells/cm^2. Media was added and the well plate was placed back in the incubator; cells were allowed to re-attach for 24 hours.

After 24 hours, the well plate was removed from the incubator and excess media was aspirated off. A single disc was placed atop the oxygenator membrane of the HARV, the top and bottom portions were screwed together, and 10 mL of media supplemented with 2000 kDa molecular weight dextran (Sigma-Aldrich, St. Louis, MO) was added via the port until the air space was no longer visible. The dextran was used to increase the viscosity of the media so that

the planar disc would remain suspended. To do this, 1 g of dextran was reconstituted in 10 mL of sterile water and autoclaved. Then, 8 mL of media was supplemented with 2 mL of the dextran solution to achieve the 10 mL HARV volume requirement. The rotational speed was adjusted until the planar disc reached an equilibrium position and remained suspended in the vessel; this occurred at 10 rpms. Cultures were de-bubbled after 24 hours and maintained for 48 hours.

Static controls for Caco-2 simulated microgravity cultures consisted of Thermanox discs cultured in a static environment in a 24-well plate for 48 hours. The media used was identical to that used in simulated microgravity; as above, media was supplemented with 2000 kDa molecular weight dextran.

Cell Culture in Simulated Microgravity Cell Culture Chamber

To culture cells in simulated microgravity using the cell culture chamber, the chamber was placed in the HARV with the cavity side facing the oxygenator membrane. In order to ensure that cells in the culture vessel were exposed to the same centripetal acceleration as cells in the unmodified HARV, rpms were converted to g-forces. Rpms are an arbitrary measurement in which the radius of the vessel is not taken into account. G-forces, on the other hand, are an unbiased indicator of the forces felt by the cells, because the radius of the vessel is factored in. Reporting data using g-forces allows reproducibility between different researchers using different experimental systems. Therefore, the following calculations were performed. Centripetal acceleration is related to angular velocity by the following formula.

$$a = \omega^2 r \qquad (3\text{-}6)$$

In order to convert from rotations/minute to angular velocity in units of radians/second, the following conversion must be used.

$$\omega = \frac{(rpm)(2)(\Pi)}{60} \tag{3-7}$$

Finally, by substituting Equation 3-7 into Equation 3-6, accounting for the fact that acceleration due to gravity is equal to 9.81 m/s^2 and simplifying, the following equation is obtained.

$$g - force = \frac{(rpm)^2(\Pi)^2(r)}{(8829)} \tag{3-8}$$

Hematopoietic Stem Cells

To culture CD34+ cells in the cell culture chamber, 1.1 mL of cell suspension was added to the well. At this volume, the well was completely filled and a meniscus formed. Then, the top part of the HARV was attached, and the HARV was affixed to the RCCS.

By using Equation 3-8 above, it was found that the 8-rpm rotational speed used when culturing cells in the "as-is" HARV is equivalent to 0.0015 g-forces, which corresponds to a rotational speed of 12.6 rpms. In other words, CD34+ cells cultured in the "as-is" HARV at 8 rpms will feel the same average centripetal acceleration as CD34+ cells cultured in the cell culture chamber at 12.6 rpms. The media, cell concentration, and duration of culture remained the same as specified above with the "as-is" HARV.

Colon Carcinoma Cells

To culture Caco-2 cells in the cell culture chamber, the planar disc was placed in the well, and 1.1 mL of media supplemented with 2000 kDa dextran was added. Then, the top part of the HARV was attached, and the HARV was affixed to the RCCS.

By using Equation 3-8 above, it was found that the 10-rpm rotational speed used when culturing cells in the "as-is" HARV is equivalent to 0.0024 g-forces, which corresponds to a rotational speed of 15.9 rpms. In other words, Caco-2 cells cultured in the "as-is" HARV at 10

rpms will feel the same average centripetal acceleration as Caco-2 cells cultured in the cell culture chamber at 15.9 rpms. The media, cell concentration, and duration of culture remained the same as specified above with the "as-is" HARV.

Reporting G-Forces

It is important to mention that not every cell in a rotating vessel feels the same g–force. Rather, the g-force felt by each cell is a function of its distance from the center of the vessel. For example, the value of 0.0015 g-forces for HSCs is a maximum force felt by a cell rotating at the largest possible orbit. The g-forces felt by the HSCs vary linearly from 0 (for cells at the center of the vessel) to 0.0015 g-forces (for cells at the outermost orbit). This is why it is more appropriate to report g-forces felt by the cells in terms of the "average" force. Equation 3-9 shows how to calculate the average g-force felt by cells in a specific environment.

$$g - force_{average} = \frac{(g - force_{\max}) + (g - force_{\min})}{2} \qquad (3\text{-}9)$$

Fixing/Staining/Mounting of Colon Carcinoma Cells

After 48 hours of culture, each disc was transferred to a clean well of a 24-well plate. Cells were fixed with 4% paraformaldehyde for 20 minutes and then rinsed 3 times with PBS. Next, cells were stained with Harris' hematoxylin (Fisher Scientific, USA) for 1 minute. Hematoxylin stains the cell's nucleus and nucleolus blue. The cells were subsequently washed with tap water, which acts as a bluing agent. Then, cells were stained with eosin (Fisher Scientific, USA) for 1 minute. Eosin stains the cell's protein portion pink. Last, cells were dipped 15 times into 95% ethanol. Finally, the discs were mounted onto a glass slide; a cover slip was attached using a glycerol/gelatin mounting agent.

Morphological Measurements of Colon Carcinoma Cells

Planar discs were viewed using a National DC3-163 digital microscope (National Optical, San Antonio, TX) with attached camera. The Motic Images 2000 1.3 program (Motic Incorporation, Ltd., Causeway Bay, Hong Kong) was used to measure the length and width of 10 representative cells from each disc. Cells were viewed using a 10X objective and 10X ocular eyepiece.

Sterilization Procedures

All work was performed in a cell culture hood, and gloves were worn at all times. Working surfaces were wiped down with a solution of 10% bleach and/or 70% ethanol before and after use. Solutions made in the lab were vacuum filtered before use. All supplies were either packaged as sterile or were autoclaved prior to use. Before and after use, the HARV was disassembled, soaked and gently scrubbed in a soap and water solution, reassembled, wrapped in aluminum foil, and autoclaved. Discarded biomaterials were treated with bleach before being placed in a biohazard receptacle.

Statistics

Student's t-tests were used to determine significance between data sets. Differences were taken to be significant at the $p \leq 0.05$ level.

Technical Approach to Specific Aims

The sections below detail the approaches which were used to accomplish each of the Specific Aims set forth in Chapter 1.

Approach to Specific Aim 1

Specific Aim 1 was to "Quantify the rheological properties of fresh and cultured cord blood stem cells and determine how these properties differ." To accomplish this, aspiration and recovery experiments were performed on fresh cells (pulled from the CD34+ fraction on day 0)

and cultured cells (grown for 1 week and then re-purified for the CD34 antigen). Experiments were performed using three different cord blood units, and a total of 10 fresh and 10 cultured cells were studied from each unit. Therefore, data was gathered on a total of n=30 fresh cells and n=30 cultured cells. Viscosity and cortical tension values were determined for cells from each population; values for each population were then averaged and analyzed to determine whether a significant difference existed.

Approach to Specific Aim 2

Specific Aim 2 was to "Study how the differentiation (colony generation) capability of cord blood-derived hematopoietic stem cells is affected by culture." To accomplish this, progenitor assays were performed on fresh cells (pulled from the CD34+ fraction on day 0) and cultured cells (grown for 1 week and then re-purified for the CD34 antigen). Fresh cell and cultured cell progenitor assays were initiated at identical CD34+ cell concentrations. Experiments were performed on cells from five different cord blood units. From each unit, culture dishes were plated in duplicate with fresh cells and in duplicate with cultured cells; the counts from the two duplicate plates were then averaged to minimize experimental error, as per the manufacturer's instructions. Therefore, data was gathered on a total of n=5 fresh cord blood samples and n=5 cultured cord blood samples. The CFU-GM and BFU-E counts from each population of cells were averaged and analyzed to determine whether a significant difference existed.

Approach to Specific Aim 3

Specific Aim 3 was to "Design a novel, economical cell culture facility to reduce the volumetric requirements of current simulated microgravity research and validate the effectiveness of this device using a "control" cell line (human colon carcinoma cells)." A culture vessel was designed and fabricated as described above. In order to test the effectiveness of this

device, it was imperative that a cell line be chosen that has been demonstrated to be positively (for example: cell growth as opposed to cell death), measurably, and significantly affected by microgravity. Consequently, the Caco-2 cell line was chosen; these cells have been shown to grow significantly longer and wider in microgravity (Anderson, 2004). In addition, the cells are readily available and the cost of maintaining them in culture is minimal. For these reasons, Caco-2 cells served as an appropriate experimental control.

Caco-2 cultures were initiated in both the "as-is" HARV and the HARV fitted with the cell culture chamber to determine whether the effects of microgravity were maintained in the culture chamber, and to verify that the culture chamber did not provide an environment that was detrimental to the cells. Viability staining and cell morphological measurements were performed on cells from both environments to determine whether a significant difference existed. Data was gathered on 10 cells from each of 3 discs from each environment, for a total of n=30 cells cultured in the "as-is" HARV and n=30 cells cultured in the cell culture chamber.

Approach to Specific Aim 4

Specific Aim 4 was to "Observe the short-term effects of simulated microgravity on cord blood stem cells (via primary simulated microgravity culture)." To accomplish this, CD34+ cells were cultured in simulated microgravity in either the "as-is" HARV or the cell culture chamber for up to four days. CD34+ cell number, nucleated cell number, cell viability, and percent CD34+ purity were assessed to determine the effects of simulated microgravity on cord blood–derived CD34+ cells. "Short-term" denotes the time period during which the cells were actually exposed to microgravity (neglecting the behavior of the cells once they were returned to static culture, which was the focus of Specific Aim 5). The control for these experiments consisted of CD34+ cells cultured for the same duration in static culture in 24-well plates.

Approach to Specific Aim 5

Specific Aim 5 was to "Observe the long-term effects of simulated microgravity by investigating the behavior of cord blood stem cells in secondary (a.) static culture, and (b.) progenitor culture." To accomplish this, cells that were primarily cultured in simulated microgravity were placed into secondary static culture. "Long-term" denotes the lasting effects of simulated microgravity on the cells, which persisted even after the cells were returned to static culture. Cells in secondary culture were assessed for CD34+ cell number, nucleated cell number, cell viability, percent CD34+ purity, and ability to generate colonies in progenitor assays. The control for these experiments consisted for CD34+ cells cultured in static culture for the entire duration.

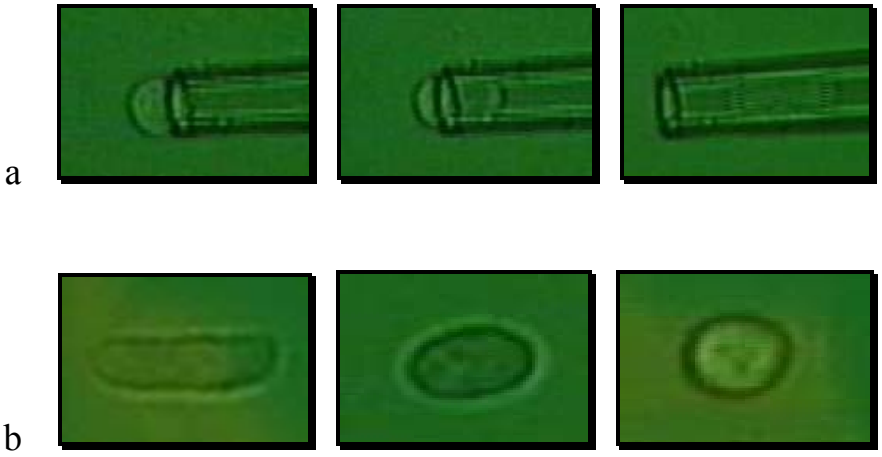

Figure 3-1. Typical aspiration and recovery experiment, shown at different time points (33X objective and 10X ocular eyepiece). a) A 10.7-µm CD34+ cell is aspirated into an 8.0-µm pipette. b) Following expulsion from the micropipette, the CD34+ cell recovers its original, undeformed shape. (Reprinted from: Watts KL, Reddy V, Tran-Son-Tay R. The effects of ex vivo expansion on the rheology of umbilical cord blood-derived CD34+ cells. Journal of Stem Cells 2007;2(1), with permission from Nova Science Publishers.)

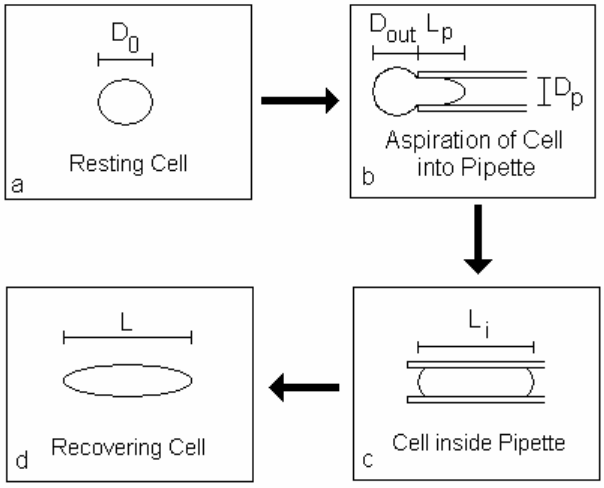

Figure 3-2. Aspiration (a, b) and recovery (c, d) experiment, showing the dimensions of interest. D_0 = resting diameter of the cell, D_{out} = diameter of the cell outside the micropipette, L_p = length of the cell inside the micropipette, D_p = diameter of the micropipette, L_i = length of the cell when completely inside the micropipette, L= length of the major axis of the recovering cell. (Reprinted from: Watts KL, Reddy V, Tran-Son-Tay R. The effects of ex vivo expansion on the rheology of umbilical cord blood-derived CD34+ cells. Journal of Stem Cells 2007;2(1), with permission from Nova Science Publishers.)

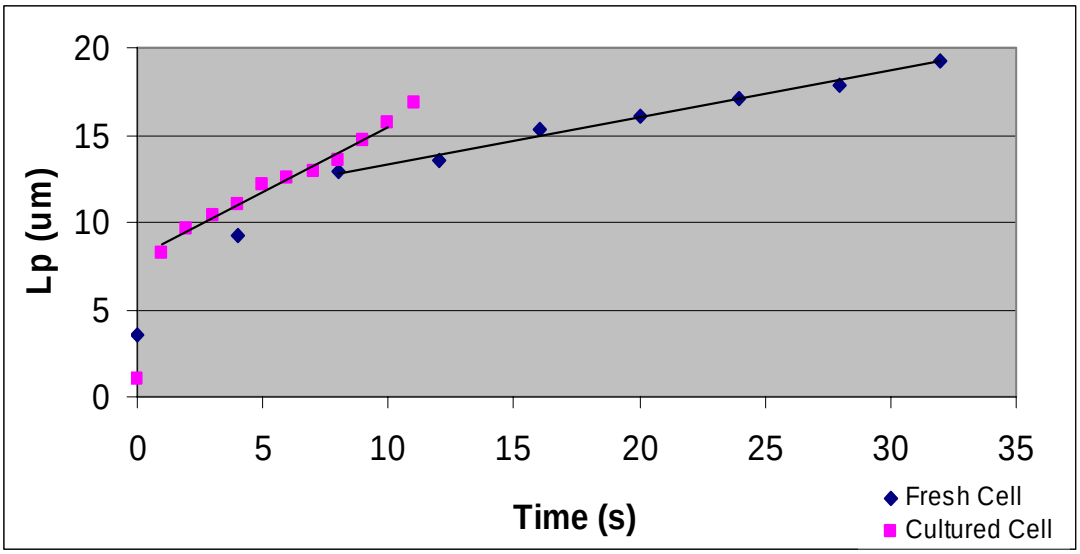

Figure 3-3. Typical aspiration curves for a fresh CD34+ cell and a cultured CD34+ cell. The cultured CD34+ cell takes much less time to be aspirated into the micropipette, which results in a higher dL_p/dt value. L_p= length of the cell inside the micropipette. (Reprinted from: Watts KL, Reddy V, Tran-Son-Tay R. The effects of ex vivo expansion on the rheology of umbilical cord blood-derived CD34+ cells. Journal of Stem Cells 2007;2(1), with permission from Nova Science Publishers.)

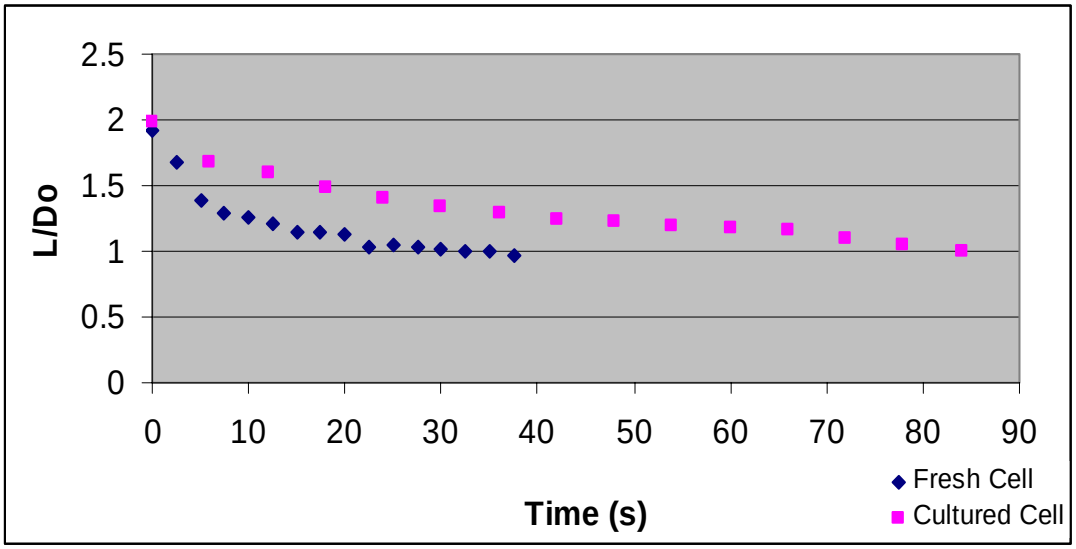

Figure 3-4. Typical recovery curves for a fresh CD34+ cell and a cultured CD34+ cell. The cultured CD34+ cell takes much longer to recover its original, undeformed shape following expulsion from the micropipette. L=length of the major axis of the recovering cell, D_0=diameter of the resting cell. (Reprinted from: Watts KL, Reddy V, Tran-Son-Tay R. The effects of ex vivo expansion on the rheology of umbilical cord blood-derived CD34+ cells. Journal of Stem Cells 2007;2(1), with permission from Nova Science Publishers.)

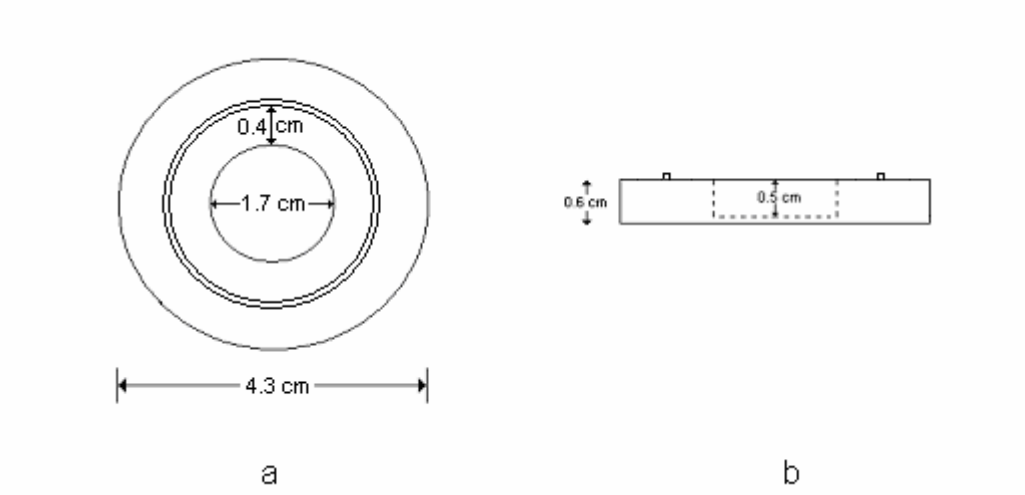

Figure 3-5. Design of simulated microgravity cell culture chamber. a) Top view. b) Side view.

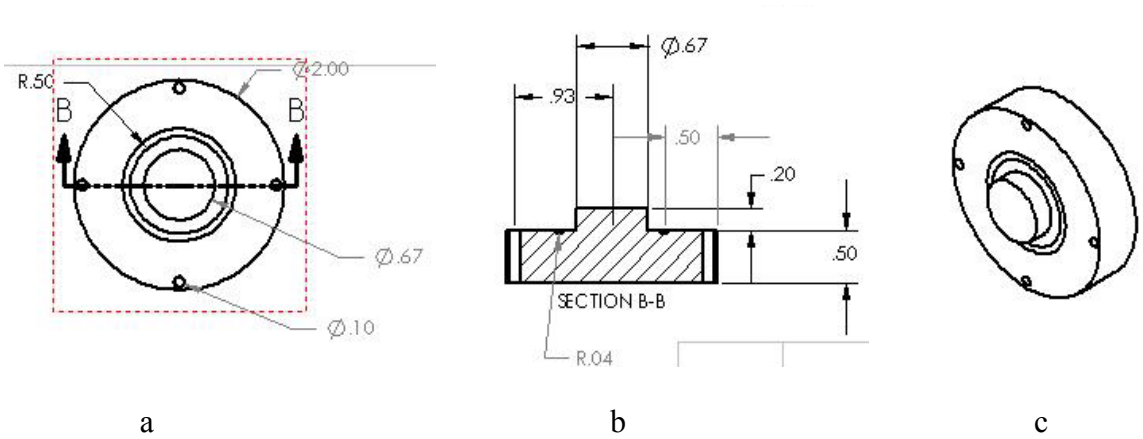

Figure 3-6. Mold base. a) Top view, showing dimensions in inches. b) Side view, showing dimensions in inches. c) Isometric view. Drawings courtesy of Ethan Sherman.

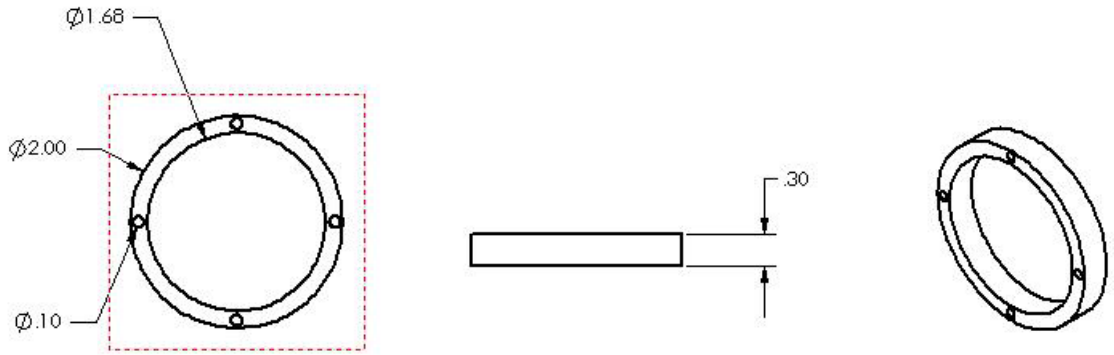

Figure 3-7. Mold ring. a) Top view, showing dimensions in inches. b) Side view, showing dimensions in inches. c) Isometric view. Drawings courtesy of Ethan Sherman.

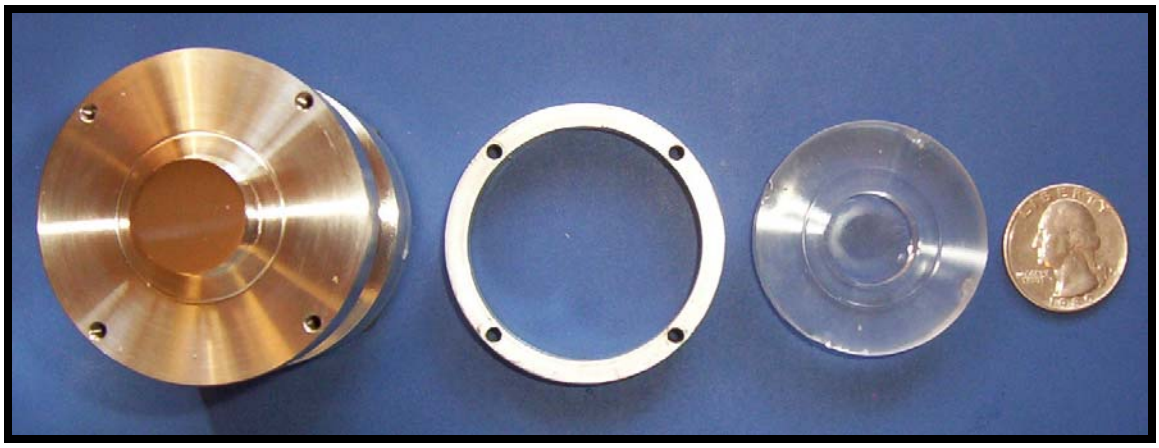

Figure 3-8. Mold and cell culture chamber. From left to right: mold base, mold ring, cell culture chamber, and quarter (to provide a dimension scale).

CHAPTER 4
RESULTS

The sections below detail the results obtained during exploration of each Specific Aim. Prior to investigating the Specific Aims, however, it was necessary to determine an optimal protocol for culture of umbilical cord blood-derived CD34+ cells. The results from this work are detailed first, and are described as "Groundwork.".

Groundwork

To begin, it was necessary to determine if the CD34+ isolation step was necessary. For peripheral blood CD34+ cells, for example, it is known that the accessory stromal elements present in whole blood aid in CD34+ cell expansion (Breems et al., 1998), and therefore CD34+ isolation is not necessary in order to promote growth. In order to determine if the same phenomenon occurs with umbilical cord blood CD34+ cells, purified and non-purified cultures were initiated (at identical CD34+ concentrations) and observed for one week. Results showed that purified cultures flourished, demonstrating an increase in nucleated cell number. Non-purified cultures, on the contrary, deteriorated and demonstrated a decrease in nucleated cell number until cultures completely perished by Day 7 (Figure 4-1). Flow cytometry verified that CD34+ cell numbers followed this trend as well: CD34+ cell numbers increased in purified cultures and decreased in non-purified cultures. Therefore, it was determined that CD34+ isolation is, in fact, a necessary step for ex vivo expansion of cord blood-derived stem cells.

Next, it was essential to determine the cell concentration that promoted maximum expansion. A series of experiments were performed using various Day 0 CD34+ cell concentrations. Figure 4-2 shows cells plated at three different concentrations. It was found that cultures plated at concentrations less than $8x10^4$ CD34+ cells/mL or greater than $4x10^5$ CD34+ cells/mL performed poorly. At concentrations below $8x10^4$ CD34+ cells/mL, it is likely that

there is insufficient cell-cell communication. At concentrations above $4x10^5$ CD34+ cells/mL, it is likely that the cells are overcrowded and compete for nutrients, thereby rapidly depleting media and growth factors. It was concluded that a concentration in the range of $8x10^4$ to $4x10^5$ CD34+ cells/mL promoted satisfactory cellular expansion.

Finally, it was important to determine an appropriate duration of culture, which required an understanding of the general growth trend of cord blood CD34+ cells. To accomplish this, cultures were initiated and their behavior was observed for a period of 3 weeks. It was discovered that nucleated cell numbers steadily climbed, reached a maximum at about 1 week, and then dropped off until there were too few cells to count by around Day 14 (Figure 4-3). This trend is logical, and is explained by the fact that as CD34+ cells mature, a portion of these cells differentiate into their terminal lineage, and at this point they are limited by a finite life span. Flow cytometry confirmed that cell viabilities (Figure 4-4) and CD34+ purities (Figure 4-5) were highest at the initiation of culture and declined throughout the remainder of the 2-week culture period. Viabilities were reasonably well-maintained for the first week of culture, but dropped off substantially by the end of the second week. It is important to mention that, even though percent CD34+ purity decreased over the first week of culture, the *absolute number of CD34+ cells* increased, which indicates that the rate of differentiation was higher than the rate of proliferation. On average, the fold increase of CD34+ cells over the first week of culture was 3.16±2.07. During the second week of culture, however, CD34+ cell numbers decreased, analogous to the decrease in nucleated cells during the second week of culture (Figure 4-3). Since it was observed that both nucleated cells and CD34+ cells thrived only during the first week of culture, a 7-day culture duration was selected for experiments comparing "fresh" and "cultured" cells (such as in Specific Aims 1 and 2).

Specific Aim 1: Rheology of CD34+ Cells

Aspiration and recovery experiments were performed on 30 fresh CD34+ cells and 30 cultured CD34+ cells derived from 3 different umbilical cord blood units. As determined by flow cytometry, CD34+ purities obtained from magnetic column separation were in the range of 85 to 98%. There was no significant difference between the CD34+ percent purity of cells used for "fresh cell" rheology experiments and "cultured cell" rheology experiments. The average fold increase of cultured CD34+ cells was 4.8±2.1 after one week of ex vivo expansion.

Results showed that the rheological properties of cultured CD34+ cells differ significantly from those of fresh CD34+ cells. Cultured cells were found to have a significantly lower viscosity than cultured cells ($p=0.0001$). Cultured cells had an average viscosity of 221.41±16.88 Pa•s, while fresh cells had an average viscosity of 515.42±62.87 Pa•s (Figure 4-6). In addition, cultured cells had a significantly lower cortical tension than fresh cells ($p<0.0001$). Cultured cells had an average cortical tension of $5.54\pm0.49\times10^{-5}$ N/m, while fresh cells had an average cortical tension of $2.14\pm0.23\times10^{-4}$ N/m (Figure 4-7).

It is important to mention that cortical tension was determined by fully aspirating each cell, expelling it, measuring the dimensions of the cell during recovery, and using Equation 3-4 as described in Chapter 3. As discussed in Chapter 2 (page 36), cortical tension can also be determined by a second method based on the Law of Laplace. In this method, the cell is held in equilibrium at the point where a hemispherical cap forms inside of the micropipette. For cultured CD34+ cells, however, this alternate method proved to be unsuccessful, because the precision associated with the pressure system of the experimental apparatus (± 0.2 cm H_20) was not fine enough to accurately measure the very small aspiration pressures needed in order to form a hemispherical projection of a cultured CD34+ cell into the pipette. Therefore, this

method was neglected in favor of the method using Equation 3-4, which allowed for more precision in data reporting. However, cortical tension data *was* able to be gathered using the Law of Laplace method for fresh CD34+ cells, and this data was in agreement with results obtained using Equation 3-4.

Specific Aim 2: Differentiation of CD34+ Cells

Progenitor assay experiments were performed in duplicate using cells from five different umbilical cord blood units. Progenitor cultures were initiated using "fresh cell" and "cultured cell" aliquots, and were scored 14 days later for CFU-GM and BFU-E.

As determined by flow cytometry, CD34+ purities obtained from magnetic column separation were in the range of 85 to 98%. There was no significant difference between the CD34+ percent purity of cells used for "fresh cell" progenitor cultures and "cultured cell" progenitor cultures. The average fold increase of cultured CD34+ cells was 4.2±1.6 after one week of ex vivo expansion.

Results showed that the colony-generation potential of cultured CD34+ cells differs from that of fresh CD34+ cells. Cultured cells generated a significantly higher number of CFU-GM (white blood cell progenitor colonies) than fresh cells ($p=0.04$). Cultured cells generated an average of 89.2±10.1 CFU-GM, while fresh cells generated an average of 62.8±4.4 CFU-GM (Figure 4-8). In addition, cultured cells generated a significantly lower number of BFU-E (red blood cell progenitor colonies) than fresh cells ($p=0.004$). Cultured cells generated an average of 65.4±11.3 BFU-E, while fresh cells generated an average of 98.8±11.2 BFU-E (Figure 4-9). Representative CFU-GM and BFU-E are depicted in Figures 4-10 and 4-11.

Specific Aim 3: Design, Fabrication, and Validation of Culture Chamber

In order to determine whether the PDMS cell culture chamber was cell-friendly, CD34+ cells were cultured in the chamber for one week under static conditions and compared to control

cells cultured in 24-well plates. This allowed for assessment of the biocompatibility of the device before addition of the "microgravity" variable. Figure 4-12 illustrates the nucleated cell fold increases of cells in both environments over one week of culture; the figure shows that cells from both environments followed a nearly identical growth trend. After seven days of culture, the fold increase of CD34+ cells was 3.81±0.47 for cells in the static PDMS cell culture chamber and 3.70±0.29 for cells in the static control.

Figure 4-13 shows the percent viability of cells from each environment on Day 0 and Day 7. On Day 0, cells from both environments had an average percent viability of 97.15±1.49%. By Day 7, cells in the static PDMS cell culture chamber had a percent viability of 94.64±1.40% and cells in the static control had a viability of 94.44±1.34%.

Figure 4-14 depicts the percent CD34+ purity of cells from each environment on Day 0 and Day 7. On Day 0, cells from both environments had an average percent CD34+ purity of 86.76±4.80%. By Day 7, cells in the static PDMS cell culture chamber had a percent CD34+ purity of 29.25±1.25% and cells in the static control had a percent CD34+ purity of 29.49±1.25%.

Figure 4-15 illustrates the colony generation of cells from primary culture in either the static PDMS culture chamber or the static control. Cells from primary culture in the static PDMS culture chamber generated 69.67±7.51 CFU-GM and 80.00±10.82 BFU-E. Cells from primary culture in the static control generated 71.00±18.52 CFU-GM and 79.67±19.55 BFU-E.

Therefore, data from nucleated cell counts, CD34+ cell counts, viability assessment, CD34+ purity assessment, and progenitor assays confirm that the PDMS culture chamber provides an environment that is as conducive, if not more so (in the case of Day 7 CD34+ cell

counts, viability, and BFU-E generation) to hematopoietic stem cell growth than that provided by 24-well plates.

The next step was to implement the "microgravity" variable by testing the culture chamber in the rotating HARV. Because Caco-2 cells have been shown to demonstrate a positive, statistically significant alteration in growth under microgravity conditions, these cells were chosen to test the chamber. Figures 4-17 and 4-18 show the length and width (respectively) of Caco-2 cells grown for 48 hours in each of three environments: "as-is" HARV, HARV with PDMS culture chamber, and static control. Cells grown in the "as-is" HARV had a length of 43.8±2.1 μm and a width of 28.2±1.4 μm. Cells grown in the HARV with culture chamber had a length of 43.9±1.7 μm and a width of 28.7±1.9 μm. Cells grown in the static control had a length of 33.0±2.4 μm and a width of 23.8±1.9 μm. There was no statistical difference between the dimensions of Caco-2 cells grown in the "as-is" HARV and those grown in the HARV with culture chamber. However, there was a statistical difference between cells grown in the "as-is" HARV and the static control, and those grown in the HARV with culture chamber and the static control. This is to be expected, and validates the findings of previous researchers that microgravity causes Caco-2 cells to grow longer and wider. It also confirms that the physics of microgravity which cause this observation are maintained in the PDMS culture chamber.

Specific Aim 4: Short-Term Effects of Simulated Microgravity

To observe the behavior of cord blood-derived CD34+ cells in simulated microgravity, cultures were initiated in three environments ("as-is" HARV, HARV with culture chamber, and static control) and observed for a period of one week (Figure 4-18). After 4 days, nucleated cell numbers in both simulated microgravity environments decreased to numbers too low to count, while cells in the static control flourished. During the first 24 hours of simulated microgravity

culture, however, cell numbers were reasonably well-maintained. After four days of culture, the fold increase of CD34+ cells was 0.01±0.00 for the "as-is" HARV, 0.00±0.00 for the HARV with culture chamber, and 1.23±0.27 for the static control. In other words, CD34+ cells died in both simulated microgravity environments, and performed well in the static environment.

Figure 4-19 depicts the percent viability of cells from each environment on Day 0 and Day 4. On Day 0, cells had an average percent viability of 95.59±0.70%. By Day 4, cells in the "as-is" HARV had a percent viability of 46.15±9.10%, cells in the HARV with culture chamber had a percent viability of 56.11±4.98%, and cells in the static control had a viability of 85.85±11.86%.

Figure 4-20 depicts the percent CD34+ purity of cells from each environment on Day 0 and Day 4. On Day 0, cells had an average percent CD34+ purity of 83.43±7.50%. By Day 4, cells in the "as-is" HARV had a percent CD34+ purity of 6.43±1.13%, cells in the HARV with culture chamber had a percent viability of 4.35±4.11%, and cells in the static control had a percent CD34+ purity of 55.19±11.70%.

Specific Aim 5: Long-Term Effects of Simulated Microgravity

In order to study the long-term behavior of cord blood CD34+ cells following a period of primary simulated microgravity culture, it was necessary to determine an appropriate duration of primary culture. Figure 4-18 shows that cell numbers are well maintained in simulated microgravity for the first 24 hours of culture. Therefore, it was determined that 24 hours would serve as the duration of primary simulated microgravity culture that would be used for subsequent experiments. At this length of time, cells have significant exposure to simulated microgravity but do not demonstrate a drop in cell number.

After 24 hours of simulated microgravity exposure, CD34+ cells were plated in secondary static culture and observed for a period of one week. After being removed from primary culture,

cells from the "as-is" HARV had a fold increase of 0.98±0.01, cells from the HARV with culture chamber had a fold increase of 0.97±0.02, and static control cells had a fold increase of 1.16±0.10. In other words, cell numbers remained reasonably constant over the 24-hour period, with simulated microgravity cells decreasing slightly in number and static cells increasing slightly in number. Viability after 24 hours of primary culture was 81.38±3.07% for cells from the "as-is" HARV, 81.06±1.84% for cells from the HARV with culture chamber, and 95.76±1.55% for cells from static controls. CD34+ purity after 24 hours of primary culture was 61.07±13.66% for cells from the "as-is" HARV, 60.91±5.28% for cells from the HARV with culture chamber, and 80.60±3.67% for cells from the static controls. Cells from each environment were plated in secondary static culture at identical concentrations of live CD34+ cells/mL.

Figure 4-21 shows the behavior of nucleated cells from each of the three primary culture environments in secondary static culture. After 7 days, cell numbers from primary culture in both of the simulated microgravity environments declined to numbers too low to count, while cell numbers from primary static culture continued to increase. After 7 days in secondary culture, the fold increase in CD34+ cells was 0.0±0.0 for cells derived from the "as-is" HARV, 0.0±0.0 for cells derived from the HARV with culture chamber, and 2.10±0.35 for cells derived from the static controls. Therefore, cells from primary simulated microgravity culture were unable to recover in secondary static culture, as evidenced by drops in nucleated cell number and CD34+ cell number.

Figure 4-22 illustrates the viability of cells from each of the three primary culture environments in secondary static culture. Cells from the "as-is" HARV had a viability of 81.38±3.07% on Day 0 and 43.62±4.20% on Day 7. Cells from the HARV with culture chamber

had a viability of 81.06±1.84% on Day 0 and 43.53±2.58% on Day 7. Cells from the static control had a viability of 95.76±1.55% on Day 0 and 91.30±1.63% on Day 7. Therefore, cells grown in 24 hours of primary microgravity culture were not able to maintain viability in secondary static culture, while cells grown in primary static culture were able to maintain viability.

Figure 4-23 depicts the percent CD34+ purity of cells from each of the three primary culture environments in secondary static culture. Cells from the "as-is" HARV had a CD34+ purity of 61.07±13.66% on Day 0 and 0.77±0.32% on Day 7. Cells from the HARV with culture chamber had a CD34+ purity of 60.91±5.28% on Day 0 and 0.63±0.18% on Day 7. Cells from the static controls had a CD34+ purity of 80.60±3.67% on Day 0 and 25.37±3.57% on Day 7. Therefore, CD34+ percent purity was better maintained in cells that were cultured in primary static control culture than in cells that were cultured in primary simulated microgravity culture.

Figure 4-24 shows the colony generation of cells from each of the three primary culture environments in secondary progenitor culture. Cells from the "as-is" HARV generated 2.33±0.58 CFU-GM and 1.00±1.00 BFU-E. Cells from the HARV with culture chamber generated 2.00±1.00 CFU-GM and 1.00±1.00 BFU-E. Cells from the static controls generated 103.33±12.66 CFU-GM and 75.17±9.33 BFU-E. Therefore, cells from primary simulated microgravity culture were not able to demonstrate satisfactory differentiation into white blood cell progenitors and red blood cell progenitors in secondary progenitor assays.

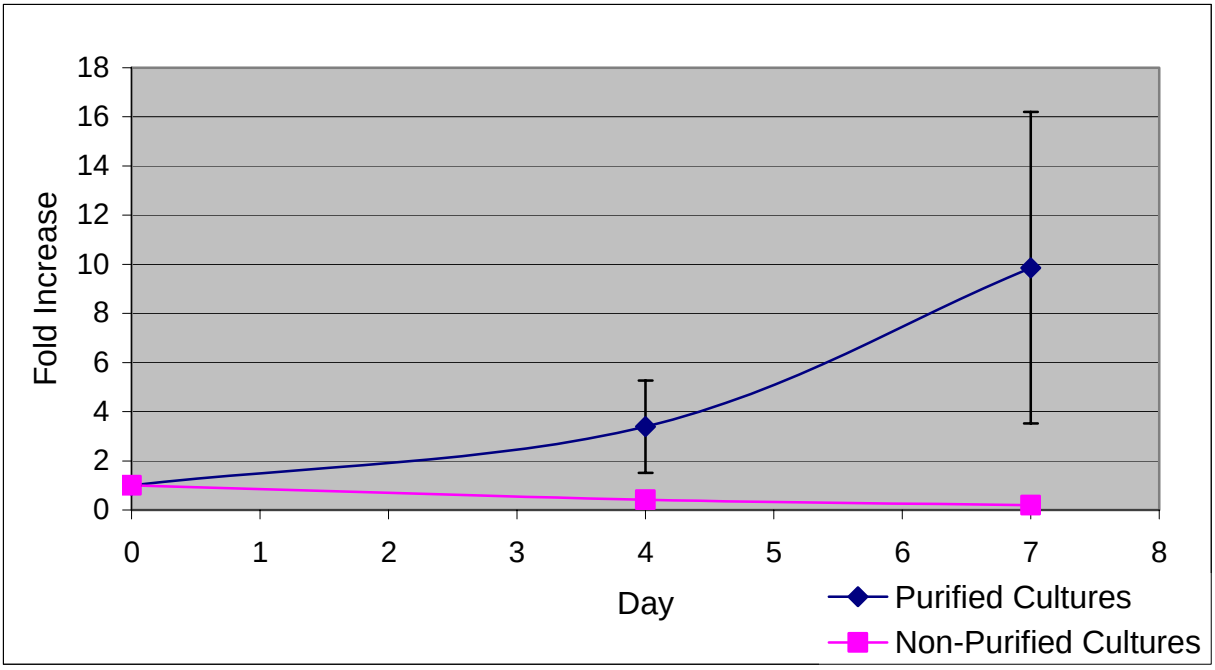

Figure 4-1. Nucleated cell fold increases of CD34+-purified cultures and non-CD34+-purified cultures (n=3).

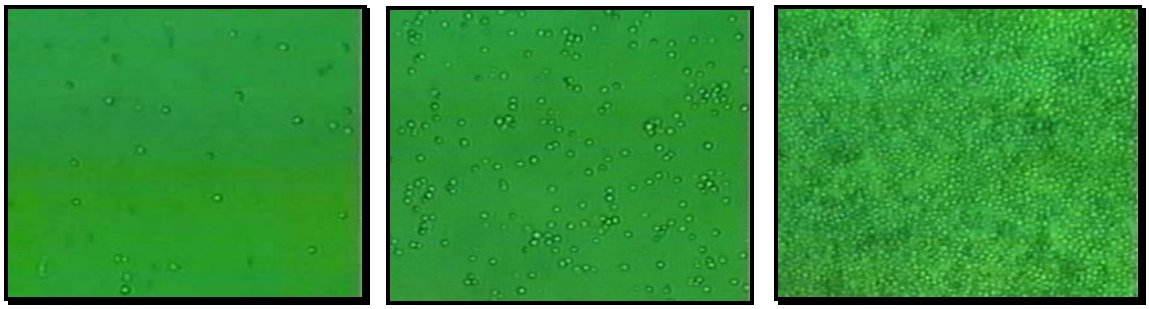

(a) (b) (c)

Figure 4-2. CD34+ cells plated at different concentrations (4X objective and 10X ocular eyepiece). (a) 1E4 CD34+ cells/ml, (b) 1E5 CD34+ cells/ml, (c) 1E6 CD34+ cells/ml.

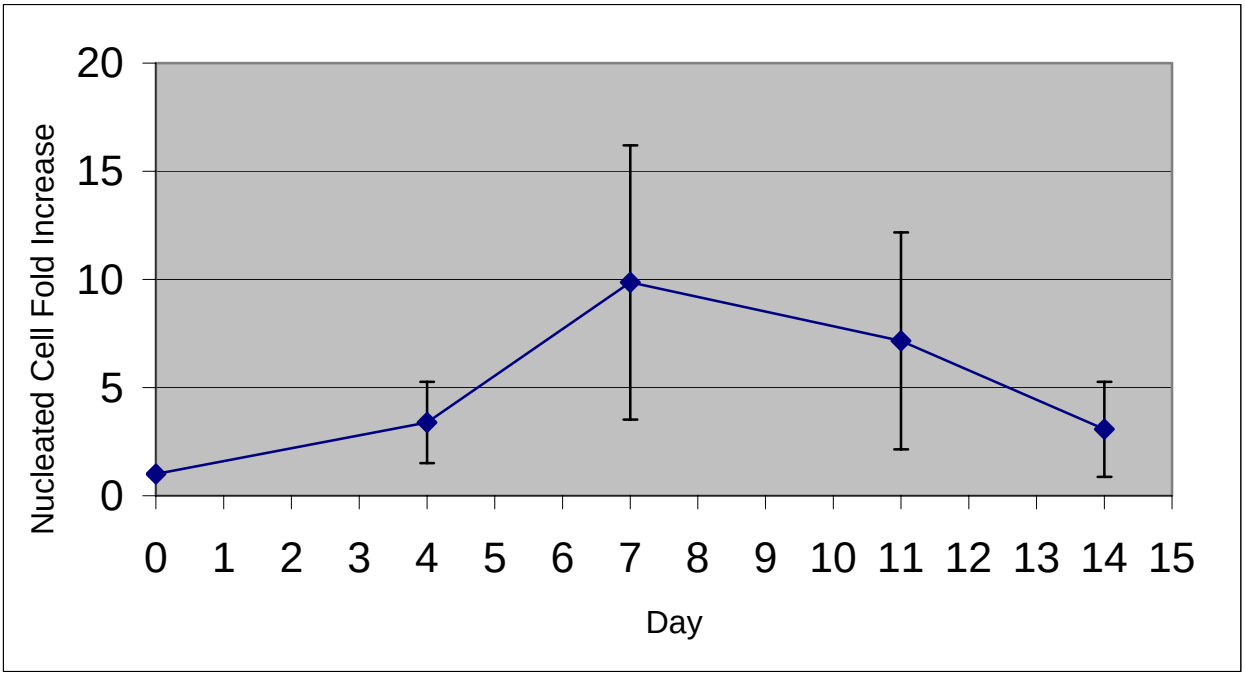

Figure 4-3. Growth trend of CD34+-purified cells over a 2-week period (n=9).

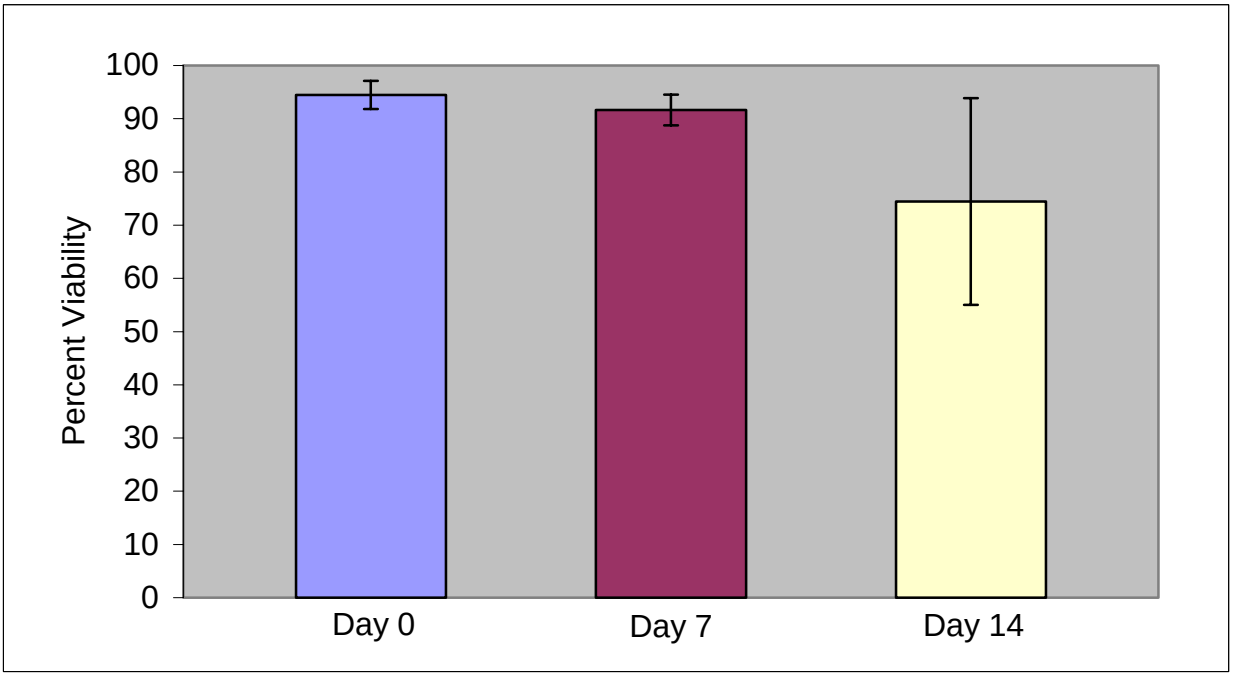

Figure 4-4. Percent viability of CD34+-purified cells, as determined by flow cytometry (n=9 for Day 0 and Day 7 cells, n=4 for Day 14 cells).

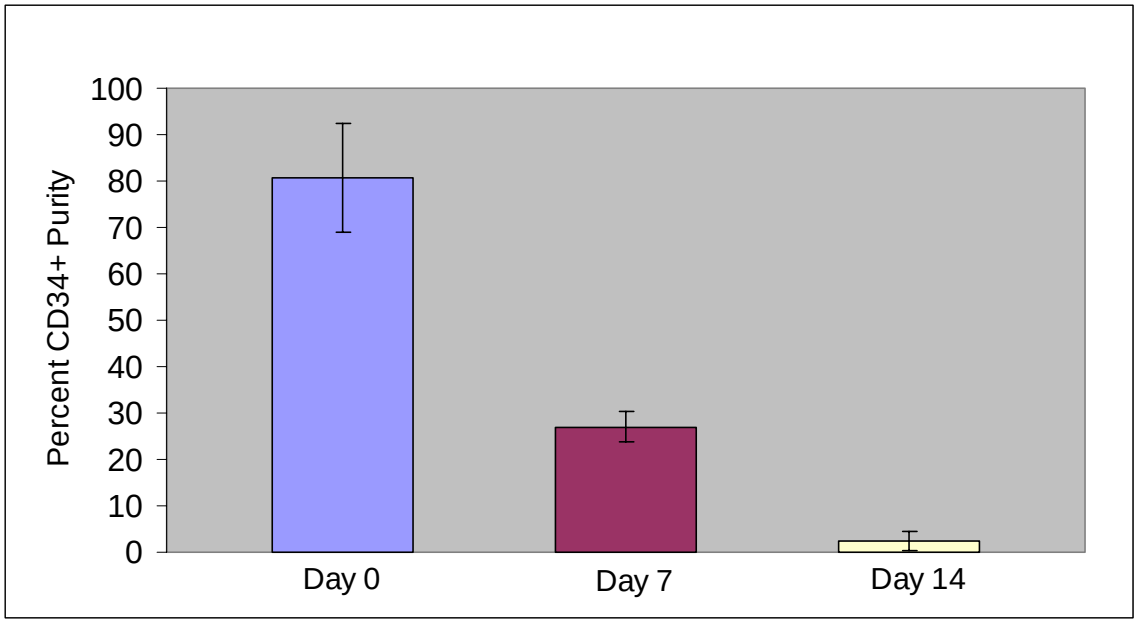

Figure 4-5. Percent CD34+ purity of cells, as determined by flow cytometry (n=9 for Day 0 and Day 7 cells, n=6 for Day 14 cells).

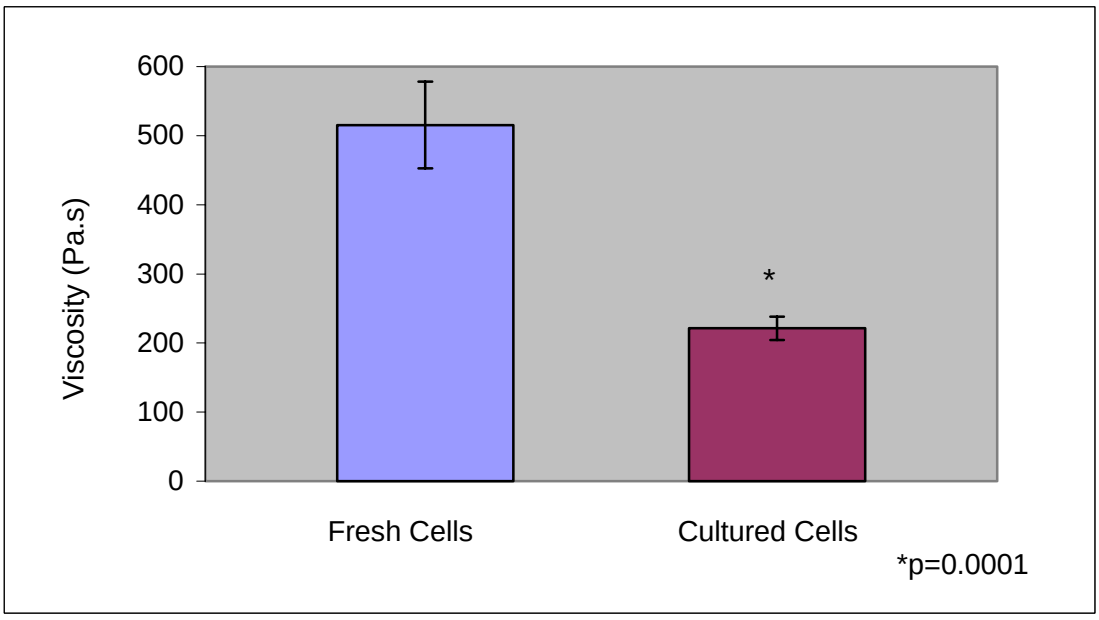

Figure 4-6. Viscosity of fresh CD34+ cells and cultured CD34+ cells (n=30). (Reprinted from: Watts KL, Reddy V, Tran-Son-Tay R. The effects of ex vivo expansion on the rheology of umbilical cord blood-derived CD34+ cells. Journal of Stem Cells 2007;2(1), with permission from Nova Science Publishers.)

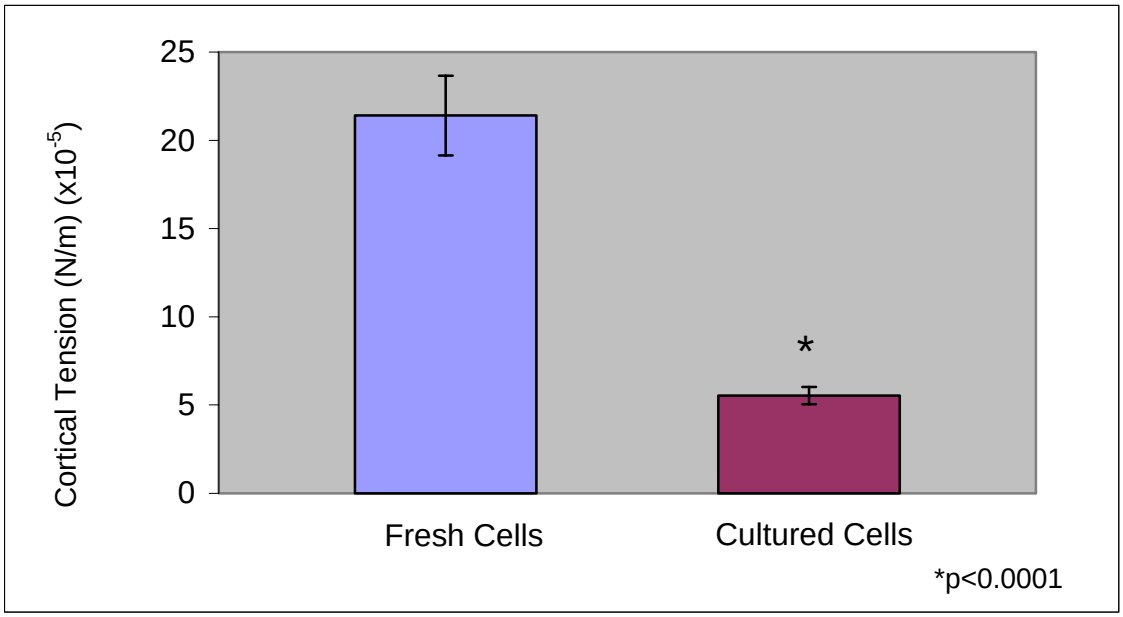

Figure 4-7. Cortical tension of fresh CD34+ cells and cultured CD34+ cells (n=30). (Reprinted from: Watts KL, Reddy V, Tran-Son-Tay R. The effects of ex vivo expansion on the rheology of umbilical cord blood-derived CD34+ cells. Journal of Stem Cells 2007;2(1), with permission from Nova Science Publishers.)

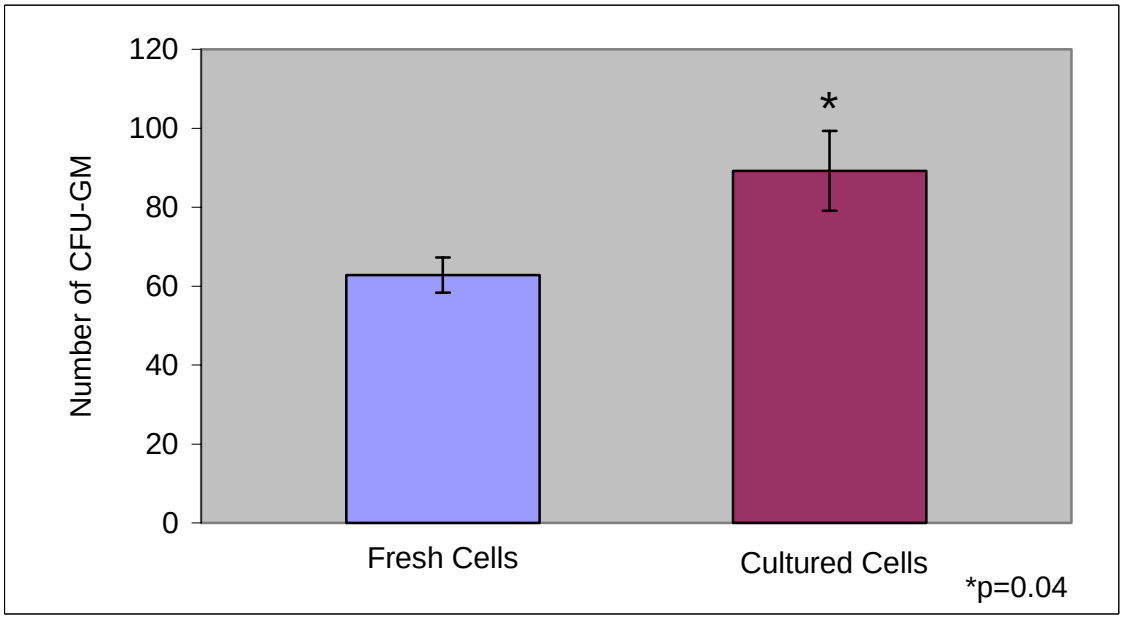

Figure 4-8. CFU-GM generated by fresh CD34+ cells and cultured CD34+ cells (n=5). (Reprinted from: Watts KL, Tran-Son-Tay R, Reddy V. The effects of ex vivo expansion on the differentiation of umbilical cord blood-derived CD34+ cells. Journal of Stem Cells 2006;(1)4, with permission from Nova Science Publishers.)

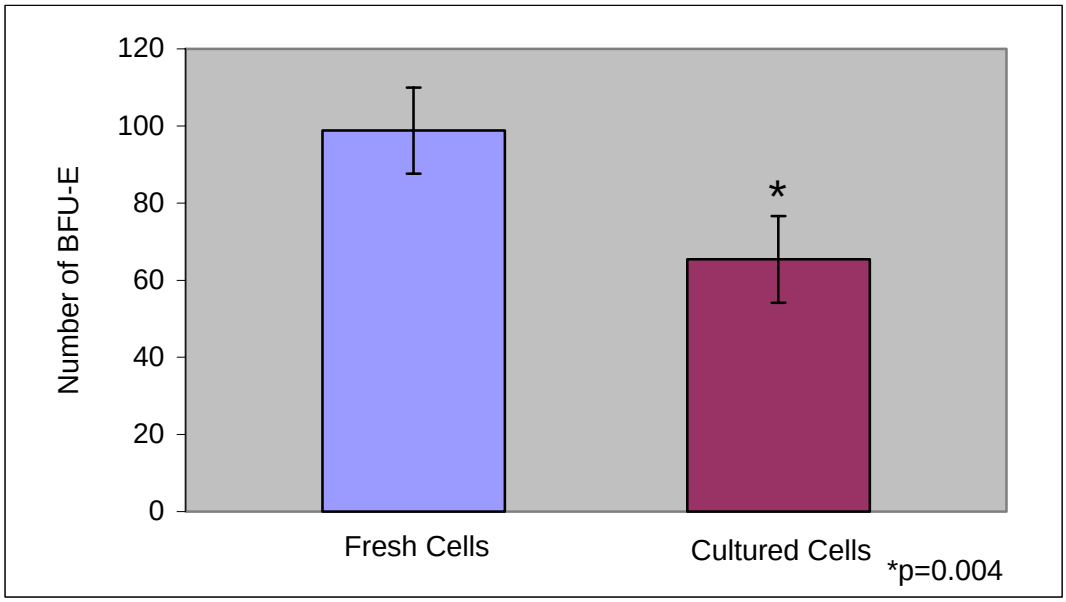

Figure 4-9. BFU-E generated by fresh CD34+ cells and cultured CD34+ cells (n=5). (Reprinted from: Watts KL, Tran-Son-Tay R, Reddy V. The effects of ex vivo expansion on the differentiation of umbilical cord blood-derived CD34+ cells. Journal of Stem Cells 2006;(1)4, with permission from Nova Science Publishers.)

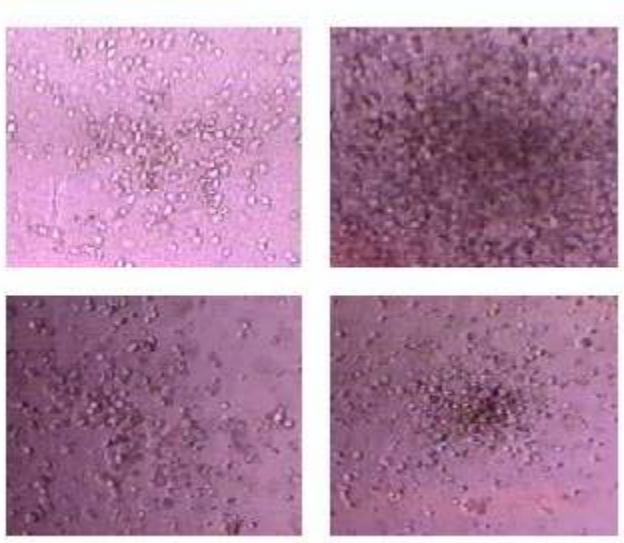

Figure 4-10. Representative CFU-GM (4X objective and 10X ocular eyepiece). Each photograph depicts a different colony. (Reprinted from: Watts KL, Tran-Son-Tay R, Reddy V. The effects of ex vivo expansion on the differentiation of umbilical cord blood-derived CD34+ cells. Journal of Stem Cells 2006;(1)4, with permission from Nova Science Publishers.)

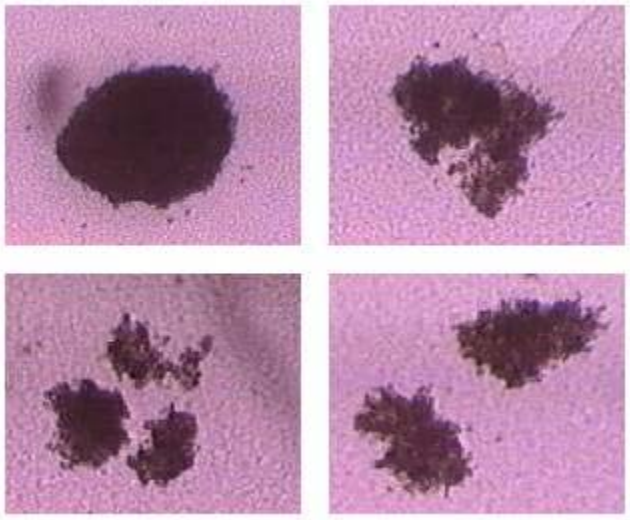

Figure 4-11. Representative BFU-E (4X objective and 10X ocular eyepiece). Each photograph depicts a different colony or cluster of colonies. (Reprinted from: Watts KL, Tran-Son-Tay R, Reddy V. The effects of ex vivo expansion on the differentiation of umbilical cord blood-derived CD34+ cells. Journal of Stem Cells 2006;(1)4, with permission from Nova Science Publishers.)

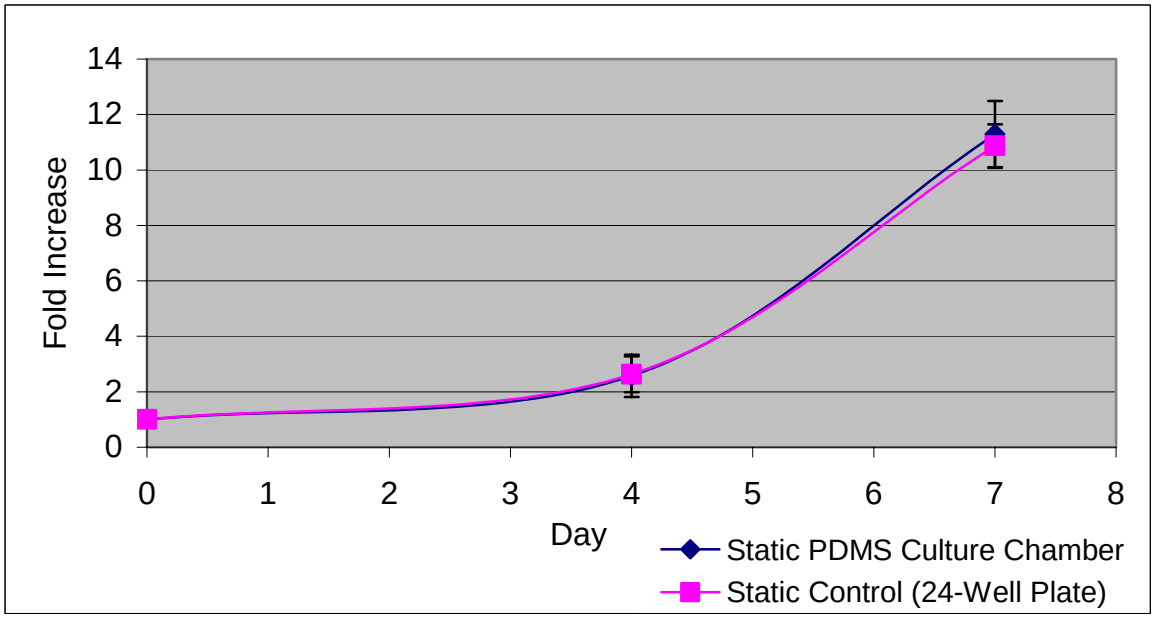

Figure 4-12. Nucleated cell fold increases of CD34+-purified cells in static PDMS culture chamber and static control (24-well plates) (n=3).

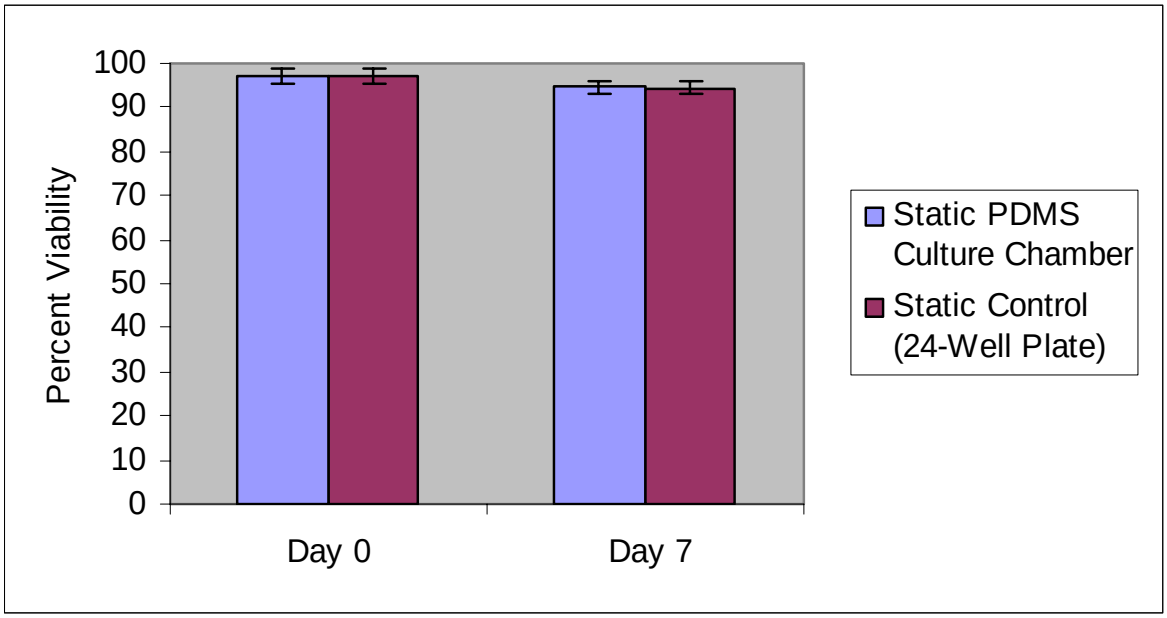

Figure 4-13. Percent viability of CD34+-purified cells grown in static PDMS culture chamber and static control (n=3). Percent viabilities for Day 0 are identical because both allotments of cells were obtained from the same cord blood unit.

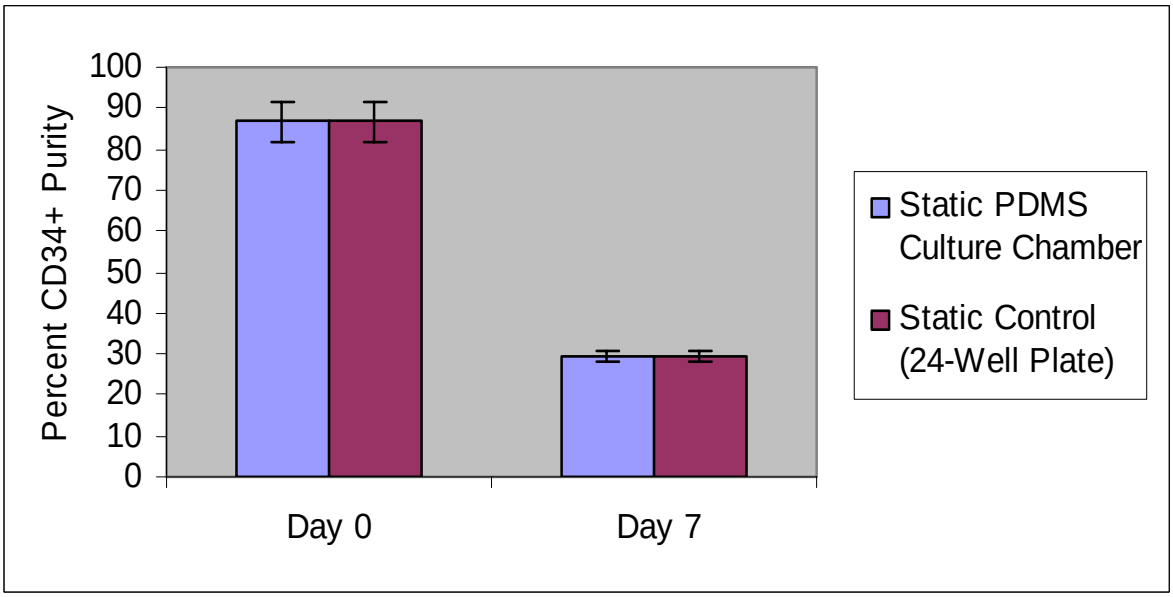

Figure 4-14. CD34+ percent purity of cells grown in static PDMS culture chamber and static control (n=3). Percent CD34+ purities for Day 0 are identical because both allotments of cells were obtained from the same cord blood unit.

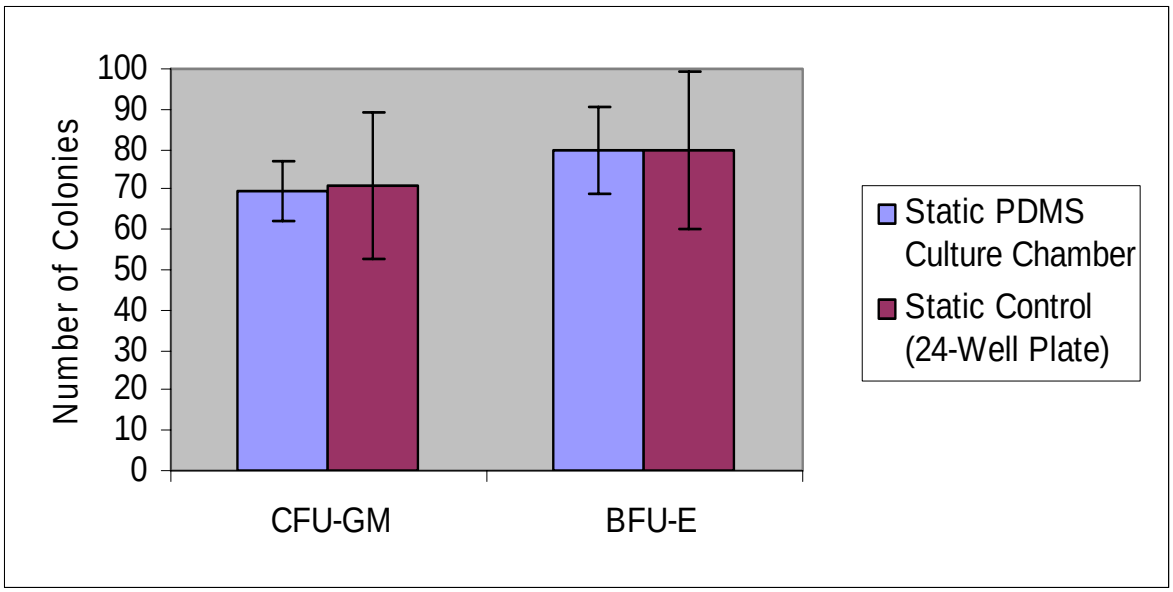

Figure 4-15. Colony generation of CD34+-purified cells in secondary progenitor culture after 7 days of primary culture in static PDMS culture chamber and static control (n=3).

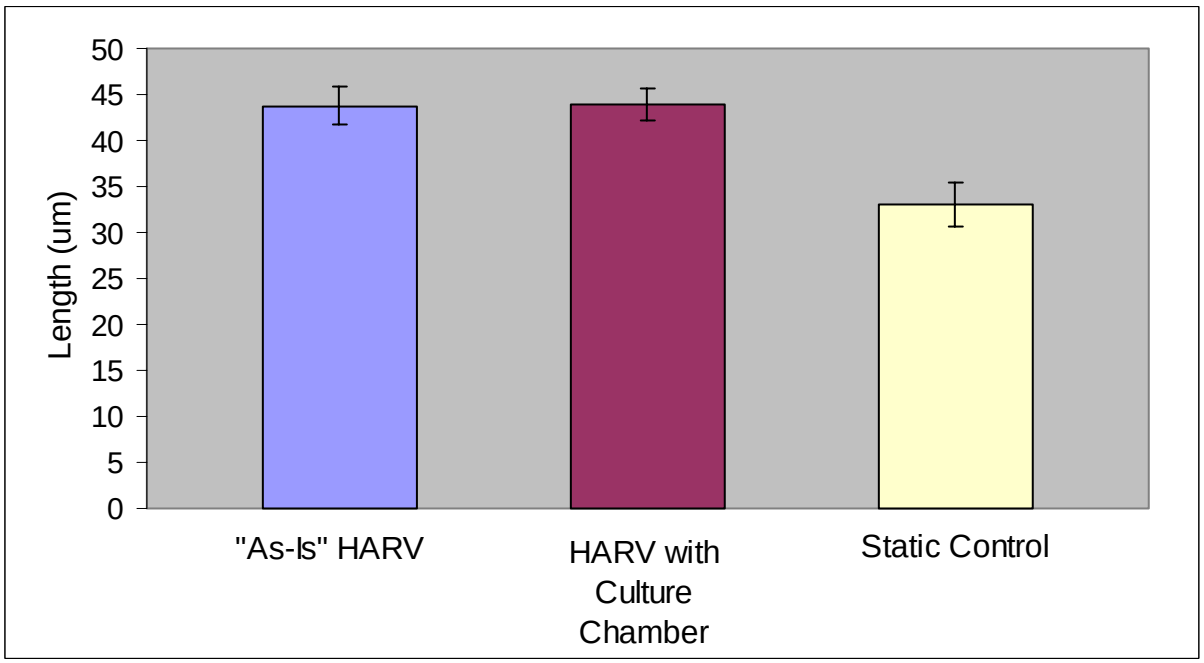

Figure 4-16. Effect of environment on length of Caco-2 cells. Cells cultured for 48 hours in "as-is" HARV, HARV with PDMS culture chamber, or static control (n=30 for "as-is" HARV and HARV with culture chamber, n=60 for static control.)

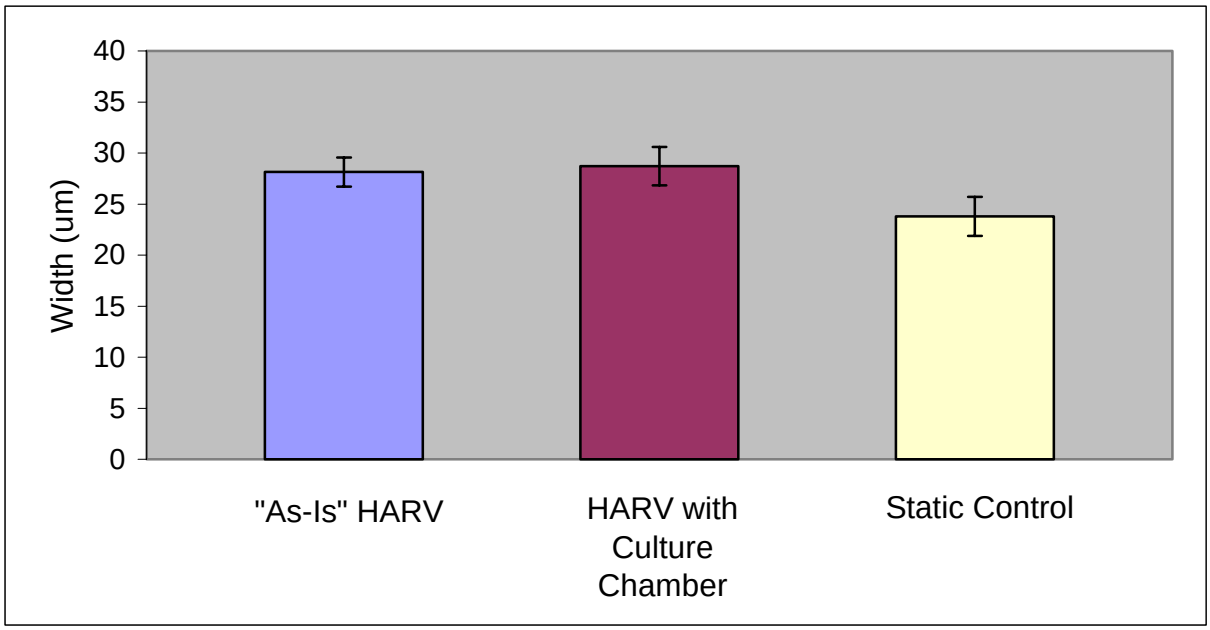

Figure 4-17. Effect of environment on width of Caco-2 cells. Cells cultured for 48 hours in "as-is" HARV, HARV with PDMS culture chamber, or static control (n=30 for "as-is" HARV and HARV with culture chamber, n=60 for static control.)

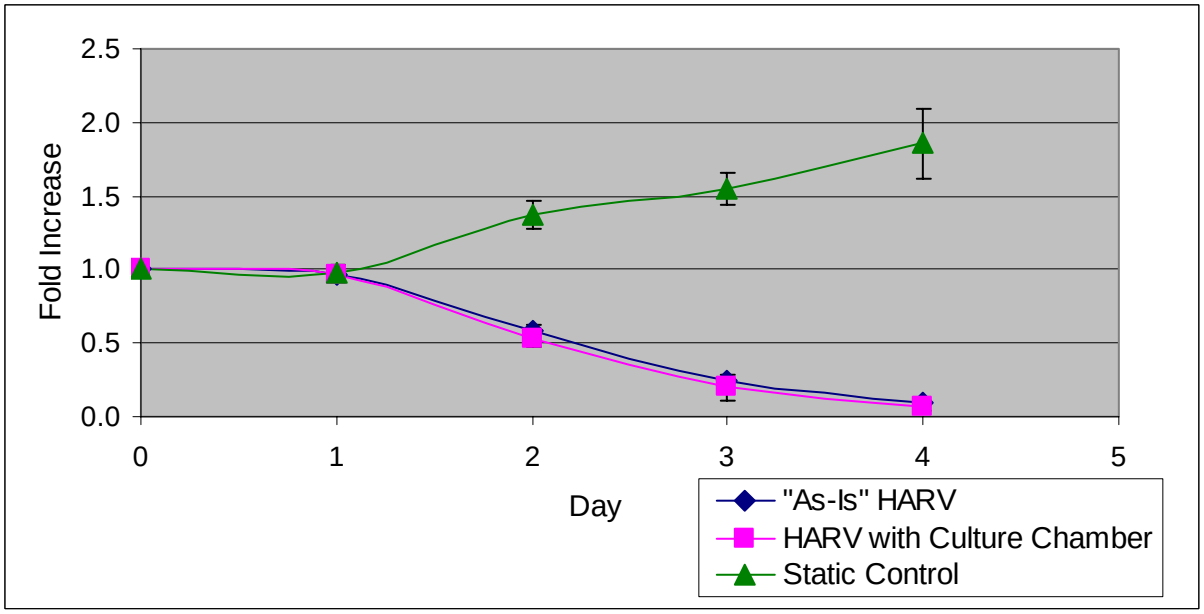

Figure 4-18. Short-term effect of environment on CD34+-purified cell growth. Fold increases of CD34+-purified cells cultured in "as-is" HARV, HARV with culture chamber, and static control over a 4-day period (n=3 for simulated microgravity cultures, n=6 for static cultures).

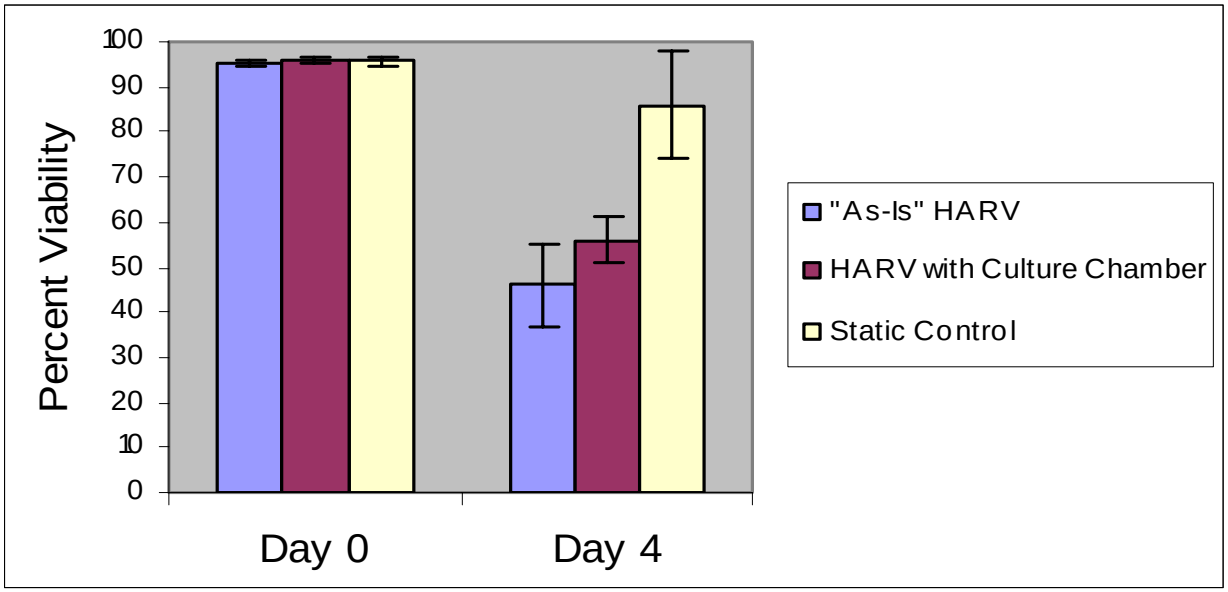

Figure 4-19. Short-term effect of environment on percent viability of CD34+-purified cells. Comparison of Day 0 and Day 4 percent viability of CD34+-purified cells grown in "as-is" HARV, HARV with culture chamber, and static control (n=3 for simulated microgravity cultures, n=6 for static cultures).

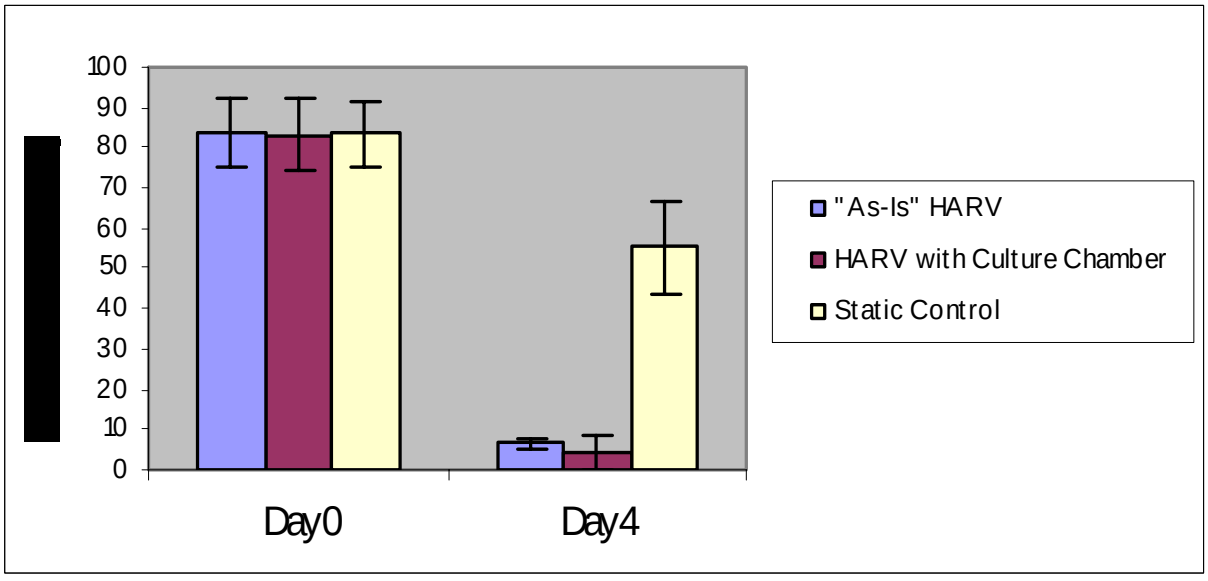

Figure 4-20. Short-term effect of environment on percent CD34+ purity. Comparison of Day 0 and Day 4 percent CD34+ purity of cells grown in "as-is" HARV, HARV with culture chamber, and static control (n=3 for simulated microgravity cultures, n=6 for static cultures).

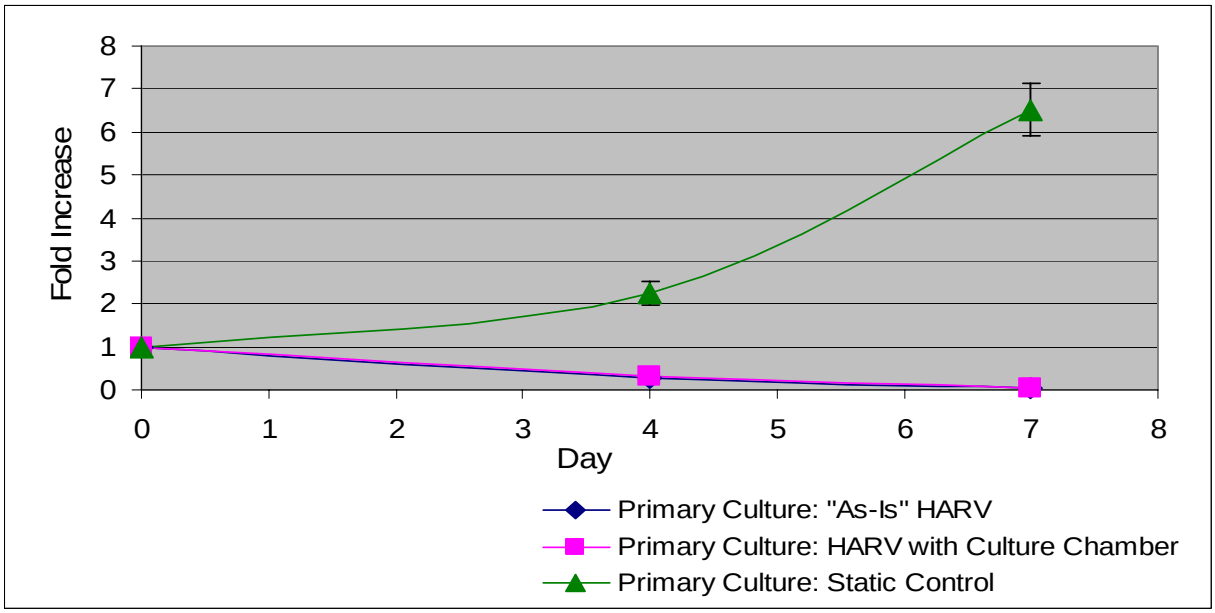

Figure 4-21. Long-term effect of environment on CD34+-purified cell growth. Fold increases of CD34+-purified cells in secondary static culture after 24 hours of primary culture in "as-is" HARV, HARV with culture chamber, or static control (n=3 for simulated microgravity cultures, n=6 for static cultures).

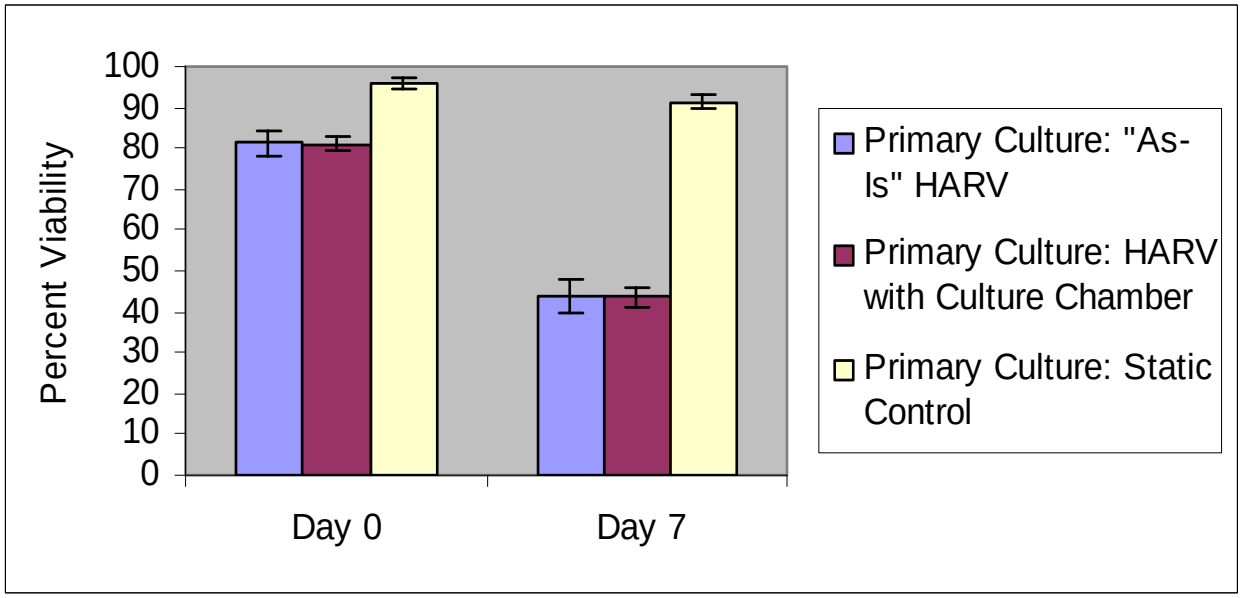

Figure 4-22. Long-term effect of environment on percent viability of CD34+-purified cells. Comparison of Day 0 and Day 7 percent viability of CD34+-purified cells in secondary static culture after 24 hours of primary culture in "as-is" HARV, HARV with culture chamber, or static control (n=3 for simulated microgravity cultures, n=6 for static cultures).

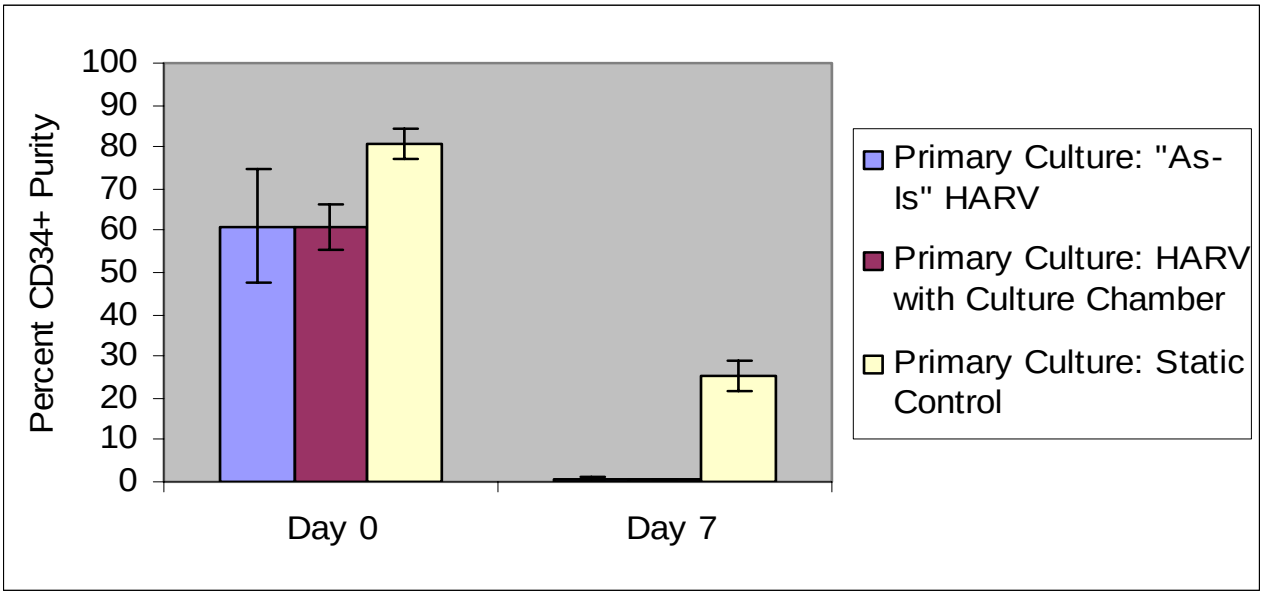

Figure 4-23. Long-term effect of environment on percent CD34+ purity. Comparison of Day 0 and Day 7 percent CD34+ purity of cells in secondary static culture after 24 hours of primary culture in "as-is" HARV, HARV with culture chamber, or static control (n=3 for simulated microgravity cultures, n=6 for static cultures).

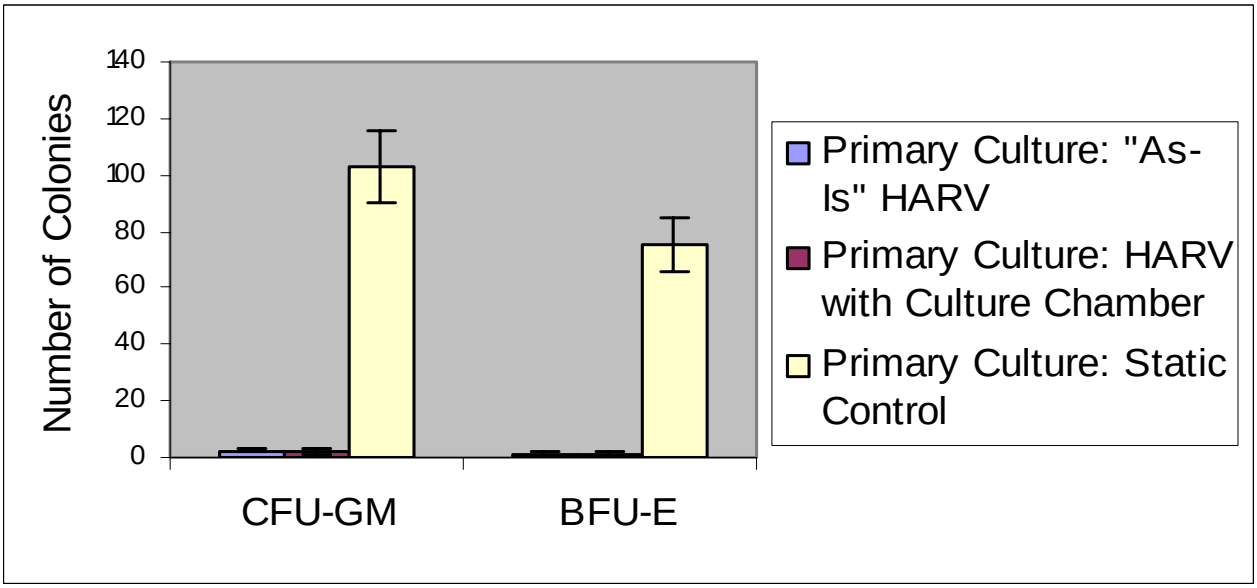

Figure 4-24. Long-term effect of environment on differentiation of CD34+ cells. Comparison of Day 0 and Day 7 colony generation of CD34+-purified cells in secondary progenitor culture after 24 hours of primary culture in "as-is" HARV, HARV with culture chamber, or static control (n=3 for simulated microgravity cultures, n=6 for static cultures).

CHAPTER 5
DISCUSSION

Specific Aim 1: Rheology of CD34+ Cells

The results from Specific Aim 1 show that cultured cord blood-derived CD34+ cells differ from fresh cord blood-derived CD34+ cells in terms of their rheological properties. These differences are manifested by a lower viscosity and a lower cortical tension of cultured cells as compared to fresh cells.

Because lineage-committed cells (i.e. neutrophils, granulocytes, lymphocytes, etc) are phenotypically unique from each other and from the primitive CD34+ progenitor, it is anticipated that their rheological properties will differ as well. In order to exclude lineage-committed cells from aspiration and recovery experiments, cultured cells were re-purified for the CD34+ antigen prior to rheological experiments to ensure that cells used for these experiments were primitive progenitors rather than lineage committed cells. This step served as an internal experimental check point to prevent committed cells from entering the experimental population and interfering with results. The data in Table 5-1 lists the viscosity and cortical tension of various types of blood cells. Viscosities vary from 5 to 1081 Pa•s, and cortical tensions range from 2.40E5 to 2.14E4 N/m. The variability in the range of values is due to different temperatures, cell treatments, and flow conditions. The viscosities of fresh and cultured CD34+ cells as determined by the current studies fall well within the range of published values for viscosity. The cortical tension of cultured CD34+ cells falls within the range of cortical tension values in the literature, while the cortical tension of fresh CD34+ cells is higher than values recorded for other types of cells. It is interesting to note that the cortical tension of fresh human CD34+ cells is highest, followed by cultured CD34+ cells, and later by the lineage-committed cells (granulocytes and neutrophils). This is logical, and provides evidence that as the cell proceeds through its life

cycle, it loses some of the elasticity of its membrane. In addition, it has been shown that cells that are cultured ex vivo for a period of time tend to alter their levels of antigen expression and gene expression (Ma et al., 2001; Li et al., 2006). Therefore, it is possible that this phenomenon leads to differences in the physical properties of the cells as well, and these variations may be manifested by a reduced rigidity in the cytoskeleton of cultured cells.

The viscosity of cultured CD34+ cells is around half of the viscosity of fresh CD34+ cells ($\mu_{cultured} \approx 1/2\mu_{fresh}$). Since viscosity is one of the determinants of the fluidity of cells, this suggests that cultured cells are able to flow more easily through the capillaries of the body than fresh cells. However, viscosity is not the only indictor of the ability of a cell to flow; cortical tension and cell size are also important variables. Furthermore, the cortical tension of cultured CD34+ cells is about one fourth of the cortical tension of fresh CD34+ cells ($T_{0,\,cultured} \approx 1/4T_{0,\,fresh}$). This suggests that cultured cells are less rigid than fresh cells. Consequently, they are likely to recover less quickly from a deformation (Figure 3-4, Chapter 3). The ratio of cortical tension to viscosity (T_0/μ) is called the recovery time constant (Evans and Yeung, 1989). Based on the results above, cultured cells have a recovery time constant that is about half that of fresh cells (as shown in Equation 5-1), explaining why they typically take twice as long to recover from a deformation.

$$\left(\frac{T_0}{\mu}\right)_{cultured} = \left[\left(\frac{T_0}{4}\right)_{fresh} \bullet \left(\frac{2}{\mu}\right)_{fresh}\right] = \frac{1}{2}\left(\frac{T_0}{\mu}\right)_{fresh} \tag{5-1}$$

It is important to mention that activated cells are poorly deformable and will not flow into the micropipette (Perrault et al., 2004). Therefore, it can be stated with certainty that the cells used for the above aspiration experiments were not activated. Furthermore, Miltenyi Biotec states that their magnetic column separation system is cell-friendly, biodegradable, compatible

with downstream applications such as cell culture, and that the binding of the antibody to the cell surface does not affect the viability or function of the cell (Heath et al., 1995; Turner and Dockrell, 1996; Parra et al., 1997). It has also been documented by others that positive selection does not interfere with the properties of CD34+ cells (Lakota et al., 2002; Koutna et al., 2006). Therefore, it is highly unlikely that the results were altered by the isolation process.

Possible Explanation of Observed Results

In vivo, the rate of proliferation is practically negligible compared to the rate of differentiation. However, because of the media and growth factors used during the ex vivo culture described in these experiments, an optimal environment has been created to promote proliferation (with very little differentiation); therefore, in this atmosphere, there is a significantly higher proportion of proliferating cells than would be found in vivo. Cells proliferate via mitosis, a pivotal phase of the cell cycle. Recall that the cell cycle consists of G1 (or first gap) phase, S (or DNA synthesis and replication) phase, G2 (second gap) phase, and M (mitosis or "nuclear division" and cytokinesis or "cytoplasm division") phase (Alberts et al., 2002).

As stated in Chapter 2: Background, the cytoskeleton is one of the major determinants of cortical tension. The roles of the cytoskeleton include mechanical interaction of the cell with its environment, motility, maintenance of cell shape, and preservation of proper internal organization. Perhaps most pivotal, however, is the cytoskeleton's role in growth and division: the cytoskeleton is responsible for pulling the chromosomes apart during mitosis and splitting the dividing cell into two. Consequently, the cytoskeleton dramatically rearranges during mitosis. The two major cytoskeletal changes that occur during the M phase of the cell cycle are (1) during mitosis, a mitotic spindle composed of microtubules and accessory proteins is formed to separate the chromosomes, and (2) during cytokinesis, a contractile ring containing actin and myosin

filaments forms around the equator of the cell (Alberts et al., 2002). Therefore, it is likely that the increased prevalence of cytoskeletal rearrangement occurring in the ex vivo expansion environment accounts for the differences seen between fresh and cultured cells.

Clinical Implications

These findings have significant implications in the field of hematopoietic stem cell transplantation. CD34+ cells that have been augmented through ex vivo expansion prior to transplantation are likely to behave differently in the body than those that have not been augmented. These results show that ex vivo expanded cells are likely to have less resistance to flow through the capillaries of the body than fresh cells. As blood cells are routinely called upon during the regular function of the hematopoietic and immune systems, this may be beneficial, resulting in more rapid cellular migration and migration-dependent physiological responses.

However, it should also be noted that a high volume of diffusion-governed mass transport occurs during periods when the cell is in direct contact with capillary walls. If the duration of contact is lessened, there is the potential for incomplete exchange between the cell and capillary wall. Furthermore, it is mentioned above that cultured cells are likely to recover more slowly from a deformation. The impact of this finding on patient health is unclear; however, it should be taken into consideration in the post-transplant care of immune-compromised patients.

In conclusion, cultured umbilical cord blood-derived CD34+ cells have different rheological properties than their fresh cell counterparts. These differences will likely cause a variation in the kinetics of cell migration in the body, and therefore should be considered when using ex vivo expanded cells for clinical transplantation.

Specific Aim 2: Differentiation of CD34+ Cells

The results from Specific Aim 2 show that fresh umbilical cord blood CD34+ cells and ex vivo expanded CD34+ cells differ in terms of their differentiation potential, as demonstrated

by *in vitro* progenitor cell assays. As compared to fresh cells, expanded cells tend to generate a significantly higher number of CFU-GM and a significantly lower number of BFU-E.

Previous studies have shown that the number of colony-forming units can be augmented through ex vivo hematopoietic stem cell expansion (Jaroscak et al., 2003). In other words, the increase in the number of primitive hematopoietic stem cells is accompanied by an increase in the number of colony-forming progenitors. Because the progenitor assay concentrations in this study were normalized prior to culture, this study shows that the differences observed in CFU potential between fresh and expanded cells are *independent of nucleated cell concentrations* and are *solely the result of the effects of the culture environment* on the biology of the individual cells.

It is not likely that the results obtained in this study were due to the growth factors used during pre-culture of CD34+ cells. It is well documented that the combination of FL and TPO stimulate extensive expansion and very minimal differentiation of cord blood derived-CD34+ cells (Gilmore et al., 2000). This combination of growth factors is recognized for its ability to promote maintenance of the primitive phenotype. In order to exclude lineage-committed cells from CFU assays, pre-cultured cells were re-purified for the CD34+ antigen prior to progenitor culture initiation to ensure that cells used for CFU assays were primitive progenitors rather than lineage committed cells. This step served as an internal experimental check point to prevent committed cells from entering progenitor assays and interfering with colony enumeration results.

Possible Explanation of Observed Results

Similar studies involving ex vivo expansion of peripheral blood CD34+ cells found that cells derived from ex vivo expansion were predominantly neutrophil precursors (Haylock et al., 1992). In addition, studies involving transplantation of ex vivo expanded peripheral blood progenitor cells have shown more rapid neutrophil recovery than historical (unexpanded)

controls (McNiece et al., 2000); it was found that the expanded cells contained more mature cells of neutrophil lineage, thus accounting for the more rapid engraftment. The findings of the current study present evidence that the same phenomenon can be recreated with UCB cells.

Additional studies provide evidence that it may be more difficult to induce erythroid differentiation in vitro than myeloid differentiation (in other words, erythroid cells are "more picky" than myeloid cells), which may explain why cultured cells generated fewer BFU-E. For example, studies involving leukemia cells showed that the majority of erythropoietic cells had not divided during culture (Tabuse et al., 1976). Likewise, it has been found that induction of erythropoietic function may require two rounds of mitosis (McClintock and Papaconstantinou, 1974), and that an expansion phase precedes terminal erythroid differentiation of progenitor cells from cord blood in vitro (Dai et al., 2000). Therefore, erythroid lineage commitment may lag behind myeloid commitment, and may require more specific environmental conditions in order to proceed.

Clinical Implications

It is likely that the same phenomenon observed ex vivo occurs in vivo as well. This has significant implications in the field of hematopoietic stem cell transplantation. Stem cells that have been expanded through ex vivo culture techniques are currently transplanted into patients suffering from various diagnoses, from leukemia to breast cancer (Devine et al., 2003). The results from this study suggest that cells that are cultured prior to transplantation are likely to behave differently in the physiological environment as compared to cells that are not cultured prior to transplantation.

There is a direct correlation between in vivo engraftment potential and the number and types of colonies obtained in ex vivo CFU assays. Emminger et al (1989) showed that CFU-GM numbers can serve as an effective predictor of engraftment kinetics. It was found that the

number of nucleated cells transplanted was directly correlated with CFU-GM numbers and inversely correlated with time to hematopoietic recovery. Therefore, one can assume that the differences in CFU potential observed between fresh and pre-cultured cells are likely to be manifested by earlier neutrophil engraftment but a prolonged period of anemia following transplantation of cultured UCB cells. Because of the delayed hematopoietic recovery associated with UCB transplants (Tse and Laughlin, 2005), the former is of increased significance.

In conclusion, culturing UCB cells prior to use in HSC transplantation may help to alleviate the delayed neutrophil engraftment associated with cord blood transplantation. It is possible, however, that ex vivo expansion may polarize CD34+ cells toward the myeloid lineage in lieu of the erythroid lineage. This may prolong post-transplant anemia and explain the delay in red cell engraftment following HSC transplantation. Therefore, the use of cultured UCB CD34+ cells in transplantation should be approached with caution.

Specific Aim 3: Design, Fabrication, and Validation of Culture Chamber

When tested in static culture using CD34+ cells, the PDMS cell culture chamber performed equally as well as traditional 24-well plates in terms of nucleated cell count, CD34+ cell count, percent viability, percent CD34+ purity, and progenitor assays. The results from these tests provide evidence that the culture chamber provides a cell-friendly, biocompatible environment. In other words, the cells did not react unfavorably to the surrounding environment. This indicates that the dominant material, physical, and chemical properties of the culture chamber (such as surface roughness, surface energy, hydrophilicity, geometry, polymer chemistry, and others) are not harmful to the cells.

Furthermore, when tested in simulated microgravity using Caco-2 cells, the PDMS culture chamber performed equally as well as the HARV in terms of cell viability and cell size. The physics of microgravity (detailed in Chapter 2: Background) that account for the significantly

larger length and width of human colon carcinoma cells are maintained in the culture chamber. Therefore, it can be concluded that the HARV and the PDMS culture chamber offer analogous culture environments in terms of such parameters as cell/disc motion, oxygenation, and nutrient circulation.

Clinical/research implications. Advances in biomedical research lead inevitably to advances in clinical practice. A smaller, more economical simulated microgravity cell culture chamber has been designed and fabricated. Based on the results above, this chamber offers the advantages of simulated microgravity while minimizing volume demands and associated supply costs. Consequently, simulated microgravity research can be carried out in a more cost-effective manner. Furthermore, simulated microgravity research can be expanded to include types of cells that are available only in small numbers. Prior to the development of this culture chamber, only abundant cells could be studied because of the large volume demanded by the HARV.

Specific Aim 4: Short-Term Effects of Simulated Microgravity

As evidenced by nucleated cell counts, CD34+ cell counts, percent viability, and percent CD34+ purity, CD34+ cells performed poorly in both the "as-is" HARV and the HARV with culture chamber. It was originally hypothesized that the major obstacle in growing cord blood-derived CD34+ cells in simulated microgravity was the large volume (10 mL) demanded by the HARV. At this volume, the cell concentration is too dilute to promote growth. However, because the same results were observed in both simulated microgravity environments ("as-is" HARV and HARV with culture chamber), one can conclude that the poor performance of the cells in simulated microgravity is not related to concentration, but is instead related to characteristics inherent to the simulated microgravity environment in the conditions tested.

However, it was observed that during the first 24 hours of culture, cell numbers were maintained relatively constant, indicating a period of quiescence (Figure 4-18). A similar period

of quiescence was found with bone marrow CD34+ cells, leading to increased proliferative potential in secondary static culture (Plett et al., 2001). Therefore, this observation provided the motivation for studying the long-term behavior of the cells in secondary static culture (Specific Aim V).

Possible Explanation of Observed Results

CD34+ cells are notoriously difficult to culture. Unlike many other types of cells, these cells are extremely fragile and particular. Because of their high degree of primitivity and unspecialized nature, CD34+ cells are highly in sync with environmental signals and ambient conditions. The data show that the simulated environment is simply too damaging for these delicate cells. As discussed in Chapter 2: Background, suspension cells generally do not fare well in this environment, perhaps because they are unable to adequately interact with their neighbors. Because of the unspecialized nature of CD34+ cells (furthermore, cord blood-derived CD34+ are among the most primitive types of CD34+ cells), this constantly changing, dynamic environment is not conducive to growth.

Collisions with the vessel wall could explain the poor performance of the cells. As discussed in Chapter 2: Background, there are a number of factors which influence the time it takes for a particle to reach the vessel wall in simulated microgravity (Gao et al., 1997). Any modifications to the simulated microgravity culture chamber in which size is minimized may decrease the time it takes for particles to collide with the vessel wall. Therefore, it becomes even more pivotal to pinpoint the ideal values for such parameters as viscosity, rotational speed, and microcarrier size, among others. In order to have a thorough understanding of the behavior of cells in this environment, it is necessary to perform an optimization study to determine the optimal values for experimental variables in order to minimize collisions with the vessel wall. Since the percent viabilities were not significantly different between cells grown in the

unmodified HARV and those grown in the HARV with PDMS culture chamber, it is not likely that cells were hitting the wall with any higher frequency in the PDMS culture chamber than in the unmodified HARV.

Clinical/Research Implications

The findings of this study suggest that the Rotary Cell Culture System used here is not a viable ex vivo expansion technique for umbilical cord blood-derived CD34+ cells. However, this finding provides motivation for further studies to determine *why* cells perform so poorly in this environment. Investigating the cellular mechanisms leading to death in microgravity may prove to be beneficial for NASA or other research institutes interested in space exploration.

Specific Aim 5: Long-Term Effects of Simulated Microgravity

Results from nucleated cell counts, CD34+ cell counts, percent viability analysis, percent CD34+ purity analysis, and progenitor assays point to a common conclusion: a period of primary simulated microgravity culture damaged CD34+ cells to a point from which they were unable to recover in secondary static culture. Cells grown in both primary culture environments ("as-is" HARV and HARV with culture chamber) performed equally poorly.

Studies by Plett et al (2001) showed that primary simulated microgravity culture conferred bone marrow CD34+ cells with an increased growth potential in secondary static culture. This same phenomenon was not seen with umbilical cord blood CD34+ cells. On the contrary, cord blood cells grown in primary simulated microgravity demonstrated a failure to thrive in secondary static culture.

Possible Explanation of Observed Results

There is a substantial body of evidence demonstrating that hematopoietic stem cells from umbilical cord blood (UCB) differ from those derived from bone marrow (BM). These dissimilarities include the following:

- UCB possesses a higher proportion of primitive hematopoietic progenitor cells than BM (Sirchia and Rebulla, 1999)
- UCB stem cells demonstrate increased proliferation and expansion potential as compared to BM stem cells (Sirchia and Rebulla, 1999)
- UCB stem cells are more appropriate than BM stem cells for genetic manipulation and gene therapy (Sirchia and Rebulla, 1999)
- UCB stem cells demonstrate higher colony efficiency, a higher percentage of colonies with mixed growth patterns, and an increased replating potential as compared to BM stem cells (Huang et al., 1998)
- When exposed to certain growth factors, UCB stem cells were found to be more quiescent than BM stem cells (Traycoff et al., 1994)
- Platelet recovery is slower following UCB stem cell transplant than BM stem cell transplant (Yasui et al., 2003)
- Over a similar dose range, UCB stem cells were stimulated by macrophage inflammatory protein-1α, yet BM stem cells were inhibited (de Wynter et al., 1998)
- Northern blot analysis showed that UCB stem cells have one macrophage inflammatory protein -1α receptor, while BM stem cells have two different receptors (de Wynter et al., 1998)

In conclusion, CD34+ cells from cord blood and bone marrow are very different, and should be expected to behave uniquely. In general, cord blood CD34+ cells tend to be much more primitive, have higher growth potential, different cell cycle kinetics, differentiate by different pathways, respond uniquely to certain signaling molecules, and have different cell surface receptors than bone marrow CD34+ cells. Therefore, it is not surprising that, though simulated microgravity was shown to promote enhanced growth of bone marrow cells, it did not have the same effect on cord blood cells. It can be concluded that a period of primary simulated microgravity culture in the Rotary Cell Culture System caused irreversible damage to cord blood cells.

Clinical/Research Implications

The results of this study show that, in the conditions tested, simulated microgravity does not confer increased expansion potential on cord blood cells in secondary static culture, and therefore is not a viable means of augmenting these cells. There may be more promise in other transplantation techniques that have gained recent recognition, such as pooled or sequential transplantation in which a second cord blood unit is transplanted following the first, with the goal of increasing cell count and improving engraftment (Ballen, 2005).

Table 5-1. Viscosity (μ) and cortical tension (T_0) of various types of human white blood cells

Cell Type	μ (Pa•s)	T_0 (N/m)	Reference(s)
CD34+ cells, fresh	515	2.14E-04	(present work)
CD34+ cells, cultured	221	5.54E-05	(present work)
Granulocytes	100 - 1000	3.50E-05	Evans and Yeung, 1989
Lymphocytes	450 - 1081	----	Thomas et al., 2003; Evans and Yeung, 1989; Needham and Hochmuth, 1992
Neutrophils	5 - 500	2.40E-5 - 3.80E-5	Zhelev et al., 1994

CHAPTER 6
CONCLUSIONS AND FUTURE WORK

It can be concluded that ex vivo expansion does, in fact, have an effect on umbilical cord blood-derived CD34+ cells. A seven-day period of ex vivo expansion causes cord blood-derived CD34+ cells to have a lower cytoplasmic viscosity and a lower cortical tension than their fresh counterparts. In addition, it causes cord blood-derived CD34+ cells to generate more cells committed to the myeloid lineage and fewer cells committed to the erythroid lineage than unexpanded cells. As cultured cells were shown to differ significantly from non-cultured cells, one can surmise that they will behave differently in the physiological milieu of a transplant patient. Therefore, it is recommended that these observations be considered when transplanting patients with expanded cells, and that the patient be monitored closely following transplantation of expanded cells. Future work in this area could assess whether *other* properties of cord blood CD34+ cells (for example: expression of surface markers, capability of differentiating into the sub-classes of white blood cells, ability to migrate in response to chemical stimuli) are affected by ex vivo expansion, as these properties are equally vital to patient health. Additionally, it would be valuable to determine whether the other types of hematopoietic stem cells (those derived from bone marrow and peripheral blood) are similarly affected by ex vivo expansion.

Extensive experimentation showed that the Rotary Cell Culture System tested here does not provide a hospitable environment for cord blood-derived CD34+ cells. However, a novel, economical, biocompatible cell culture chamber has been built and validated; this chamber minimizes the volume requirement of current simulated microgravity technology while maintaining the properties of the environment. This chamber did not offer promise for cord blood-derived CD34+ cells, as it was shown that cell concentration is <u>not</u> the obstacle hindering the growth of these cells in microgravity. However, with the implementation of this culture

chamber, research can proceed with cell lines that previously could not be studied in simulated microgravity because of the 10-mL volume requirement. This includes families of cells in which the cells themselves are few in number, or those in which the cost of supplies and reagents prohibits in-depth study.

As discussed previously, any modifications to the simulated microgravity culture chamber in which size is minimized may decrease the time it takes for particles to collide with the vessel wall. Therefore, it is crucial to understand the motion of the cells within the chamber to ascertain that collisions with the vessel wall are negligible. Consequently, it would be useful to perform a visualization experiment (perhaps using fluorescently tagged cells viewed using a camera with fluorescence capabilities) to observe the paths of the cells. Results from this visualization study could be used to fine-tine experimental parameters such as viscosity, rotational speed, and microcarrier size to minimize cell damage.

Additional future work could consist of designing, building, and testing a similar device for the alternate simulated microgravity culture vessel (the STLV, seen in Figure 2-6(d)). Studies using the STLV are also hindered by a large volume requirement; therefore, this culture vessel would benefit from a micro-well device.

APPENDIX A
GROUNDWORK DATA

Table A-1. Non-CD34+ purified cultures: nucleated cell fold increases

	Day 0	Day 4	Day 7
n=1	1.00	0.27	0.22
n=1	1.00	0.45	0.19
n=3	1.00	0.53	0.16
mean	1.00	0.42	0.19
std dev	0.00	0.13	0.03

Table A-2. CD34+ purified cultures: nucleated cell fold increases

	Day 0	Day 4	Day 7	Day 11	Day 14
n=1	1.00	2.70	5.21	1.58	0.07
n=2	1.00	2.20	3.86	0.97	0.03
n=3	1.00	1.86	5.00	7.07	3.07
n=4	1.00	4.92	13.99	12.39	3.65
n=5	1.00	2.45	5.72	5.17	2.83
n=6	1.00	7.30	23.50	17.00	7.40
n=7	1.00	1.88	11.69	7.89	3.48
n=8	1.00	4.87	12.77	5.59	4.07
n=9	1.00	2.33	7.00	6.78	3.03
mean	1.00	3.39	9.86	7.16	3.07
std dev	0.00	1.88	6.34	5.01	2.20

Table A-3. Fold increases of CD34+ cells over a 1-week period

	Day 0 NC Conc. (cells/ml)	Day 0 CD34+ Purity (%)	Day 0 CD34+ Conc. (cells/ml)	Day 7 NC Conc. (cells/ml)	Day 7 CD34+ Purity (%)	Day 7 CD34+ Conc. (cells/ml)	Day 7 Fold Increase
n=1	1.27E+05	67.86	8.62E+04	6.60E+05	23.16	1.53E+05	1.77
n=2	5.06E+05	67.86	3.43E+05	1.95E+06	30.08	5.87E+05	1.71
n=3	6.38E+04	88.57	5.65E+04	3.19E+05	24.67	7.87E+04	1.39
n=4	9.75E+04	88.57	8.64E+04	1.37E+06	25.66	3.52E+05	4.07
n=5	3.55E+05	61.39	2.18E+05	2.03E+06	22.47	4.56E+05	2.09
n=6	4.20E+04	90.62	3.81E+04	9.85E+05	30.75	3.03E+05	7.96
n=7	1.30E+05	81.29	1.06E+05	1.52E+06	27.79	4.22E+05	4.00
n=8	1.95E+05	92.85	1.81E+05	2.49E+06	24.91	6.20E+05	3.43
n=9	1.05E+05	86.67	9.10E+04	7.35E+05	25.03	1.84E+05	2.02
						mean	3.16
						std dev	2.07

NC = Nucleated Cell; Conc. = Concentration

Table A-4. Percent viability of CD34+ cells over a 2-week period

	Day 0 % Viability	Day 7 % Viability	Day 14 % Viability
n=1	90.32	93.21	
n=2	90.32	87.93	
n=3	94.22	91.64	89.31
n=4	94.22	90.27	80.46
n=5	97.10	93.86	
n=6	96.89	88.74	45.90
n=7	97.28	97.38	
n=8	95.43	90.52	82.14
n=9	94.29	91.27	
mean	94.45	91.65	74.45
std dev	2.65	2.87	19.42

Table A-5. Percent CD34+ purity of cells over a 2-week period

	Day 0 % CD34+ Purity	Day 7 % CD34+ Purity	Day 14 % CD34+ Purity
n=1	67.86	23.16	0.00
n=2	67.86	30.08	2.44
n=3	88.57	27.93	1.67
n=4	88.57	24.96	0.66
n=5	61.39	22.47	
n=6	90.62	30.75	4.67
n=7	81.29	27.79	
n=8	92.85	31.38	5.22
n=9	86.67	25.03	
mean	80.63	27.06	2.44
std dev	11.77	3.31	2.12

APPENDIX B
SPECIFIC AIM 1 DATA

Table B-1. Viscosity and cortical tension of fresh and cultured CD34+ cells

	Viscosity Fresh Cells (Pa•s)	Viscosity Cultured Cells (Pa•s)	Cortical Tension Fresh Cells (N/m)	Cortical Tension Cultured Cells (N/m)
n=1	1009.19	356.09	0.000365	0.000145
n=2	1189.98	79.45	0.000358	0.000005
n=3	140.30	245.76	0.000060	0.000016
n=4	165.29	405.19	0.000067	0.000029
n=5	317.52	198.09	0.000179	0.000039
n=6	267.29	229.58	0.000022	0.000053
n=7	108.40	157.19	0.000070	0.000053
n=8	1197.55	399.61	0.000436	0.000042
n=9	108.62	331.02	0.000210	0.000047
n=10	1140.42	121.62	0.000292	0.000050
n=11	189.30	209.48	0.000089	0.000048
n=12	289.49	133.68	0.000384	0.000068
n=13	229.49	380.36	0.000084	0.000052
n=14	308.54	283.66	0.000384	0.000073
n=15	489.39	164.69	0.000284	0.000058
n=16	193.08	295.97	0.000392	0.000018
n=17	576.39	190.68	0.000097	0.000067
n=18	567.39	199.47	0.000374	0.000059
n=19	896.49	184.60	0.000086	0.000062
n=20	936.79	159.30	0.000198	0.000067
n=21	503.78	36.43	0.000280	0.000046
n=22	284.07	118.23	0.000193	0.000091
n=23	937.43	300.30	0.000084	0.000038
n=24	749.39	193.48	0.000244	0.000067
n=25	274.98	208.38	0.000096	0.000020
n=26	454.69	188.96	0.000292	0.000087
n=27	739.44	307.88	0.000233	0.000050
n=28	539.49	200.88	0.000099	0.000058
n=29	378.03	173.78	0.000199	0.000068
n=30	280.39	188.30	0.000273	0.000086
mean	515.42	221.41	0.000214	0.000055
std error	62.87	16.88	0.0000226	0.0000049

APPENDIX C
SPECIFIC AIM 2 DATA

Table C-1. Number of CFU-GM generated by fresh and cultured CD34+ cells

Cord Blood Unit	Fresh Cells	Cultured Cells
1	52	64
2	78	92
3	66	124
4	61	76
5	57	90
mean	62.80	89.20
std error	4.44	10.07

Table C-2. Number of BFU-E generated by fresh and cultured CD34+ cells

Cord Blood Unit	Fresh Cells	Cultured Cells
1	70	34
2	138	100
3	98	74
4	100	49
5	88	70
mean	98.80	65.40
std error	11.15	11.29

APPENDIX D
SPECIFIC AIM 3 DATA

Table D-1. Nucleated cell fold increases of CD34+-purified cells in control culture (static 24-well plate)

	Day 0	Day 4	Day 7
n=1	1.00	1.88	11.69
n=2	1.00	3.03	10.16
n=3	1.00	2.98	10.76
mean	1.00	2.63	10.87
std dev	0.00	0.65	0.77

Table D-2. Nucleated cell fold increases of CD34+-purified cells in static PDMS chip

	Day 0	Day 4	Day 7
n=1	1.00	1.69	12.46
n=2	1.00	3.02	10.05
n=3	1.00	3.01	11.35
mean	1.00	2.57	11.29
std dev	0.00	0.77	1.21

Table D-3. Fold increases of CD34+ cells over a 1-week period in control culture (static 24-well plate)

	Day 0 NC Conc. (cells/ml)	Day 0 CD34+ Purity (%)	Day 0 CD34+ Conc. (cells/ml)	Day 7 NC Conc. (cells/ml)	Day 7 CD34+ Purity (%)	Day 7 CD34+ Conc. (cells/ml)	Day 7 Fold Increase
n=1	1.30E+05	81.29	1.06E+05	1.52E+06	27.79	4.22E+05	4.00
n=2	2.06E+05	90.26	1.86E+05	2.09E+06	30.46	6.37E+05	3.42
n=3	2.32E+05	88.72	2.06E+05	2.50E+06	30.22	7.56E+05	3.67
						mean	3.70
						std dev	0.29

NC = Nucleated Cell; Conc. = Concentration

Table D-4: Fold increases of CD34+ cells over a 1-week period in static PDMS chip

	Day 0 NC Conc. (cells/ml)	Day 0 CD34+ Purity (%)	Day 0 CD34+ Conc. (cells/ml)	Day 7 NC Conc. (cells/ml)	Day 7 CD34+ Purity (%)	Day 7 CD34+ Conc. (cells/ml)	Day 7 Fold Increase
n=1	1.30E+05	81.29	1.06E+05	1.62E+06	27.81	4.51E+05	4.26
n=2	2.06E+05	90.26	1.86E+05	2.07E+06	29.92	6.19E+05	3.33
n=3	2.32E+05	88.72	2.06E+05	2.63E+06	30.02	7.90E+05	3.84
						mean	3.81
						std dev	0.47

NC = Nucleated Cell; Conc. = Concentration

Table D-5. Percent viability of CD34+-purified cells over a 1-week period in control culture (static 24-well plate)

	Day 0 % Viability	Day 7 % Viability
n=1	97.70	95.38
n=2	95.46	92.91
n=3	98.28	95.03
mean	97.15	94.44
std dev	1.49	1.34

Table D-6. Percent viability of CD34+-purified cells over a 1-week period in static PDMS chip

	Day 0 % Viability	Day 7 % Viability
n=1	97.70	95.28
n=2	95.46	93.03
n=3	98.28	95.61
mean	97.15	94.64
std dev	1.49	1.40

Table D-7. Percent CD34+ purity of cells over a 1-week period in control culture (static 24-well plate)

	Day 0 % CD34+ Purity	Day 7 % CD34+ Purity
n=1	81.29	27.79
n=2	90.26	30.46
n=3	88.72	30.22
mean	86.76	29.49
std dev	4.80	1.48

Table D-8. Percent CD34+ purity of cells over a 1-week period in static PDMS chip

	Day 0 % CD34+ Purity	Day 7 % CD34+ Purity
n=1	81.29	27.81
n=2	90.26	29.92
n=3	88.72	30.02
mean	86.76	29.25
std dev	4.80	1.25

Table D-9. Number of CFU-GM and BFU-E generated by CD34+ cells pre-cultured for 1 week in control culture (static 24-well plate)

	CFU-GM	BFU-E
n=1	52	100
n=2	89	61
n=3	72	78
mean	71.00	79.67
std dev	18.52	19.55

Table D-10. Number of CFU-GM and BFU-E generated by CD34+ cells pre-cultured for 1 week in static PDMS chip

	CFU-GM	BFU-E
n=1	62	92
n=2	77	71
n=3	70	77
mean	69.67	80.00
std dev	7.51	10.82

Table D-11. Length of Caco-2 cells grown in static culture, “as-is” HARV, and HARV with culture chamber

	Static Control	"As-Is" HARV	HARV with Culture Chamber
n=1	38.5	46.3	44.5
n=2	29.3	41.3	44.7
n=3	30.1	42.3	42.7
n=4	32.9	46.7	46.4
n=5	34.4	41.8	43.8
n=6	36.1	45.8	44.7
n=7	32.7	44.3	44.9
n=8	34.5	43.2	42.1
n=9	30.6	46.9	41.6
n=10	31.4	48.4	43.8
n=11	34.7	41.2	44.7
n=12	29.1	39.9	42.7
n=13	34.8	42.3	45.7
n=14	33.4	45.4	44.7
n=15	30.5	44.8	46.1
n=16	31.1	46.3	42.3
n=17	34.8	42.3	44.3
n=18	33.2	43.5	41.0
n=19	33.1	41.2	42.8
n=20	31.4	44.7	45.7
n=21	33.7	45.7	45.2
n=22	35.2	42.6	44.6
n=23	29.1	42.4	43.8
n=24	34.8	43.9	42.7
n=25	33.9	44.0	41.6
n=26	35.9	42.5	46.8
n=27	35.0	42.8	45.8
n=28	29.2	46.4	44.6
n=29	35.8	42.6	41.3
n=30	34.2	41.8	40.2
n=31	33.7		
n=32	31.6		
n=33	36.2		
n=34	32.7		
n=35	33.9		
n=36	28.4		
n=37	29.4		
n=38	35.8		
n=39	32.4		
n=40	33.8		
n=41	35.7		
n=42	35.2		
n=43	31.1		
n=44	30.7		
n=45	30.4		
n=46	29.1		
n=47	34.2		
n=48	36.2		
n=49	29.1		
n=50	29.4		
n=51	30.2		
n=52	33.8		
n=53	32.9		
n=54	34.3		
n=55	36.4		
n=56	34.3		
n=57	32.5		
n=58	34.7		
n=59	33.1		
n=60	35.7		
mean	32.9	43.9	44.0
std dev	2.4	2.2	1.5

Table D-12. Width of Caco-2 cells grown in static culture, “as-is” HARV culture, and HARV with culture chamber

	Static Control	"As-Is" HARV	HARV with Culture Chamber
n=1	26.3	30.4	28.1
n=2	20.3	27.9	30.2
n=3	20.4	28.9	28.0
n=4	26.9	27.0	27.9
n=5	27.3	26.4	30.4
n=6	24.2	25.9	29.4
n=7	25.2	29.0	27.5
n=8	20.3	30.4	29.1
n=9	23.9	29.1	24.6
n=10	25.1	28.1	29.9
n=11	27.2	26.5	29.7
n=12	22.9	28.2	30.4
n=13	24.0	29.4	29.3
n=14	22.1	30.5	25.7
n=15	23.9	28.3	29.9
n=16	24.4	25.9	28.0
n=17	24.2	29.5	29.4
n=18	21.2	26.6	25.6
n=19	24.9	28.0	24.9
n=20	24.1	28.1	29.6
n=21	23.0	29.5	27.8
n=22	23.7	25.9	30.9
n=23	21.7	27.3	31.4
n=24	26.4	25.9	29.8
n=25	22.9	28.7	30.4
n=26	25.1	29.4	28.4
n=27	22.8	27.0	25.2
n=28	23.1	28.9	29.3
n=29	27.2	28.4	30.6
n=30	24.1	29.4	29.9
n=31	23.8		
n=32	25.3		
n=33	24.1		
n=34	24.7		
n=35	26.3		
n=36	22.1		
n=37	20.6		
n=38	21.3		
n=39	22.5		
n=40	23.5		
n=41	25.2		
n=42	25.1		
n=43	23.8		
n=44	22.1		
n=45	22.8		
n=46	24.7		
n=47	23.6		
n=48	25.3		
n=49	23.5		
n=50	22.6		
n=51	24.8		
n=52	21.5		
n=53	19.9		
n=54	20.4		
n=55	25.3		
n=56	23.9		
n=57	22.3		
n=58	24.3		
n=59	27.5		
n=60	25.9		
mean	23.8	28.2	28.7
std dev	1.9	1.4	1.9

APPENDIX E
SPECIFIC AIM 4 DATA

Table E-1. Nucleated cell fold increases of CD34+-purified cells over a 4-day period in static culture

	Day 0	Day 1	Day 2	Day 3	Day 4
n=1	1.00	1.00	1.40	1.36	2.20
n=2	1.00	0.94	1.36	1.62	1.88
n=3	1.00	0.96	1.39	1.58	2.02
n=4	1.00	0.99	1.20	1.54	1.55
n=5	1.00	1.06	1.47	1.52	1.79
n=6	1.00	0.92	1.40	1.67	1.69
mean	1.00	0.98	1.37	1.55	1.86
std dev	0.00	0.05	0.09	0.11	0.23

Table E-2. Nucleated cell fold increases of CD34+-purified cells over a 4-day period in "as-is" HARV culture

	Day 0	Day 1	Day 2	Day 3	Day 4
n=1	1.00	0.98	0.60	0.20	0.07
n=2	1.00	0.91	0.53	0.26	0.11
n=3	1.00	0.99	0.62	0.27	0.10
mean	1.00	0.96	0.58	0.24	0.09
std dev	0.00	0.04	0.05	0.04	0.02

Table E-3. Nucleated cell fold increases of CD34+-purified cells over a 4-day period in HARV with PDMS culture chamber

	Day 0	Day 1	Day 2	Day 3	Day 4
n=1	1.00	0.97	0.48	0.10	0.09
n=2	1.00	0.99	0.52	0.21	0.04
n=3	1.00	0.95	0.61	0.30	0.07
mean	1.00	0.97	0.54	0.20	0.07
std dev	0.00	0.02	0.07	0.10	0.03

Table E-4. Fold increases of CD34+ cells over a 4-day period in static culture

	Day 0 NC Conc. (cells/ml)	Day 0 CD34+ Purity (%)	Day 0 CD34+ Conc. (cells/ml)	Day 4 NC Conc. (cells/ml)	Day 4 CD34+ Purity (cells/ml)	Day 4 CD34+ Conc. (cells/ml)	Day 4 Fold Increase
n=1	1.25E+05	73.69	9.21E+04	2.75E+05	49.12	1.35E+05	1.47
n=2	4.50E+04	87.44	3.93E+04	8.46E+04	65.53	5.54E+04	1.41
n=3	8.74E+04	89.90	7.86E+04	1.77E+05	60.35	1.07E+05	1.36
n=4	5.83E+04	73.27	4.27E+04	9.02E+04	34.07	3.07E+04	0.72
n=5	8.20E+04	90.26	7.40E+04	1.47E+05	60.78	8.93E+04	1.21
n=6	1.28E+05	86.04	1.10E+05	2.16E+05	61.29	1.32E+05	1.20
						mean	1.23
						std dev	0.27

NC = Nucleated Cell; Conc. = Concentration

Table E-5. Fold increases of CD34+ cells over a 4-day period in "as-is" HARV culture

	Day 0 NC Conc. (cells/ml)	Day 0 CD34+ Purity (%)	Day 0 CD34+ Conc. (cells/ml)	Day 4 NC Conc. (cells/ml)	Day 4 CD34+ Purity (%)	Day 4 CD34+ Conc. (cells/ml)	Day 4 Fold Increase
n=1	1.25E+05	73.69	9.21E+04	8.75E+03	5.13	4.49E+02	0.00
n=2	4.50E+04	87.44	3.93E+04	5.00E+03	7.12	3.56E+02	0.01
n=3	8.74E+04	89.90	7.86E+04	8.74E+03	7.04	6.15E+02	0.01
						mean	0.01
						std dev	0.00

NC = Nucleated Cell; Conc. = Concentration

Table E-6. Fold increases of CD34+ cells over a 4-day period in HARV with PDMS culture chamber

	Day 0 NC Conc. (cells/ml)	Day 0 CD34+ Purity (%)	Day 0 CD34+ Conc. (cells/ml)	Day 4 NC Conc. (cells/ml)	Day 4 CD34+ Purity (%)	Day 4 CD34+ Conc. (cells/ml)	Day 4 Fold Increase
n=1	5.83E+04	73.27	4.27E+04	5.00E+03	0.00	0.00E+00	0.00
n=2	8.20E+04	90.26	7.40E+04	3.28E+03	4.89	1.60E+02	0.00
n=3	1.28E+05	86.04	1.10E+05	8.96E+03	8.16	7.31E+02	0.01
						mean	0.00
						std dev	0.00

NC = Nucleated Cell; Conc. = Concentration

Table E-7. Percent viability of CD34+-purified cells over a 4-day period in static culture

	Day 0 % Viability	Day 4 % Viability
n=1	94.86	92.54
n=2	95.01	88.38
n=3	96.23	92.88
n=4	96.10	61.93
n=5	94.91	88.73
n=6	96.43	90.63
mean	95.59	85.85
std dev	0.74	11.86

Table E-8. Percent viability of CD34+-purified cells over a 4-day period in "as-is" HARV culture

	Day 0 % Viability	Day 4 % Viability
n=1	94.86	35.67
n=2	95.01	52.05
n=3	96.23	50.73
mean	95.37	46.15
std dev	0.75	9.10

Table E-9. Percent viability of CD34+-purified cells over a 4-day period in HARV with PDMS culture chamber

	Day 0 % Viability	Day 4 % Viability
n=1	96.10	50.38
n=2	94.91	58.52
n=3	96.43	59.42
mean	95.81	56.11
std dev	0.80	4.98

Table E-10. Percent CD34+ purity of cells over a 4-day period in static culture

	Day 0 % CD34+ Purity	Day 4 % CD34+ Purity
n=1	73.69	49.12
n=2	87.44	65.53
n=3	89.90	60.35
n=4	73.27	34.07
n=5	90.26	60.78
n=6	86.04	61.29
mean	83.43	55.19
std dev	7.87	11.70

Table E-11. Percent CD34+ purity of cells over a 4-day period in "as-is" HARV culture

	Day 0 % CD34+ Purity	Day 4 % CD34+ Purity
n=1	73.69	5.13
n=2	87.44	7.12
n=3	89.90	7.04
mean	83.68	6.43
std dev	8.74	1.13

Table E-12. Percent CD34+ purity of cells over a 4-day period in HARV with PDMS culture chamber

	Day 0 % CD34+ Purity	Day 4 % CD34+ Purity
n=1	73.27	0.00
n=2	90.26	4.89
n=3	86.04	8.16
mean	83.19	4.35
std dev	8.85	4.11

APPENDIX F
SPECIFIC AIM 5 DATA

Table F-1. Nucleated cell fold increases of CD34+-purified cells removed from primary static culture

	Day 0	Day 4	Day 7
n=1	1.00	2.33	7.00
n=2	1.00	1.86	5.72
n=3	1.00	2.61	6.91
n=4	1.00	1.96	6.01
n=5	1.00	2.42	7.21
n=6	1.00	2.28	6.23
mean	1.00	2.24	6.51
std dev	0.00	0.28	0.61

Table F-2. Nucleated cell fold increases of CD34+-purified cells removed from primary "as-is" HARV culture

	Day 0	Day 4	Day 7
n=1	1.00	0.27	0.00
n=2	1.00	0.20	0.00
n=3	1.00	0.31	0.08
mean	1.00	0.26	0.03
std dev	0.00	0.06	0.05

Table F-3. Nucleated cell fold increases of CD34+-purified cells removed from primary culture in HARV with PDMS culture chamber

	Day 0	Day 4	Day 7
n=1	1.00	0.32	0.04
n=2	1.00	0.29	0.00
n=3	1.00	0.33	0.02
mean	1.00	0.31	0.02
std dev	0.00	0.02	0.02

Table F-4. Fold increases of CD34+ cells removed from primary static culture

	Day 0 NC Conc. (cells/ml)	Day 0 CD34+ Purity (%)	Day 0 CD34+ Conc. (cells/ml)	Day 7 NC Conc. (cells/ml)	Day 7 CD34+ Purity (%)	Day 7 CD34+ Conc. (cells/ml)	Day 7 Fold Increase
n=1	1.05E+05	86.67	9.10E+04	7.35E+05	25.03	1.84E+05	2.02
n=2	8.36E+04	75.82	6.34E+04	4.78E+05	20.15	9.63E+04	1.52
n=3	2.17E+05	81.92	1.78E+05	1.50E+06	22.91	3.44E+05	1.93
n=4	6.57E+04	78.18	5.14E+04	3.95E+05	30.26	1.20E+05	2.33
n=5	1.26E+05	80.82	1.02E+05	9.08E+05	27.84	2.53E+05	2.48
n=6	1.02E+05	80.19	8.18E+04	7.28E+05	26.01	1.89E+05	2.32
						mean	2.10
						std dev	0.35

NC = Nucleated Cell; Conc. = Concentration

Table F-5. Fold increases of CD34+ cells removed from primary "as-is" HARV culture

	Day 0 NC Conc. (cells/ml)	Day 0 CD34+ Purity (%)	Day 0 CD34+ Conc. (cells/ml)	Day 7 NC Conc. (cells/ml)	Day 7 CD34+ Purity (%)	Day 7 CD34+ Conc. (cells/ml)	Day 7 Fold Increase
n=1	1.31E+05	69.50	9.10E+04	0.00E+00	0.66	0.00E+00	0.00
n=2	9.27E+04	68.40	6.34E+04	0.00E+00	0.51	0.00E+00	0.00
n=3	3.92E+05	45.31	1.78E+05	3.14E+04	1.13	3.55E+02	0.00
						mean	0.00
						std dev	0.00

NC = Nucleated Cell; Conc. = Concentration

Table F-6. Fold increases of CD34+ cells removed from primary culture in HARV with PDMS culture chamber

	Day 0 NC Conc. (cells/ml)	Day 0 CD34+ Purity (%)	Day 0 CD34+ Conc. (cells/ml)	Day 7 NC Conc. (cells/ml)	Day 7 CD34+ Purity (%)	Day 7 CD34+ Conc. (cells/ml)	Day 7 Fold Increase
n=1	7.73E+04	66.48	5.14E+04	3.09E+03	0.79	2.44E+01	0.00
n=2	1.82E+05	55.97	1.02E+05	0.00E+00	0.43	0.00E+00	0.00
n=3	8.28E+04	60.27	4.99E+04	3.22E+03	0.68	2.19E+01	0.00
						mean	0.00
						std dev	0.00

NC = Nucleated Cell; Conc. = Concentration

Table F-7. Percent viability of CD34+-purified cells removed from primary static culture

	Day 0 % Viability	Day 7 % Viability
n=1	94.29	91.27
n=2	98.42	89.17
n=3	94.64	90.62
n=4	95.19	90.41
n=5	96.76	93.62
n=6	95.27	92.73
mean	95.76	91.30
std dev	1.55	1.63

Table F-8. Percent viability of CD34+-purified cells removed from primary "as-is" HARV culture

	Day 0 % Viability	Day 7 % Viability
n=1	84.85	48.30
n=2	80.27	42.36
n=3	79.02	40.19
mean	81.38	43.62
std dev	3.07	4.20

Table F-9. Percent viability of CD34+-purified cells removed from primary culture in HARV with PDMS culture chamber

	Day 0 % Viability	Day 7 % Viability
n=1	81.52	45.82
n=2	79.04	40.73
n=3	82.63	44.03
mean	81.06	43.53
std dev	1.84	2.58

Table F-10. Percent CD34+ purity of cells removed from primary static culture

	Day 0 % CD34+ Purity	Day 7 % CD34+ Purity
n=1	86.67	25.03
n=2	75.82	20.15
n=3	81.92	22.91
n=4	78.18	30.26
n=5	80.82	27.84
n=6	80.19	26.01
mean	80.60	25.37
std dev	3.67	3.57

Table F-11. Percent CD34+ purity of cells removed from primary "as-is" HARV culture

	Day 0 % CD34+ Purity	Day 7 % CD34+ Purity
n=1	69.50	0.66
n=2	68.40	0.51
n=3	45.31	1.13
mean	61.07	0.77
std dev	13.66	0.32

Table F-12. Percent CD34+ purity of cells removed from primary culture in HARV with PDMS culture chamber

	Day 0 % CD34+ Purity	Day 7 % CD34+ Purity
n=1	66.48	0.79
n=2	55.97	0.43
n=3	60.27	0.68
mean	60.91	0.63
std dev	5.28	0.18

Table F-13. Number of CFU-GM and BFU-E generated by CD34+ cells pre-cultured in primary static culture

	CFU-GM	BFU-E
n=1	124	74
n=2	95	61
n=3	89	80
n=4	111	89
n=5	97	71
n=6	104	76
mean	103.33	75.17
std dev	12.66	9.33

Table F-14. Number of CFU-GM and BFU-E generated by CD34+ cells pre-cultured in primary "as-is" HARV culture

	CFU-GM	BFU-E
n=1	2	2
n=2	3	0
n=3	2	1
mean	2.33	1.00
std dev	0.58	1.00

Table F-15. Number of CFU-GM and BFU-E generated by CD34+ cells pre-cultured in HARV with PDMS culture chamber

	CFU-GM	BFU-E
n=1	3	0
n=2	1	1
n=3	2	2
mean	2.00	1.00
std dev	1.00	1.00

LIST OF REFERENCES

Alberts B, Johnson A, Lewis J, Raff M, Roberts K, Walter P. Molecular Biology of the Cell (Fourth Edition), Garland Science, New York 2002.

Alcaraz J, Buscemi L, Grabulosa M, Trepat X, Fabry B, Farre R, Navajas D. Microrheology of human lung epithelial cells measured by atomic force microscopy. Biophys J 2003;84:2071-79.

Anderson RK. Effects of simulated microgravity and shear on cell behavior. (University of Florida, Gainesville, PhD dissertation.) 2004.

Atkins RE, Schroedl NA, Gonda SR, Hartzell CR. Neonatal rat heart cells cultured in simulated microgravity. In Vitro Cell Dev Biol Anim 1997;33:337-43.

Ballen KK. New trends in umbilical cord blood transplantation. Blood 2005:105;3786-92.

Branham ML, Tran-Son-Tay R, Schoonover C, Davis P, Allen S, Shyy W. Rapid prototyping of micropatterned substrates using conventional laser printers. J Mat Res 2002;17:1559-62.

Breems DA, Blokland EAW, Siebel KE, Mayen AEM, Engels LJA, Ploemacher RE. Stroma-contact prevents loss of hematopoietic stem cell quality during ex vivo expansion of CD34+ mobilized peripheral blood stem cells. Blood 1998;91:111-17.

Brugger W, Heimfeld S, Berenson RJ, Mertelsmann R, Kanz L. Reconstitution of hematopoiesis after high-dose chemotherapy by autologous progenitor cells generated ex vivo. New Engl J Med 1995;333: 283-7.

Bucaro MA, Fertala J, Adams CS, Steinbeck M, Ayyaswamy P, Mukundakrishnan K, Shapiro IM, Risbud MV. Bone cell survival in microgravity: Evidence that modeled microgravity increases osteoblast sensitivity to apoptogens. Ann NY Acad Sci 2004;1027:64-73.

Chan RJ and Yoder MC. The multiple facets of hematopoietic stem cells. Current Neurovascular Research 2004;1:197-206.

Clejan S, O'Conner KC, Cowger NL, Cheles MK, Haque S, Primavera AC. Effects of simulated microgravity on DU 145 human prostate carcinoma cells. Biotechnol Bioeng 1996;50:587-97.

Copelan EA. Hematopoietic stem-cell transplantation. New Engl J Med 2006;354:1813-26.

Cotrupi S, Ranzani D, Maier JA. Impact of modeled microgravity on microvascular endothelial cells. Biochim Biophys Acta 2005;1746:163-8.

Dai MS, Mantel CR, Xia ZB, Broxmeyer HE, Lu L. An expansion phase precedes terminal erythroid differentiation of hematopoietic progenitor cells from cord blood in vitro and is

associated with up-regulation of cyclin E and cyclin-dependent kinase 2. Blood 2000;96:3985-7.

de Wynter EA, Durig J, Cross MA, Heyworth CM, Testa NG. Differential response of CD34+ cells isolated from cord blood and bone marrow to MIP-1α and the expression of MIP-1α receptors on these immature cells. Stem Cells 1998;16:349-56.

Devine SM, Lazarus HM, Emerson SG. Clinical applications of hematopoietic progenitor cell expansion: current status and future prospects. Bone Marrow Transplant 2003;31:241-2.

Dong C, Skalak R, Sung K-LP. Cytoplasmic rheology of passive neutrophils. Biorheology 1991;28:557-67.

Dong C, Skalak R, Sung K-LP, Schmid-Schonbein GW, Chien S. Passive deformation analysis of human leukocytes. J Biomech Eng 1988;110:27-36.

Emminger W, Emminger-Schmidmeier W, Hocker P, Hinterberger W, Gadner H. Myeloid progenitor cells (CFU-GM) predict engraftment kinetics in autologous transplantation in children. Bone Marrow Transplant 1989;4:415-20.

Eridani S, Mazza U, Massaro P, La Targia ML, Maiolo AT, Mosca A. Cytokine effect on ex vivo expansion of haemopoietic stem cells from different human sources. Biotherapy 1998;11:291-6.

Evans E. White cell mechanics: Basic science and clinical aspects. In: HJ Meiselman, MA Lichman, PL LaCelle (ed.) Allan R Liss, New York 1984:53.

Evans EA, Yeung A. Apparent viscosity and cortical tension of blood granulocytes determined by micropipette aspiration. Biophys J 1989;56:151-60.

Fung YC. Foundations of Solid Mechanics. Prentice-Hall Inc., Englewood Cliffs, NJ 1965.

Gammaitoni L, Bruno S, Sanavio F, Gunetti M, Kollet O, Cavalloni G, Falda M, Fagioli F, Lapidot T, Aglietta M, Piacibello W. Ex vivo expansion of human adult stem cells capable of primary and secondary hemopoietic reconstitution. Exp Hematol 2003;31:261-70.

Gao H, Ayyaswamy PS, Ducheyne P. Dynamics of a microcarrier particle in the simulated microgravity environment of a rotating wall vessel. Microgravity Sci Technol 1997:154-65.

Gill, A. Optimization of microfluidic cell sorter concepts using rapid-prototyping techniques. (University of Florida, Gainesville, MS thesis) 2003.

Gilmore GL, DePasquale DK, Lister J, Shadduck RK. Ex vivo expansion of human umbilical cord blood and peripheral blood CD34+ hematopoietic stem cells. Exp Hematol 2000; 28:1297-305.

Goodwin TJ, Prewett TL, Spaulding GF, Becker JL. Three-dimensional culture of a mixed mullerian tumor of the ovary: Expression of in vivo characteristics. In Vitro Cell Dev Biol Anim 1997;33:366-74.

Hammond TG, Hammond JM. Optimized suspension culture: the rotating-wall vessel. Am J Physiol Renal Physiol 2001;281:F12-25.

Haylock DN, To LB, Dowse TL, Juttner CA, Simmons PJ. Ex vivo expansion and maturation of peripheral blood CD34+ cells into myeloid lineage. Blood 1992;80:1405-12.

Heath SL, Tew JG, Tew JG, Szakal AK, Burton GF. Follicular dendritic cells and human immunodeficiency virus infectivity. Nature 1995;26:740-4.

Heike T, Nakahata T. Ex vivo expansion of hematopoietic stem cells by cytokines. Biochimica et Biophysica Acta 2002;1592:313-21.

Hochmuth RM, Ting-Beall HP, Beaty BB, Needham D, Tran-Son-Tay R. Viscosity of passive human neutrophils undergoing small deformations. Biophys J 1993;64;1596-1601.

Huang S, Law P, Young D, Ho AD. Candidate hematopoietic stem cells from fetal tissues, umbilical cord blood vs. adult bone marrow and mobilized peripheral blood. Exp Hematol 1998;26:1162-71.

Jaroscak J, Goltry K, Smith A, Waters-Pick B, Martin PL, Driscoll TA, Howrey R, Chao N, Douville J, Burhop S, Fu P, Kurtzberg J. Augmentation of umbilical cord blood (UCB) transplantation with ex vivo expanded UCB cells: results of a phase 1 trial using the AastromReplicell System. Blood 2003;101:5061-70.

Jessup JM, Frantz M, Sonmez-Alpan E, Locker J, Skena K, Waller H, Battle P, Nachman A, Bhatti, Weber ME, Thomas DA, Curbeam RL, Baker TL, Goodwin TJ. Microgravity culture reduces apoptosis and increases the differentiation of a human colorectal carcinoma cells line. In Vitro Dev Cell Biol Anim 2000;36:367-73.

Kan HC, Shyy W, Udaykumar HS, Vigneron P, Tran-Son-Tay R. Effects of nucleus of leukocyte recovery. Annals of Biomedical Engineering 1999;27:648-55.

Kan HC, Udaykumar HS, Shyy W, Tran-Son-Tay R. Hydrodynamics of a compound drop with application to leukocyte modeling. Physics of Fluids 1998;10:760-74.

Klement BJ, Young QM, George BJ, Nokkaew M. Skeletal tissue growth, differentiation, and mineralization in the NASA rotating wall vessel. Bone 2004;34:487-98.

Koutna I, Klabusay M, Kohutova V, Krontorad P, Svoboda Z, Kozubek M, Mayer J. Evaluation of CD34+ - and Lin- -selected cells from peripheral blood stem cell grafts of patients

with lymphoma during differentiation in culture ex vivo using a cDNA microarray technique. Exp Hematol 2006;34:832-40.

Lakota J, Ballova V, Drgona L, Durkovic P, Vranovsky A. Use of selected CD34+ cells in the treatment of relapsed/progressive HD: experiences from a single center. Cytotherapy 2002;4:177-80.

Lanza F, Healy L, Sutherland DR. Structural and functional features of the CD34 antigen: an update. J Biol Regul Homeost Agents 2001;15:1-13.

Li Q, Cai H, Liu Q, Tan WS. Differential gene expression of human CD34+ hematopoietic stem and progenitor cells before and after culture. Biotechnol Lett 2006;6:389-94.

Licato LL, Grimm EA. Multiple interleukin-2 signaling pathways differentially regulated by microgravity. Immunopharmacology 1999;44:273-9.

Lim CT, Zhou EH, Quek ST. Mechanical models for living cells – a review. J Biomech 2006;39:195-216.

Lui Y, Liu T, Fan X, Ma X, Cui Z. Ex vivo expansion of hematopoietic stem cells derived from umbilical cord blood in rotating wall vessel. J Biotech 2006;124:592-601.

Ma DC, Jin BQ, Sun YH, Chang KZ, Dai B, Chu JJ, Liu YG. Changes in cyclin expression during proliferation and differentiation of CD34+ cells derived from fetal liver induced by thrombopoietin. Sheng Li Xue Bao 2001;53:296-302.

Maggakis-Kelemen C, Biselli M, Artmann GM. Determination of the elastic shear modulus of cultured human red blood cells. Biomed Tech 2002;47 Suppl 1 Pt 1:106-9.

McClintock PR, Papaconstantinou J. Regulation of hemoglobin synthesis in a murine erythroblastic leukemia cell; the requirement for replication to induce hemoglobin synthsis. Proc Natl Acad Sci USA 1974;71:4551-5.

McNiece I, Jones R, Bearman SI, Cagnoni P, Nieto Y, Franklin W, Ryder J, Steele A, Stoltz J, Russell P, McDermitt J, Hogan C, Murphy J, Shpall EJ. Ex vivo expanded peripheral blood progenitor cells provide rapid neutrophil recovery after high-dose chemotherapy in patients with breast cancer. Blood 2000;96:3001-7.

Needham D, Hochmuth RM. Rapid flow of passive neutrophils into a 4 μm pipet and measurement of cytoplasmic viscosity. J Biomech Eng 1990;112:269-76.

Needham D, Hochmuth, RM. A sensitive measure of surface stress in the resting neutrophil. Biophys J 1992;61:1664-70.

Paquette RL, Dergham ST, Karpf E, Wang H-J, Slamon DJ, Souza L, Glaspy JA. Ex vivo expanded unselected peripheral blood: progenitor cells reduce posttransplantation

neutropenia, thrombocytopenia, and anemia in patients with breast cancer. Blood 2000;96:2385-90.

Parra E, Wingren AG, Hedlund G, Kalland T, Dohlsten M.The role of B7-1 and LFA-3 in costimulation of CD8+ T cells. J Immunol 1997;158:637-42.

Perrault CM, Bray EJ, Didier N, Ozaki CK, Tran-Son-Tay R. Altered rheology of lymphocytes in the diabetic mouse. Diabetologia 2004;47:1722-6.

Piacibello W, Sanavio F, Garetto L, Severino A, Bergandi D, Ferrario J, Fagioli F, Berger M, Aglietta M. Extensive amplification and self-renewal of human primitive hematopoietic stem cells from cord blood. Blood 1997; 89:2644-53.

Plett PA, Abonour R, Frankovitz SM, Orschell CM. Impact of modeled microgravity on migration, differentiation, and cell cycle control of primitive human hematopoietic progenitor cells. Exp Hematol 2004;32:773-781.

Plett PA, Frankovitz SM, Abonour R, Orschell-Traycoff CM. Proliferation of human hematopoietic bone marrow cells in simulated microgravity. In Vitro Cell Dev Biol-Animal 2001;37:73-78.

Reiffers J, Cailliot C, Dazey B, Attal M, Caraux J, Boiron J-M. Abrogation of post-myeloablative chemotherapy neutropenia by ex vivo expanded autologous CD34-positive cells. Lancet 1999;354:1092-3.

Roberson JA, Crowe CT. Engineering Fluid Mechanics (Third Edition), Houghton Mifflin Company, Boston 1985.

Savary C, Grazziuti ML, Przepiorka D, Tomasovic SP, McIntyre BW, Woodside DG, Pellis NR, Pierson DL, Rex JH. Characteristics of human dendritic cells generated in a microgravity analogue culture system. In Vitro Cell Dev Biol Anim 2001;37:216-22.

Schmid-Schonbein GW, Sung KL, Tozeren H, Skalak R, Chien S. Passive mechanical properties of human leukocytes. Biophys J 1981;36:243-56.

Shin D, Athanasiou K. Cytoindentation for obtaining cell biomechanical properties. J Orthop Res 1999;17:880-90.

Shpall EJ, Quinones R, Giller R, Zeng C, Baron AE, Jones RB, Bearman SI, Nieto Y, Freed B, Madinger N, Hogan CJ, Slat-Vasquez V, Russell P, Blunk B, Schissel D, Hild E, Malcolm J, Ward W, McNiece IK. Transplantation of ex vivo expanded cord blood. Biol Blood Marrow Transplant 2002;8:368-76.

Simons DM, Garder EM, Lelkes PI. Dynamic culture in a rotating-wall vessel bioreactor differentially inhibits murine T-lymphocyte activation by mitogenic stimuli upon return to static conditions in a time-dependent manner. J Appl Physiol 2006;100:1287-92.

Sirchia G, Rebulla P. Placental/umbilical cord blood transplantation. Haematologica 1999;84:738-47.

Sytkowski AJ, Davis KL. Erythroid cell growth and differentiation in vitro in the simulated microgravity environment of the NASA rotating wall vessel bioreactor. In Vitro Cell Dev Biol Anim 2001;37:79-83.

Tabuse Y, Kawamura M, Furusawa M. Induction of haemoglobin synthesis in Friend leukaemia cells without the necessity of mitosis. Differentiation 1976;7:1-5.

Tanavde VM, Malehorn MT, Lumkul R, Gao Z, Wingard J, Garrett ES, Civin CI. Human stem-progenitor cells from neonatal cord blood have greater hematopoietic expansion capacity than those from mobilized adult blood. Exp Hematol 2002;30:816-23.

Theret DP, Levesque MJ, Sato M, Nerem RM, Wheeler LT. The application of a homogeneous half-space model in the analysis of endothelial cell micropipette measurements. J Biomech Eng 1988;110:190-99.

Thomas S, Bolch W, Kao KJ, Bova F, Tran-Son-Tray R. Effects of x-ray radiation on the rheologic properties of platelets and lymphocytes. Transfusion 2003;43:502-8.

Tran-Son-Tay R, Needham D, Yeung A, Hochmuth RM. Time-dependent recovery of passive neutrophils after large deformation. Biophys J 1991;60:856-66.

Traycoff CM, Abboud MR, Laver J, Clapp DW, Srour EF. Rapid exit from G0/G1 phase of cell cycle in response to stem cell factor confers on umbilical cord blood CD34+ cells an enhanced ex vivo expansion potential. Exp Hematol 1994;22:1264-72.

Tsai MA, Frank RS, Waugh RE. Passive mechanical behavior of human neutrophils: power-law fluid. Biophys J 1993;65:2078-88.

Tse W, Laughlin M. Cord blood transplantation in adult patients. Cytotherapy 2005;7:228-42.

Turner J, Dockrell HM. Stimulation of human peripheral blood mononuclear cells with live Mycobacterium bovis BCG activates cytolytic CD8+ T cells in vitro. Immunology 1996;87:339-42.

Vincent L, Avancena P, Cheng J, Rafii S, Rabbany S. Simulated microgravity impairs leukemic cell survival through altering VEGFR-2/VEGF-A signaling pathway. Annals of Biomed Eng 2005;33:1405-10.

Volokh, K. Cytoskeletal architecture and mechanical behavior of living cells. Biorheology 2003;40:213-20.

Wagner JE, Barker JN, DeFor TE, Baker KS, Blazar BR, Eide C, Goldman A, Kersey J, Krivit W, MacMillan ML, Orchard PJ, Peters C, Weisdorf DJ, Ramsay NK, Davies SM.

Transplantation of unrelated donor umbilical cord blood in 102 patients with malignant and non-malignant diseases: Influence of CD34 cell dose and HLA disparity on treatment-related mortality and survival. Blood 2002;100:1611-18.

Wang N, Naruse K, Stamenovic D, Fredberg JJ, Mijailovich SM, Tolic-Norrelykke IM, Polte T, Mannix R, Ingber DE. Mechanical behavior in living cells consistent with the tensegrity model. Proc Natl Acad Sci USA 2001;98:7765-70.

Watts KL, Reddy V, Tran-Son-Tay R. The effects of ex vivo expansion on the rheology of umbilical cord blood-derived CD34+ cells. Journal of Stem Cells 2007;2(1):pages x-x (in print).

Watts KL, Tran-Son-Tay R, Reddy V. The effects of ex vivo expansion on the differentiation of umbilical cord blood-derived CD34+ cells. Journal of Stem Cells 2006;(1)4:pages x-x (in print).

Yasui K, Matsumoto K, Hirayama F, Tani Y, Nakano T. Differences between peripheral blood and cord blood in the kinetics of lineage-restricted hematopoietic cells: implications for delayed platelet recovery following cord blood transplantation. Stem Cells 2003;21:143-51.

Yeung A, Evans EA. Cortical shell-liquid core model for passive flow of liquid-like spherical cells into micropipets. Biophys J 1989;56:139-49.

Zhelev DV, Needham D, Hochmuth RM. Role of the membrane cortex in neutrophil deformation in small pipets. Biophys J 1994;67:696-705.

BIOGRAPHICAL SKETCH

Korashon Lynn Watts received a Bachelor of Science degree with high honors in agricultural and biological engineering from the University of Florida in May of 2003. During her undergraduate career, she participated in an NSF-sponsored Research Experience for Undergraduates program at the Center for Biofilm Engineering at Montana State University, where she worked with Dr. Phil Butterfield on the development of a method to automate the measurement of Biodegradable Dissolved Organic Carbon levels in drinking water. She successfully completed the Honors Program and was awarded the following undergraduate scholarships: Robert Byrd Foundation Scholarship, John Andrew Bostrom Foundation Scholarship, Gator Club of Volusia County Scholarship, Daughters of the American Revolution Scholarship, American Society of Agricultural Engineers Scholarship, US Sugar Farmers' Corporation Scholarship, and Ernest F. Lamothe Scholarship.

Miss Watts was awarded an Alumni Fellowship for graduate study at the University of Florida in the department of Biomedical Engineering, where she specialized in Cell and Tissue Engineering. She began her graduate work in the Fall of 2003 and received a Master of Science degree in December of 2004. She is currently a member of the Society of Women Engineers, the National Society of Collegiate Scholars, and the Biomedical Engineering Society. While completing her Ph.D. research, she published two peer-reviewed manuscripts detailing her findings.